PROTEIN EXPRESSIONS OF *Acinetobacter sp.* ISOLATES LT1A AND V2 DURING HYDROCARBON DEGRADATION

By: Karyn Pretorius

Submitted in fulfillment of the academic requirements for the degree of Master of Science in the School of Biochemistry, Genetics, and Microbiology, University of KwaZulu-Natal, Westville.

March 2012

As the candidate's supervisor I have approved this dissertation for submission.

Signed:_____ **Name:** Prof. Johnson Lin **Date:** _____

FACULTY OF SCIENCE AND AGRICULTURE

DECLARATION 1 – PLAGIARISM

I, Karyn Pretorius, declare that

1. The research reported in this thesis, except where otherwise indicated, and is my original research.

2. This thesis has not been submitted for any degree or examination at any other university.

3. This thesis does not contain other persons' data, pictures, graphs or other information, unless specifically acknowledged as being sourced from other persons.

4. This thesis does not contain other persons' writing, unless specifically acknowledged as being sourced from other researchers. Where other written sources have been quoted, then:

    a. Their words have been re-written but the general information attributed to them has been referenced
    b. Where their exact words have been used, then their writing has been placed in inside quotation marks, and referenced.

5. This thesis does not contain text, graphics or tables copied and pasted from the Internet, unless specifically acknowledged, and the source being detailed in the thesis and in the References sections.

Signed

……..... ……

Declaration Plagiarism 22/05/08 FHDR Approved

FACULTY OF SCIENCE AND AGRICULTURE

DECLARATION 2 – PUBLICATIONS

DETAILS OF CONTRIBUTION TO PUBLICATIONS that form part and/or include research presented in this thesis (include publications in preparation, submitted, *in press* and published and give details of the contributions of each author to the experimental work and writing of each publication)

NOT APPLICABLE

Signed:

…… ……

Declaration Publications FHDR 22/05/08 Approved

TABLE OF CONTENTS

CONTENTS **PAGE**

PREFACE

The experimental work described in this dissertation was carried out in the School of Biochemistry, Genetics, Microbiology, University of KwaZulu-Natal, Westville, from January 2010 to December 2011, under the supervision of Professor Johnson Lin.

These studies represent original work by the author and have not otherwise been submitted in any form for any degree or diploma to any tertiary institution. Where use has been made of the work of others it is duly acknowledged in the text.

_____

Karyn Pretorius (206504758)
March 2012

ACKNOWLEDGEMENTS

The author would like to express her gratitude to the following people:

My supervisor, Prof. J. Lin for his motivation, supervision and support during this study;

The staff and postgraduate students of the Microbiology department (University of KwaZulu-Natal, Westville Campus) for their support and much appreciated assistance;

Atheesha Ganesh for her mentorship and guidance throughout the study;

Prof. Peter Owira, in the School of pharmacology for use of the XRS gel documentation system;

Her family and friends for their belief, motivation and encouragement;

The National Research Foundation for financial assistance.

ABSTRACT

Bacteria of the genus *Acinetobacter* are known to be involved in the degradation, leaching and removal of various hazardous compounds from the environment. Several studies of *Acinetobacter* spp. have reported on the genes involved in alkane degradation; but less is known about the proteins that are expressed at certain points within the degradation period. *Acinetobacter* sp. LT1A and *Acinetobacter* sp. V2 were isolated from diesel- and used engine oil-contaminated soils respectively. In a previous investigation (Toolsi, 2008), these isolates have been shown to demonstrate different gene expression patterns during diesel degradation using real time PCR. The real time PCR data showed that isolate V2 made use of multiple alkane hydroxylases whereas LT1A made use of only one, and the expression of the alkane hydroxylase regulator *alkR* and secretory protein *xcpR* also revealed multiple product formations in isolate V2 as compared to LT1A. Thus the objectives for the current investigation were to monitor the hydrocarbon degradation ability of *Acinetobacter* sp. isolates V2 and LT1A using medium chain (C_{14}) and long chain (C_{28}) hydrocarbon substrates and to compare the hydrocarbon degradation abilities and protein expression patterns of both isolates. To achieve this, the isolates were grown for 20 days in Bushnell Haas liquid medium supplemented with tetradecane (C_{14}) or octocosane (C_{28}) as a sole carbon source. Gravimetric analysis was used to monitor degradation and whole cell protein was extracted from the culture medium throughout the 20-day study period. The protein expression patterns were visualized using 1D and 2D PAGE. The 2D PAGE images were analyzed using the PDQuest Advanced 2D image analysis software (BIORAD). By day 20, approximately 90% of C_{14} was degraded by both isolates, whereas only 36% of C_{28} had been broken down. In both the C_{14} and C_{28} degradation assays, the isolates achieved significant amounts of hydrocarbon degradation as compared to the abiotic controls. One-dimensional and 2D SDS-PAGE gels indicated that there are observable differences in protein expression patterns between the isolates during C_{14} and C_{28} degradation. Both isolates achieved similar rates of hydrocarbon usage, but appear to do so using different, unidentified, protein systems. Analysis of the 2D-SDS PAGE gel images revealed that more proteins were required for the utilization of the long chain alkane (C_{28}) as compared to the medium chain alkane (C_{14}) for both isolates. Potential spots of interest were identified from the 2D SDS-PAGE images and sequenced. The identities of these proteins were found to be: a conserved hypothetical protein, TonB-dependent receptor

protein, Peptidyl-prolyl-cis-trans isomerase and a Protein containing DUF1559. No alkane hydroxylase components were detected in this study. This investigation demonstrated the need for more studies at the proteomic level. Future investigations should focus on the insoluble subproteome of the isolates and make use of larger sample sizes (replicates) to reduce variation in spot detection and quantification. Genomic sequencing of the isolates will also shed light on the genetics and biochemistry of alkane metabolism in these *Acinetobacter* sp. isolates.

LIST OF FIGURES

LIST OF TABLES

CHAPTER ONE

INTRODUCTION AND LITERATURE REVIEW

1.1 INTRODUCTION

Widespread use of hydrocarbons as energy sources and the associated transport of such compounds have resulted in an increasing risk of environmental pollution (Throne-Holst *et al*., 2007, Sheppard *et al.*, 2011). Thankfully, wax-like alkanes are also naturally synthesized by plants, algae and other organisms, and it is well known that they serve as carbon sources for a variety of bacteria (Smits *et al*., 2002; Park, 2005; Piccolo *et al*., 2010). Microbes involved in diesel degradation are known as hydrocarbon degraders and were first isolated almost a century ago (Head *et al.,* 2006). The first bacterium isolated was capable of degrading methane and longer chain alkanes. Since then the microbial degradation of alkanes by microorganisms has been well investigated (van Beilen *et al*., 2003). Many microorganisms including bacteria, yeasts and fungi contribute to hydrocarbon degradation in the environment (Head *et al*., 2006; Kim *et al*., 2009). In fact, approximately 79 bacterial genera have been reported to utilize hydrocarbons as a sole source of carbon and energy (Head *et al*., 2006).

In 1992 Rosenberg *et al*. defined two essential characteristics that hydrocarbon utilizing bacteria needed to possess in order to successfully degrade hydrocarbons, these were: i) membrane-bound group specific oxygenases and, ii) mechanisms for optimizing contact between the microbe and the insoluble hydrocarbon (Manilla-Perez *et al*., 2010). Gram negative bacteria are usually the most dominant organisms after an oil spill (Ganesh and Lin, 2011); known diesel and hydrocarbon degraders include: *Acinetobacter* sp., *Pseudomonas* sp*., Citrobacter* sp., and *Alcanivorax* sp. (Hara *et al.,* 2003; van Gestel *et al*., 2003; Singh and Lin, 2007). Of particular interest is the *Acinetobacter* genus that has been shown in the literature to be a versatile biocatalyst, utilizing a wide range of compounds for both carbon and energy sources (Abdel-El-Haleem, 2003; Barbe *et*

al., 2004; Doughari *et al*., 2011). It has been shown that *Acinetobacter* spp. may employ a variety of *n*-alkane-degrading mechanisms that include the presence of alternative oxidative pathways, implementation of different methods of adhesion, and emulsification (Toolsi, 2008).

The microorganism-mediated biodegradation of hydrocarbons has been investigated for many years, and numerous factors have been shown to influence the utilization of such compounds (Kang and Park, 2010). Many of the studies involving alkane degradation are investigated at the nucleic acid level; however the disadvantage with this approach is that not all genes that may be present in an organism(s) are necessarily expressed, especially if the organism possesses 2 or more related genes (Smits *et al*., 1999; Callister *et al*., 2008). Since it is not always possible to verify the expression of these genes of interest due to time and cost factors, a gap in our knowledge base exists (Callister *et al*., 2008). Genetic characterization of bacterial biodegradation pathways has been achieved to some extent; however, there is a lack of information at the proteomic level (Kim *et al*., 2007). Thus the study of protein expression is a promising alternative to that of nucleic acid based research because proteins reflect the functionality of metabolic reactions and regulatory pathways directly (Benndorf *et al*., 2007). In order to complete the picture of *n*-alkane utilization of the *Acinetobacter* sp. isolates V2 and LT1A, this study investigated the protein expression patterns of both organisms when grown on chemically defined media, containing either a medium or long chain alkanes.

1.2 THE HARMFUL EFFECTS AND BIOREMEDIATION OF DIESEL AND OIL SPILLAGES

Public attention is always drawn to large oil spills such as that of the Exxon Valdez in 1989 and the massive oil spill in 2010 that resulted from an explosion on the Deepwater Horizon Oil Rig (Kerr, 2010). Attention is gained because large numbers of marine mammals and sea birds are killed from the resulting pollution and devastating effects that the spilt oil has on the surrounding ecosystems. These spills have negative, irreversible effects on the quality and health of the environment (Andreoni and Gianfreda, 2007). It has been well documented that crude oil contains mutagenic, carcinogenic and growth-inhibiting chemicals that, even in small quantities, can destroy microalgae

and juvenile forms of marine organisms (Gutnick and Rosenberg, 1977). Petroleum compounds have also been reported to inhibit microbial decomposition of organic matter by affecting chemotaxis (Gutnick and Rosenberg, 1977). Smaller oil spills are often overlooked, even though the threat they pose to human health is still significant (Zhu *et al*., 2004). For example, acute exposure to the volatile components of diesel and other hydrocarbons can cause neurological symptoms such as headaches and nausea, and some of these volatile components can be carcinogenic (Rodriguez-Trigo *et al*., 2007). Contamination of the environment is associated with the manufacture, storage, and transport of hydrocarbons and can also be as a result of losses from motor vehicles as well as from illegal dumping (Harrison *et al*., 2000; Marchal *et al.,* 2003; Bento *et al*., 2005).

Many physical and chemical methods are available nowadays to cleanup diesel-contaminated areas; however these methods are often tedious and can expose workers to potentially dangerous toxic substances (Rodriguez-Trigo *et al*., 2007). A combination of biological, physical or chemical methods can be employed to treat hydrocarbon-contaminated soils, but the role and activity of microorganisms in this degradation process is the most important contributing factor to successful degradation (Greenwood *et al*., 2009). Bioremediation is an inexpensive alternative to physical and chemical methods of remediation that has the added advantage of being able to convert hazardous chemicals into less or non-toxic forms (Abdel-El-Haleem, 2003). Bioremediation can be defined as: „any process that uses microbes or their enzymes to return the environment altered by contaminants to its original condition' (Okoh and Trejo-Hernandez, 2006). Microbes have an inherent ability to survive in almost any environment making use of a wide range of chemical compounds as carbon and energy sources (Peixoto *et al*., 2011). *n*-Alkanes are one such source of carbon and energy and are particularly relevant since they comprise the major hydrocarbon component of crude oil, usually between 20 to 50% (Marin *et al*., 2003; Rojo, 2005). A range of techniques can be used for bioremediation, each having certain advantages over others (Atlas, 1995). The obvious advantage of utilizing microbial enzymes for remediation is that the enzymes are active under mild conditions, are easier to work with than whole organisms and they are environment-friendly biocatalysts, which would have wide public acceptance as a „green technology' without the release of genetically modified or exotic organisms into an environment (Mohebali and Ball, 2008; Peixoto *et al*., 2011).

Diesel is a complex substrate made up of a carbon range from C_9 to C_{25}. It is comprised mainly of un-branched *n*-alkanes that can be described as short, medium, long or very long-chain *n*-alkanes based on the length of their carbon chains. According to Wentzel *et al.* (2007), a long chain *n*-alkane is generally ten carbon atoms or more but for the purposes of this study, long chain alkanes will contain 16 or more carbon atoms. There may also be alkenes, cycloalkanes, aromatic hydrocarbons and olefins. Hydrocarbons, measured mainly as total petroleum hydrocarbons (TPHs) comprise the majority components in crude oils (Al-Mutairi *et al.*, 2008). Petroleum hydrocarbons can be divided into four classes: the saturates, the aromatics, the asphaltenes (phenols, fatty acids, ketones, esters and porphyrins) and the resins (pyridines, quinolines, carbazoles, sulfoxides and amides) (Leahy and Colwell, 1990). Petroleum can be distilled into several products, like engine fuels such as diesel oil and gasoline (Vanzella *et al.*, 2007). Alkanes themselves are components of natural gas, petroleum, petrochemicals and coal and it is obvious then that they have a widespread distribution (Berthe-Corti and Fetzner, 2002). There are many enzymes and alternative pathways for biodegradation. Some organisms preferentially degrade short chain alkanes over long chain alkanes. Liquid and low solid *n*-alkanes are less soluble in water and are thus less toxic to microorganisms. Their toxicity arises because alkanes have the ability to destroy bacterial cell membranes and they can affect protein transport systems (Plohl *et al.*, 2002). Liquid and low solid *n*-alkanes are then more readily degraded as compared to shorter chain hydrocarbons (Plohl *et al.*, 2002).

1.3 HYDROCARBON DEGRADATION BY *ACINETOBACTER* spp.

Gram negative organisms have been revealed by most studies to be the most prevalent microorganisms in oil polluted sites (Alonso-Gutierrez *et al.*, 2011). One such Gram negative organism, *Acinetobacter* is one of the most common bacterial species isolated from petroleum contaminated sites (Toolsi, 2008). *Acinetobacter* spp. are known to be involved in the degradation, leaching and removal of various hazardous compounds from the environment and it is for this reason that they are of interest from a biotechnological point of view (Abdel-El-Haleem, 2003; Vanbroekhoven *et al.*, 2004; Doughari *et al.*, 2011). *Acinetobacter* as a genus have been described as being nutritionally versatile organisms with a range of substrates that can be used as sole carbon and energy sources matching that of the Pseudomonads (Abdel-El-Haleem, 2003; Barbe *et al.*,

2004; Doughari *et al*., 2011). These non-motile, Gram-negative coccobacilli are widespread in nature, and are adept to using a wide range of carbon sources including various oil components and diesel (Abdel-El-Haleem, 2003; Kang and Park, 2010). How *Acinetobacter* spp. utilizes these hydrocarbons shows the versatility of these organisms. There are multiple variations in the choice of enzymes or metabolic systems used amongst the genus (Ratajczak *et al*., 1998a). One of the major biotechnological applications of *Acinetobacter* spp. is in „Lipid Biotechnology' which is defined as the microbial production and biotransformation of lipids and lipid soluble compounds (Manila-Perez *et al*., 2010). The storage lipids (TAGs and wax esters) generated by various bacterial species during growth on alkanes are used for biotechnological product development which includes the production of cosmetics and pharmaceuticals (Ishige *et al*., 2002; Manilla-Perez *et al*., 2010). Other major biotechnological applications of this versatile bacterial genus include:

i) The bioremediation of waste water effluents; whereby these bacteria have been reported to facilitate the removal of phosphates, degrade petrochemicals and breakdown organic pollutants.

ii) Bioremediation of soils and effluents contaminated with heavy metals; this includes the effluent from the textile or tannery industries, lead that may be present in digested sewage sludge, chromium in activated sludge or waste water or the silver in photographic wastewater.

iii) The production of biopolymers and biosurfactants; these have been investigated for the prevention of dental plaque, for use in the paper making industry, for the emulsification of oil waste and for the incorporation in cosmetics, detergents and shampoos.

iv) Clinical use; *Acinetobacter* spp. are involved in the production of glutaminase-sparaginase and L (-) carnitine (Doughari *et al*., 2011).

Acinetobacter strains are considered to be one of the most efficient oil degraders and are highly rated in their ability to degrade hydrocarbons (George-Okafor *et al*., 2009). They are well equipped to utilize hydrocarbons because they are one of several hydrocarbon degrading bacteria that are capable of producing biotensides (or biosurfactants) that facilitate the use of hydrocarbons as

carbon sources. Without these biosurfactants, the hydrocarbon substrates are not bioavailabe for catabolism. Biosurfactants are known to greatly improve the degradation process since the limiting and most critical step in the utilization of hydrocarbons is that of hydrocarbon emulsification (Vasconcellos *et al*., 2011). Biosurfactants improve the degradation process by stabilizing the hydrocarbon-water emulsions and by enhancing cell adherence to the oil droplet surface (Berthe-Corti and Fetzner, 2002; Bach *et al*., 2003). The biosurfactants produced by microorganisms are cell-wall associated, or extracellular surface active agents, and the two most commonly discussed examples are those of Liposan and Emulsan (Vasconcellos *et al*., 2011). According to Berthe-Corti and Fetzner (2002) most of the work done on biotensides in terms of their structure and function has been with *Acinetobacter* strains. The most extensively studied biosurfactant produced by *Acinetobacter* spp. is Emulsan (Bach *et al*., 2003). The genes responsible for the biosynthesis and regulation of Emulsan have been shown to exist in a single gene cluster denoted the *wee* regulon, however very little is known about the protein component of this system (Bach *et al*., 2003). Another biotechnological benefit of biosurfactant production is that it can facilitate the growth of other organisms and thus increase the cometabolic effects that take place in alkane degrading microbial communities (Berthe-Corti and Fetzner, 2002).

Acinetobacter spp. are also known to possess specialized adherence strategies for access to the insoluble hydrocarbon substrates (Baldi *et al*., 1999; Bihari *et al*., 2007). Certain species of *Acinetobacter* can make use of proteins that mediate attachment to oil droplets, further enhancing their abilities to degrade such compounds (Baldi *et al.*, 1999; Toolsi, 2008). In *Acinetobacter* sp. strain A3 adhesion occurs via two proteins of 26.5 kDa and 56 kDa (Hanson *et al*., 1994), and via a possible glycoprotein of 65 kDa in *Acinetobacter* sp. strain MJT/F5/199A (Toolsi, 2008). Bihari *et al*. (2007) isolated an *Acinetobacter haemolyticus* strain AR-46 that was capable of degrading alkanes between the C_{12}-C_{35}. The interesting findings from their study were that their isolate possessed a very unusual adherence strategy (via thicker fimbriae) that prevented the cells from being separated from the substrate, even with intensive centrifugation. It has also been suggested that *Acinetobacter* sp. RAG-1, when grown on hexadecane, utilizes its cell surface fimbriae to facilitate the attachment and consequent uptake of hydrophobic substrates such as those of the long chain alkanes (Wentzel *et al*., 2007).

Acinetobacter sp. isolates have been shown to degrade hydrocarbons in the range of C_9 to C_{34} (Wentzel *et al*., 2007) and *Acinetobacter* strain M-1 has been shown to grow on alkanes up to C_{44} (Sakai *et al*., 1994). Previous studies in our laboratory have revealed that *Acinetobacter* sp. V2 had the greatest percentage reduction of engine oil as compared to the other isolates (Mandri and Lin, 2007). Results from other work in our laboratory revealed that the isolates made use of different strategies for the breakdown of the diesel substrate, as was shown using real time PCR; isolate V2 made use of multiple alkane hydroxylases whereas LT1A contained only one (Toolsi, 2008). This is known to be a common occurrence, since the presence of multiple alkane hydroxylases enable hydrocarbon degraders to grow on a broad range of substrates (van Beilen *et al*., 2003). Both isolates are capable of producing biosurfactants (Zhao and Wong, 2009).

1.4 METABOLIC PATHWAYS FOR *n*-ALKANE AND ACETATE DEGRADATION

Bacterial oxidation of *n*-alkanes is a frequent occurrence in both soil and water, in fact it is estimated that several million tons of these alkanes are geochemically recycled every year (Smits *et al*., 2002). It is no surprise then that several enzyme systems for the activation of aliphatic hydrocarbons under aerobic conditions have evolved in both prokaryotes and eukaryotes (van Beilen and Funhoff, 2005; Wentzel *et al.,* 2007). These include the cytochrome P450 enzymes, integral membrane di-iron alkane hydroxylases, soluble di-iron methane monoxygenases and membrane-bound copper-containing methane monoxygenases (van Beilen and Funhoff, 2005). Questions regarding the importance of such enzyme systems in the environment have been raised and it thus for this reason that any information regarding the prevalence and distribution of said enzymes and pathways is of interest (Heiss-Blanquet *et al*., 2005). Alkane hydroxylase genes for example can be used as marker genes to predict the potential of an environment for oil degradation (van Beilen *et al*., 2003). Also, the enzymes involved in alkane degradation are useful in the petroleum industry since they have application in the formation of activated intermediates for the polymer and bulk chemical industries (van Beilen and Funhoff, 2005).

Alkanes are saturated hydrocarbons that can take a linear, cyclic or branched form (Rojo, 2009; Wentzel *et al*., 2007). These non-polar compounds lack functional groups and at 20°C at atmospheric pressure they can be gaseous (C_1 to C_4), liquid (C_5 to C_{16}) or solid (> C_{16}) (Berthe-Corti and Fetzner, 2002). Alkanes are major components of fuels and oils, which means that they play an important role in modern life (Wentzel *et al*., 2007). Metabolism of alkanes poses various challenges for microorganisms, due to their low water solubility, their tendancy to accumulate in cell membranes and the fact that alkanes are inert molecules that require energy for activation in order to facilitate further metabolic steps (van Beilen *et al*., 2003; Rojo, 2009). It has been stated that the hydrophobic nature of the bacterial cell surface plays an important role in degradation. This is because the initial step in the degradation of aliphatic and aromatic hydrocarbons is often mediated by the oxidative reactions that are catalyzed by cell-surface-associated oxygenases (Wentzel *et al.,* 2007). There are two mechanisms used to access these hydrophobic substrates namely: interfacial accession by direct contact of the cell with the hydrocarbon and biosurfactant-mediated accession by cell contact with emulsified hydrocarbons (Wentzel *et al.*, 2007). Hydrocarbons tend to partition into the area between the monolayers of the cytoplasmic membrane and outer membrane of Gram negative organisms due to their lipophillic nature, which can have two effects on the cell. The partitioning of the hydrocarbons in this way increases the bioavailability of the substrate, but it can also be detrimental to the cell due to the toxicity of the substrate (Sikkema *et al*., 1995). The insertion of the hydrocarbons into the membrane alters the membrane structure by changing membrane fluidity, protein conformations and it disrupts the barrier and energy transduction functions of the membrane (Sikkema *et al*., 1995; van Hamme *et al*., 2003). It also affects the activity of membrane bound enzymes (Sikkema *et al*., 1995; van Hamme *et al*., 2003). So microorganisms have to devise strategies to overcome these potentially harmful effects in order to successfully degrade and survive in the presence of the hydrocarbon. Some of these strategies include: the modification of cell membranes, cell walls, S-layer, and active excretion of the hydrocarbon (Sikkema *et al*., 1995).

Many studies carried out on environmental samples have demonstrated the abundance of alkane degraders and have resulted in the identification of new species (van Beilen and Funhoff, 2007). These organisms possess alkane hydroxylases, which are thought to play an important role in the microbial degradation of oil, chlorinated hydrocarbons and many other compounds (van Beilen and Funhoff, 2007). The microbial processing of hydrocarbons follows the general pathways seen in

Figure 1.1 (Das and Chandran, 2011). Cellular intermediates necessary for growth are synthesized using hydrocarbons as a sole source of carbon and energy. The first and most important step in the process is the uptake of the insoluble material, followed by the activation step by oxygenase enzymes requiring molecular oxygen and this is then followed by several other pathways that result in the production of fatty acids for the β-oxidation cycle (peripheral pathways). The acetyl-CoA resulting from these steps then enters the TCA cycle producing cellular intermediates for growth. As seen in Figure 1.1 and later in Figure 1.4. Acetyl-CoA (C2) is condensed onto an oxaloacetate molecule (C4) giving rise to citrate (C6) which is then subsequently modified though oxidation, decarboxylation etc, into cis-aconitate, isocitrate and then a C5 compound α-ketoglutarate. This is then followed by oxidation, phosphorylation and hydration to yield C4 compounds succinyl-CoA, succinate, fumarate, malate and eventually oxaloacetate to continue the cycle.

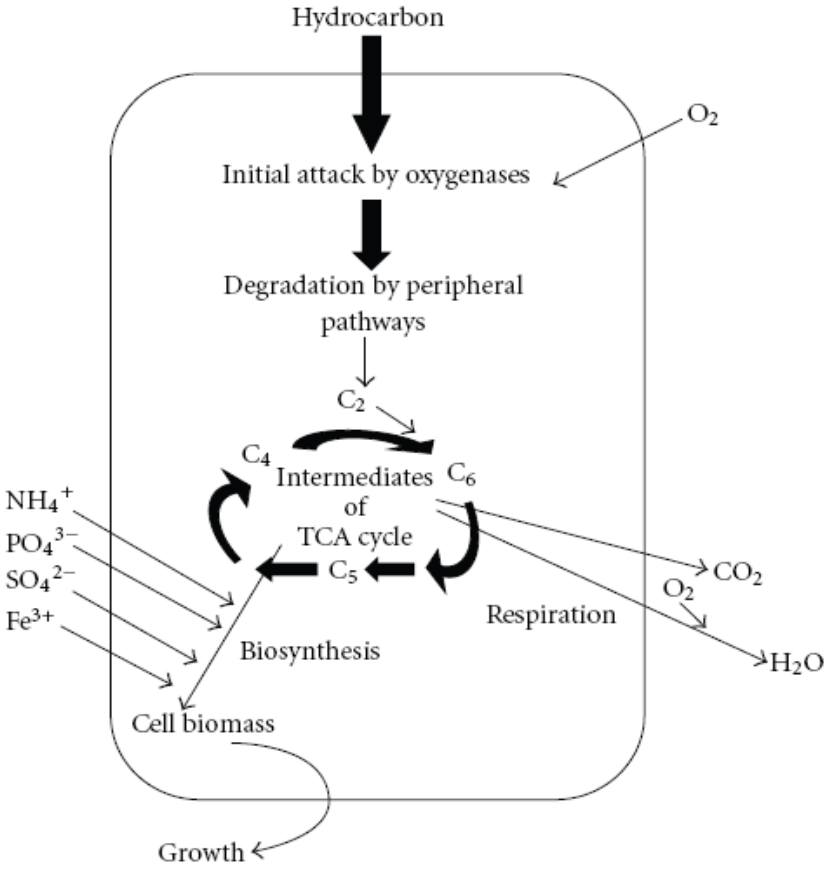

Figure 1.1. Representative diagram illustrating the pathway of hydrocarbon utilization in microbial cells (Das and Chandran 2011). C_2: Acetyl-CoA, C_6: citrate, cis-aconitate, isocitrate C_5: α-ketoglutarate, succinyl-CoA, succinate, fumarate, malate, oxaloacetate.

Alkane-oxidizing bacteria can be divided into three groups namely: the methane-oxidizing bacteria, the bacteria utilizing other gaseous alkanes and those growing on liquid or solid alkanes (Berthe-Corti and Fetzner, 2002). Depending on the chain length of the alkane substrate, different enzyme systems are utilized to incorporate/introduce oxygen into the alkane to facilitate biodegradation (van Beilen and Funhoff, 2007). Table 1.1 gives a good representation of the different enzyme systems that can be employed by different microbial species when degrading hydrocarbons of different chain lengths. It provides a brief overview of what information can be gathered from the literature. In general, oxygenase enzymes introduce oxygen atoms into the hydrocarbon molecules, monooxygenase enzymes introduce one oxygen atom, and dioxygenase introduce two (Peixoto *et al*., 2011). Methane monooxygenases are involved in carbon cycling in the biosphere, and they are involved in the degradation of xenobiotics in the environment, they also catalyze the oxidation of short-chain alkanes (C_1-C_4) such as methane and butane (van Beilen and Funhoff, 2007). In the presence of copper, the aerobic degraders make use of membrane-bound particulate copper containing enzymes known as pMMO (particulate methane monooxygenase), but under copper-limiting conditions they express soluble non-heme di-iron monooxygenases, sMMO (soluble methane monooxygenase) (van Beilen and Funhoff, 2007). In terms of the other short chain alkanes, such as ethane and propane, there are enzymes that have similarities to the sMMO and pMMO for example the butane monooxygenases (BMO) (van Beilen and Funhoff, 2007).

Table 1.1. Enzymes involved in biodegradation of petroleum compounds (Das and Chandran, 2011)

Enzymes	Substrates	Microorganisms
Soluble methane monoxygenases	C1-C8 alkanes, alkenes and cycloalkanes	*Methylococcus, Methylosinus, Methylocystis, Methylomonas, Methylocella*
Particulate methane monoxygenases	C1-C5 (halogenated) alkanes and cycloalkanes	*Methylococcus, Methylocystis, Methylobacter*
AlkB related alkane hydroxylases	C5-C16 alkanes, fatty acids, alkyl benzenes, cycloalkanes	*Pseudomonas, Burkholderia, Rhodococcus, Mycobacterium*
Eukaryotic P450	C10-C16 alkanes, fatty acids	*Candida maltose, Candida tropicalis, Yarrowia lipolytica*
Bacterial P450	C5-C16 alkanes, cycloalkanes	*Acinetobacter, Caulobacter, Mycobacterium*
Dioxygenases	C10-C30 alkanes	*Acinetobacter* sp.

The oxidation of medium or long chain alkanes under aerobic conditions occurs via monoterminal, biterminal or subterminal pathways (Berthe-Corti and Fetzner, 2002). Under these conditions the first oxidation step, required for the activation of these inert molecules, is carried out by oxygenases (such as the rubredoxin dependent hydroxylases or cytochrome P450 enzymes) (Berthe-Corti and Fetzner, 2002; Van Beilen *et al*., 2003). These enzymes introduce oxygen into the alkane substrate. Figure 1.2 provides an overview of the various reactions and enzymes involved in the breakdown of hydrocarbon substrates. The activation of the alkane generally depends on its chain length; usually this occurs via the monoterminal oxidation pathway to form a primary alcohol. This alcohol is further oxidized by alcohol and aldehyde dehydrogenases to produce fatty acids for the β-oxidation cycle (Geiβdorfer *et al*., 1999; van Beilen *et al*., 2003; van Hamme *et al*., 2003; Wentzel *et al*., 2007). Subterminal oxidation has also been suggested for the oxidation of long and short chain alkanes by organisms such as *Penicillium*, *Bacillus*, *Pseudomonas* and *Rhodococcus* sp.. Here the alkane is oxidized by a monooxygenase to the corresponding secondary alcohol followed by a ketone which is then oxidized by a Baeyer-Villiger monooxygenase to an ester. The ester is then subsequently hydrolyzed by an esterase to an alcohol and a fatty acid (Whyte *et al.*, 1998; van Beilen *et al*., 2003; Rojo, 2009).

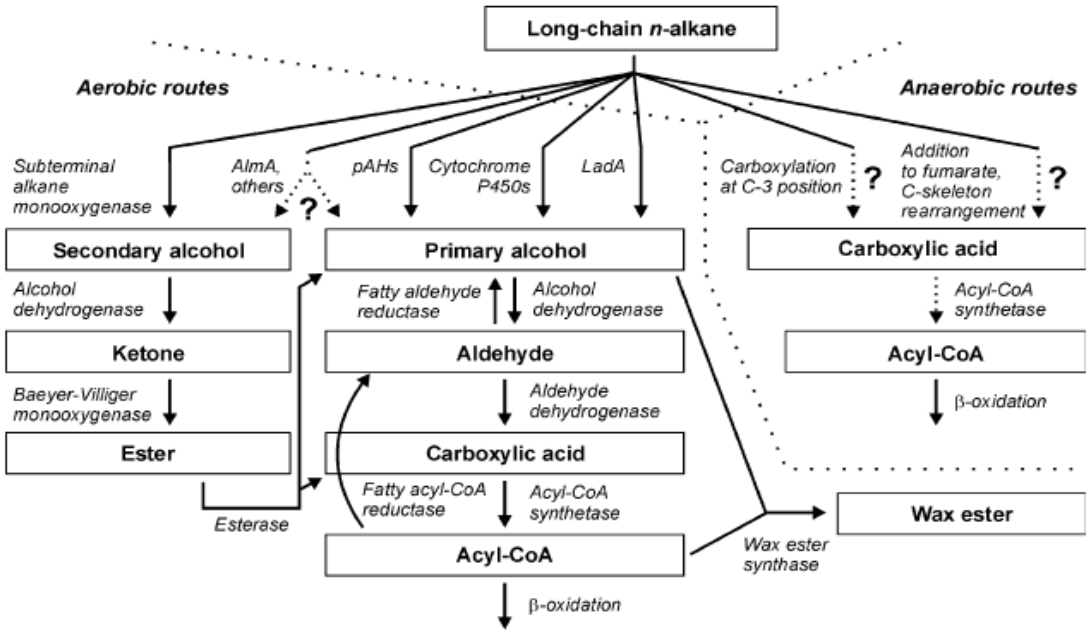

Figure 1.2. Aerobic and Anaerobic *n*-alkane degradation pathways (Wentzel *et al*., 2007). The figure provides an overview of the reactions and enzymes involved in hydrocarbon degradation. *AlmA*: putative monooxygenase, *pAHs*: particulate alkane hydroxylase, *LadA*: long chain alkane hydroxylase

The genes and enzyme systems involved in the utilization of long chain *n*-alkanes have been well characterized and have resulted in a good (but not complete) understanding of their metabolism (Wentzel *et al*., 2007; Toolsi, 2008). Long-chain liquid alkanes can be utilized by both Gram negative and Gram positive bacteria. The alkane hydroxylase system of the Gram negative *Pseudomonas oleovorans* has been well characterized (Hamamura *et al*., 2001) and it consists of an integral membrane monooxygenase, 1 to 2 rubredoxins and a rubredoxin reductase (Van Beilen *et al*., 2003). The alkane hydroxylase complex of *P. oleovorans* is encoded on the OCT plasmid, and comprises three polypeptides namely: AlkB encoding a hydroxylase, AlkG encoding a rubredoxin and AlkT encoding a rubredoxin reductase (Hamamura *et al*., 2001). The oxygenase component AlkB is an integral membrane protein that not only carries out alkane hydroxylation, but also catalyzes the oxidation of substituted cyclic alkanes, the hydroxylation of alkyl substituents and various other reactions (Berthe-Corti and Fetzner, 2002). The *alk* pathway has been thoroughly reviewed by van Hamme *et al*. (2003): The *alkBFGHJKL* operon encodes those genes responsible for converting the alkanes into acetyl-CoA. The *alkST* genes encode rubredoxin reductase (AlkT) and positive regulator (AlkS) for the *alkBFGHJKL* operon and *alkST* genes. The two operons are separated by a 9.7 kb of DNA. Within this DNA segment there is the gene *alkN* which encodes for a methylaccepting transducer protein. This protein may be involved in alkane chemotaxis. The *alkL* genes' function remains unknown but is suspected to be involved in transport/uptake. The AlkL protein product is located in the outer membrane; the AlkB (a non-heme iron integral membrane protein, alkane hydroxylase, which carries out the hydroxylation reaction), AlkN and AlkJ (alcohol dehydrogenase) protein products are located within the inner membrane; AlkF and AlkG (rubredoxins - the simplest of the iron-sulphur containing redox active proteins/ferredoxins) (van Beilen *et al*., 2003), AlkH (aldehyde dehydrogenase), AlkK (acyl-CoA synthetase) and AlkT are located in the cytoplasm. The rubredoxins transfer electrons from the NADH-dependent flavoprotein rubredoxin reductase to AlkB (Smits *et al*., 2002). AlkB then transfers one oxygen atom from O_2 to one of the terminal methyl groups of the alkane molecule rendering an alcohol, while the other oxygen atom is reduced to H_2O by the electrons transferred by rubredoxin (Rojo, 2005).

Two, less common, enzymatic pathways have been suggested for the initial oxidation of short chain alkanes between C_5-C_{11} for bacteria and these involve the cytochrome P450 monooxygenase and a dioxygenase (Heiss-Blanquet *et al*., 2005; Rojo, 2009). The cytochrome P450 enzymes are more

commonly associated with yeasts and fungi and limited evidence has shown them to be found in all bacteria (van Beilen *et al*., 2003). They belong to a superfamily of heme proteins which catalyze monooxygenation of a wide variety of organic molecules (Maier *et al*., 2001; Sabirova *et al*., 2006; Rojo, 2009). The P450 enzymes require an electron transport system involving a ferredoxin (iron-sulphur protein) and a ferredoxin reductase (FAD containing protein) that transfer electrons from NAD(P)H to the cytochrome (van Beilen *et al*., 2003; Rojo, 2009). Van Beilen *et al*. (2003) noted that reports on bacterial cytochrome P450 enzymes involved in alkane degradation are scarce; *Acinetobacter calcoaceticus* EB104 was reported to possess a P450 enzyme involved in alkane degradation that showed very little similarity to other P450 enzymes, it was assigned to its own class, bacterial class I P450s family CYP153 (Maier *et al*., 2001). The P450 isolated from *Acinetobacter calcoaceticus* EB104 was found to be a soluble protein with a high molecular weight of between 52-53.6 kDa.

The dioxygenase enzymes are said to be involved in the „Finnerty pathway' which proposes that the oxidation of long chain *n*-alkanes to the corresponding alcohol and fatty acid proceeds via the formation of an alkane hydroperoxide, peroxy acid and an aldehyde without the production of an alcohol intermediate (Maeng *et al*., 1996; Rojo, 2009). It is accepted to be a non-conventional pathway for alkane oxidation (Maeng *et al*., 1996) and there is some evidence in the literature to support this theory (Berthe-Corti and Fetzner, 2002; Van Hamme *et al*., 2003). In order for one to conclude that the pathway is present in an organism, the following requirements must be met: i) the bacterium must be dependent on molecular oxygen for oxidation of *n*-alkanes, ii) peroxy acid oxidation should be detected in a cell extract system, iii) no alkane hydroxylase activity should be detected and iv) enzymes involved in long-chain fatty alcohol oxidation should have a lower level of activity than several types of aldehyde dehydrogenases (Maeng *et al*., 1996). In 1996, Sakai *et al*. validated the existence of the Finnerty pathway in the *Acinetobacter* sp. M-1 isolate growing on long chain alkanes C_{16}, C_{20} and C_{30}. It has been demonstrated by Sakai *et al*. that *Acinetobacter* strain M-1 makes use of three alkane dioxygenases, which are assumed to be involved in the oxidation of those alkanes that are slightly dissolved into the cytosol or inclusion bodies in the cell (Geiβdorfer *et al*., 1999; Tani *et al*., 2001). In *Acinetobacter* strain M1, the dioxygenases require molecular oxygen in order to catalyze the oxidation of *n*-alkanes (C_{10} to C_{30}) and alkenes (C_{12} to

C_{20}) without the production of oxygen radicals. The dioxygenase enzymes do not require rubredoxins or NAD(P)H and are thought to contain Cu^{2+} (Van Hamme *et al*., 2003).

Different *Acinetobacter* strains have been shown to employ alternative strategies for the breakdown of alkane substrates, for example multicomponent monooxygenase, cytochrome P450 and dioxygenase activity in *Acinetobacter* strain M1 (Berthe-Corti and Fetzner, 2002). It is evident that different long-chain alkane oxidation pathways exist in strains of *Acinetobacter*. Alkane dioxygenases degrade alkanes ranging from C_{13} to C_{44} in *Acinetobacter* sp. strain M-1. Other strains utilize the P-450 monoxygenase system, and in *Acinetobacter* sp. strain ADP1 an alkane hydroxylase homologous to that found in *P. oleovorans*, is used (Hamamura *et al*., 2001). The genetics of the alkane monooxygenase system in *Acinetobacter calcoaceticus* ADP1 has been studied and it was revealed that this organism possesses a monooxygenase system that is similar to that of *P. oleovorans* in that it too contains a hydroxylase (*alk*M), rubredoxin (*rub*A) and rubredoxin reductase (*rub*B), however the organization of the genes encoding these proteins, differs significantly from that of *P. oleovorans* (Tani *et al*., 2001; Berthe-Corti and Fetzner, 2002). Evidence from Tani *et al*., (2001) showed that *Acinetobacter* strain M1 was found to contain genes that are homologous to those found in *Acinetobacter calcoaceticus* strain ADP1, namely the genes encoding the alkane hydroxylase. However an observation by these authors was that there were two genes encoding the alkane hydroxylase and these genes were differentially induced depending on the length of the hydrocarbon chain (Tani *et al*., 2001). It should also be noted that it is not atypical to observe multiple alkane hydroxylases in a single bacterial strain, and several possible explanations for such occurrences have been provided by van Beilen and Funhoff (2005). These include:

1. The fact that the presence of more than one alkane hydroxylase allows microorganisms to make use of more than one alkane substrate;
2. Different alkane hydroxylases might be active at certain phases of growth;
3. Some enzymes have different affinity constants for different alkanes;
4. Some enzymes preferentially oxidize certain alkanes and,
5. It has also been suggested that some alkane hydroxylase genes may be pseudogenes.

As seen in Figure 1.1, alkanes are eventually metabolized by bacteria into acetyl-CoA that enters the TCA cycle. The metabolism of acetate undergoes a similar pathway to that of hydrocarbons. It is metabolized into acetyl-CoA via the action of acetate kinase and phosphate acetyltransferase as demonstrated in *Corynebacterium glutamicum* or through the action of acetyl-CoA synthetase as seen in *Escherichia coli* (Camarena *et al*., 2010). According to Abbott *et al*. (1973), there are 2 mechanisms for the formation of acetyl-CoA from acetate and both require Mg^{2+}; the one utilizes only one enzyme, namely acetyl-CoA synthetase, and the other (only found in bacteria) uses two enzymes as seen in Figure 1.3. Many bacterial species possess both (Pirog *et al*., 2002). Once acetate is converted into acetyl-CoA it enters the TCA cycle where in *Acinetobacter* spp. the glyoxylate bypass reactions take place as illustrated in Figure 1.4 (Cozzone, 1998; Camarena *et al*., 2010). The purpose of the glyoxylate bypass is to minimize the amount of carbon lost as carbon dioxide in the TCA cycle, thus conserving carbon for cellular intermediates such as amino acids (Cozzone, 1998). In the glyoxlate bypass, highlighted by the darker region in Figure 1.4, the enzymes isocitrate lyase and malate synthase are upregulated. They facilitate the conversion of citrate to glyoxylate and with the incorporation of another acetyl-coa molecule, glyoxylate to malate. The release of hydrogen results in the formation of oxaloacetate, which gives rise to cellular intermediates such as amino acids, coenzymes and nucleotides. Upon degradation of fatty acids (or hydrocarbons), one molecule of acetyl- CoA is generated from each two-carbon segment of a fatty-acid (or hydrocarbon) molecule. This reaction results in the production of one equivalent each of $FADH_2$ and NADH, which is used in ATP synthesis. In acetate degradation, this ATP is not formed (Cozzone, 1998). Ultimately, hydrocarbons and acetate share the same eventual fate once they are broken into acetyl-CoA molecules as shown in Figure 1.4.

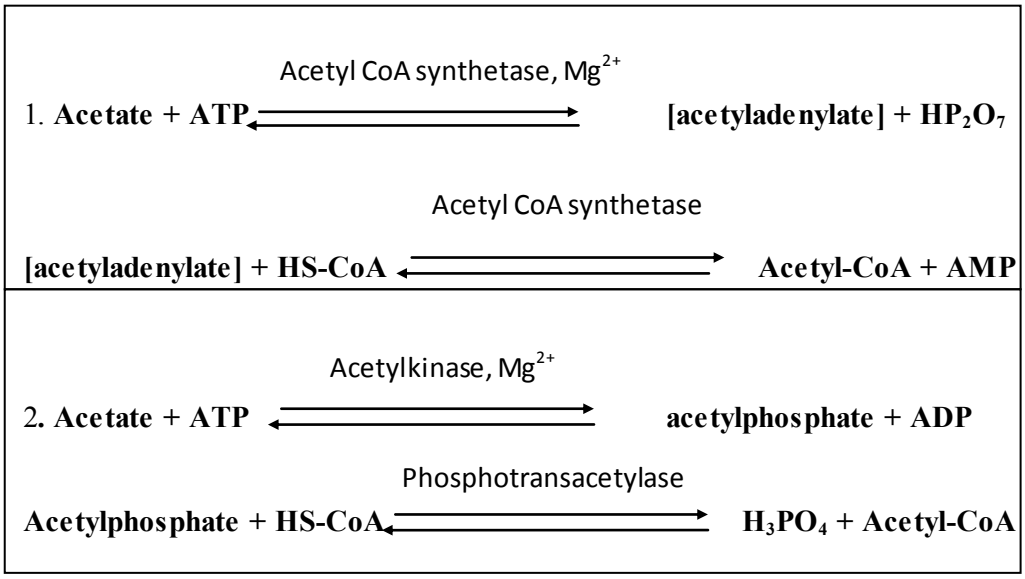

Figure 1.3. Metabolic reactions involving the conversion of acetate to acetyl-CoA (Abbott *et al.*, 1973)

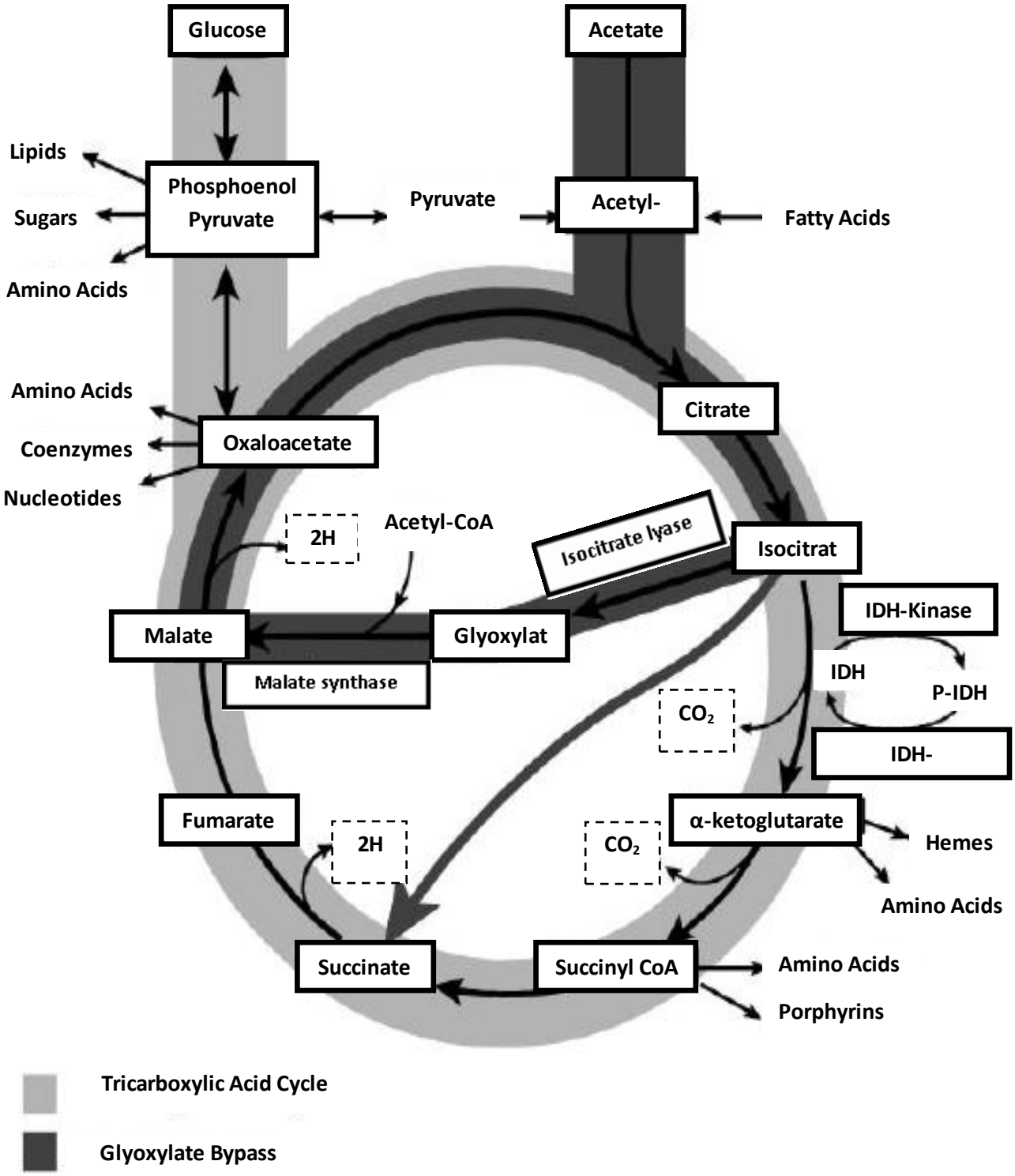

Figure 1.4. TCA cycle showing the glyoxylate bypass whereby acetate and fatty acids are metabolized to produce cellular intermediates for microbial growth (Cozzone, 1998)

It is important to remember that the distribution of these enzyme systems is recognized to be ubiquitous in the environment (van Beilen and Funhoff, 2005). In bioremediation studies where consortia of bacteria are added into contaminated areas, it is essential to investigate the indigenous microbial community and their contributions to the degradation process in order to control the release of contaminants at a polluted site (Heiss-Blanquet *et al*., 2005). Since in natural habitats microorganisms live in communities whose metabolic potentials may involve cooperation and co-metabolism of certain substrates (Berthe-Corti and Fetzner, 2002), it is imperative to also consider the community as a whole. Molecular approaches are used since they are culture-independent and specific for biodegradation activity (Heiss-Blanquet *et al*., 2005). But at the same time, the classical approach of using pure cultures to investigate metabolic routes allows for the genetic and biochemical characterization of pathways and enzyme systems involved in alkane degradation (Berthe-Corti and Fetzner, 2002). This approach is an essential step in characterizing and understanding the degradation process fully. The disadvantage with the use of culture-independent molecular approaches for the analysis of biodegradation activity is that the catabolic pathways and the corresponding genes have to be known (Heiss-Blanquet *et al*., 2005). Although many pathways have been proposed, alternative pathways may also be possible and are as yet uncharacterized (Berth-Corti and Fetzner, 2002). Hence comparative proteomic analysis is a useful initial step for the elucidation of degradation pathways (Kim *et al*., 2003).

1.5 PROTEOMIC STUDIES FOR THE ANALYSIS OF BACTERIAL BIODEGRADATION PATHWAYS

Proteome analysis has become a powerful tool for the investigation of global changes in prokaryotic gene expression that allows for high throughput screening of induced proteins as a function of environmental changes (Pessione *et al*., 2003; Kim *et al*., 2003). The term ‘’proteomics’’ encompasses a broad range of topics including: the identification, and quantification of proteins in cells, tissues and biological fluids; analysis of changes in protein expression under different conditions; characterization of post-translational modifications; and investigations into protein-protein interactions (Beranova-Giorgianni, 2003). The data generated through proteomic investigations is invaluable to the research area of microbial biodegradation because it incorporates a comparative analysis of biodegradation enzymes, it allows for the separation and identification of

various post-translationally modified proteins, and allows for the analysis of open reading frames that are induced under certain conditions (Kim *et al*., 2007). Important information on the life cycle, regulation and post-translational modification of proteins can also be provided by proteomic investigations (Kim *et al*., 2007). Proteins are the key structural and functional molecules within the cell; hence one requires the characterization of proteomes on the molecular level in order to attain a complete understanding of biological systems (Beranova-Giorgianni, 2003).

An advantage to proteomic studies is that a larger number of proteins involved in a particular pathway can be identified at one time and the data generated, allows for a better understanding of bacterial metabolism as well as the overall physiological responses and regulatory processes involved in the utilization of various substrates (Kim *et al*., 2009). However, there are several disadvantages to the use of proteomic technologies that make use of 2-Dimensional Electrophoresis (2-DE); a major disadvantage is that it is not possible to view and analyze the entire proteome and this can be attributed to a couple of factors:

i) Low-abundance proteins are difficult to detect, so too are membrane proteins (Lilley *et al*., 2001; Pessione *et al*., 2003) and proteins with extreme molecular weights or isoelectric points (Görg *et al*., 2000; Lilley *et al*., 2001; Kim *et al*., 2009).

ii) The staining technique employed as it determines which proteins can be viewed in a sample. A sensitive stain can detect low abundance proteins and is the method of choice for analytical gels. The conventional stain Coomassie blue only detects the most abundant proteins (Görg, 2000).

iii) The separation of membrane proteins posses various challenges due to their poor solubility in extraction solutions, their low abundance (Beranova-Giorgianni, 2003) and the conditions required for 2-DE separation based on their hydrophobic nature (Pessione *et al*., 2003; Hecker *et al*., 2008).

The fact that membrane proteins are difficult to analyze with 2DE technologies means that a great deal of very important proteins are over looked. Many of these proteins are involved in alkane degradation; these include the terminal hydroxylases, enzymes involved in fatty acid oxidation and enzymes responsible for transport of nutrients across the membrane as well as cell-surface proteins

and receptors (Sabirova *et al*., 2006; Singh and Nagaraj, 2006). Bearing these disadvantages in mind, most of the proteomic data from literature has involved both 2-DE and MALDI-MS technologies (Brötz-Oesterhelt *et al*., 2005; Kim *et al*., 2009).

Conventionally proteomic analyses comprise two steps: protein separation by two- dimensional electrophoresis or chromatographic techniques followed by protein identification using modern bioinformatics tools and mass spectrometry (Garbis *et al*., 2005; Fulekar and Sharma, 2008). Figure 1.5 illustrates the basic outline of the workflow involved in a proteomic investigation. An essential starting point in planning such a study is the selection of a suitable protein identification strategy, and this is dependent on whether or not the genome of the target bacterium has been sequenced or not (Kim *et al*., 2007; de Souza and Wiker, 2009). The genome and proteome of an organism are tightly connected; without the genome sequence, one cannot identify the proteins within the proteome via Mass spectrometry (MS) technologies (Hecker *et al*., 2008). A 2-DE/MS approach to the analysis of bacterial biodegradative pathways is a suitable tool because the enzymes involved in these pathways are said to be abundant under specific culture conditions (Kim *et al*., 2007). For those organisms whose genomes are not known, the availability of technologies such as Electrospray ionization quadrupole-time of flight mass spectrometry (ESI-Q-TOF MS) for de novo sequencing of proteins allow for cheaper alternatives with improved sensitivity, and speed as opposed to the older technologies of N-terminal or Edman chemistry (Kim *et al*., 2004).

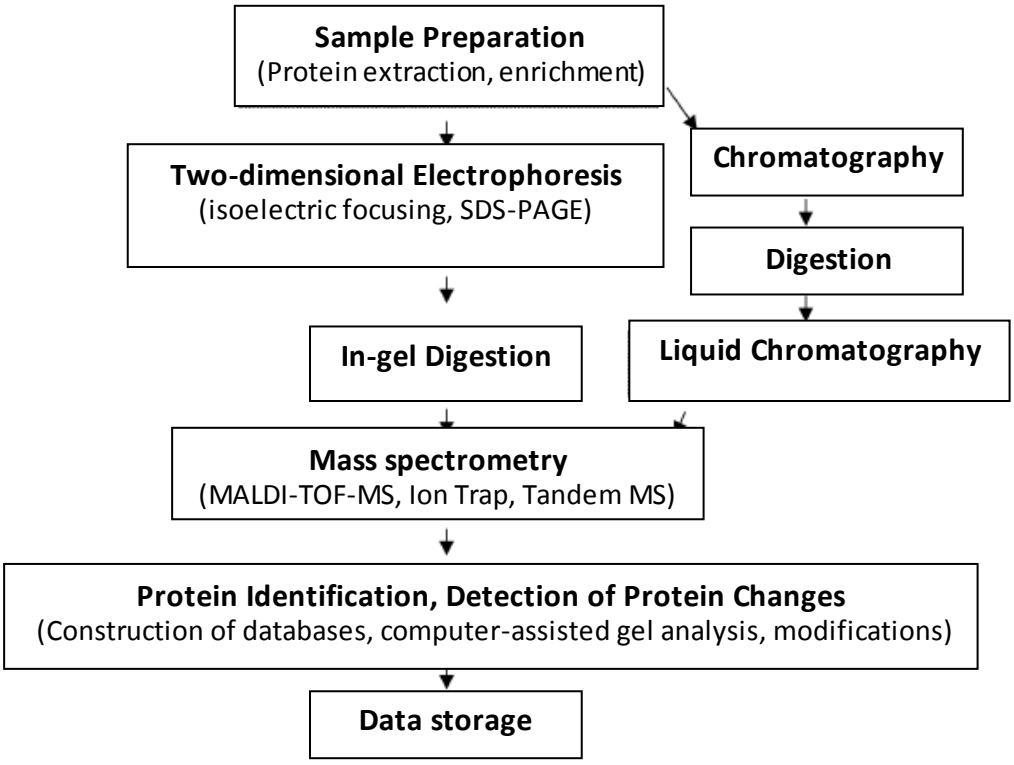

Figure 1.5. Basic workflow involved in proteomic investigations. Both the 2-dimensional SDS-PAGE and Liquid chromatography separation methods are illustrated, both requiring mass spectrometry for the second phase of protein identification following separation by the abovementioned techniques. (Garbis *et al.*, 2005)

The induction of proteins involved in biodegradative pathways is achieved through the growth of microbial cells on a variety of substrates available in an environment or culture medium (Pessione *et al.*, 2003; Kim *et al.*, 2009). Various extraction techniques are available in the literaure to recover desired proteins from the host cell; these may involve physical, chemical or enzymatic means to disintegrate the cell and commercial preparations for such tasks are available for almost any cell type (Ganesh and Lin, 2011). Once isolated, the proteins are separated by electrophoresis on a 2-Dimensional polyacrylamide gel (2D-PAGE), a technique that is well established to allow for qualitative and quantitative comparisons of different protein expression profiles (Choi *et al.*, 2000; Fulekar and Sharma, 2008; Kim *et al.*, 2009). Over half a century ago, it was recognized that the separation of proteins in a single dimension was inadequate for the resolution of complex

protein mixtures; it was acknowledged then that a combination of two electrophoretic processes would allow for a better resolution of the protein mix (Issaq and Veenstra, 2008). The first dimension separation of the protein samples is through isoelectric focusing (IEF) which is usually performed on immobilized pH gradient strips (IPG strips). This separation is based entirely on the isoelectric points of the proteins (Issaq and Veenstra, 2008). This is then followed by the separation of the proteins based on molecular weight in the presence of sodium dodecyl sulphate (SDS) in the second dimension (Issaq and Veenstra, 2008). Once electrophoresis is completed, the gels are stained with a suitable, Mass Spectrometry compatible stain and the image is analysed. The resulting protein spots allow one to characterize the proteins in terms of their net charges and molecular weights. Various forms of proteins, including isoforms, glycosylated or phosphorylated forms, can be resolved based on the altered isoelectric points or molecular weights thus facilitating the retrieval of information regarding post-translational modification of such proteins (Kim *et al*., 2007).

A major driving factor in the progress made into proteomics, has been improvements in mass spectrometry, bioinformatics and 2D electrophoresis technologies (Beranova-Giorgianni, 2003). These technological advances have aimed at improving separation, increasing sensitivity and resolution and dealt with proteins that possessed unfavourable properties for 2-DE and reducing costs associated with this often expensive technique (Brötz-Oesterhelt *et al*., 2005). One of the most recent technological advances has been the major competitor to 2–DE, liquid chromatography coupled to mass spectrometry (LC-MS). This technology circumvents some of the limitations experienced with conventional 2-DE, and is said to be capable of identifying up to 10 times more proteins in a single experiment (Brötz-Oesterhelt *et al*., 2005; de Souza and Wiker, 2009). LC-MS is also more amenable to the identification of membrane proteins (de Souza and Wiker, 2009). But the reasons that 2-DE/MS is still the most widely used approach is because the major advantages it possesses over LC-MS, is the fact that it allows for the simultaneous visualization of the protein spots, it allows for the quantification of their levels, detection of post-translational modifications, and it is robust (Garbis *et al.*, 2005; Issaq and Veenstra, 2008). All in all however, LC-MS and any other technologies boasting advantages over 2-DE should be used to complement it as it is likely that it is a technology that will be around for many years to come (Lilley *et al*., 2001).

The staining technologies for 2-DE have also undergone a vast improvement with a wider range available to the end user, each with their own advantages and disadvantages (Westermeier and Marouga, 2005). The selection of the most appropriate protein detection method is essential, since the quantitative changes in expression levels need to be accurately measured. Sadly, the ideal protein detection method that meets all the requirements (fast and easy to perform, non-toxic, environmentally friendly, wide dynamic range, mass-spectrometry compatible and affordable) is currently not available and the user has to weigh up the advantages and disadvantages for each (Westermeier and Marouga, 2005). Another major hurdle is that the relationship between the actual protein quantity in the sample, and the measured spot intensity on the analysis software, is influenced by many factors (Berth *et al*., 2007):

i) Loss of sample during entry into the IEF gel,
ii) Efficiency of transfer from first to second dimension,
iii) Protein loss during staining,
iv) Staining efficiency,
v) A proteins staining curve over time,
vi) Staining curve over concentration, and
vii) Dye bleaching.

Highly sensitive detection of protein spots can be achieved using silver stain or other commercially available fluorescent stains, both of which can be compatible with mass spectrometry (Görg *et al*., 2000). Silver stain has the advantage in that the higher sensitivities allow for the detection and analysis of trace amounts of proteins in a sample with a detection limit of 0.1 ng per spot; however the corresponding disadvantages with this stain include: poor reproducibility, limited dynamic range, poor staining of some proteins, and the silver staining procedure itself is also time consuming (Görg *et al*., 2000; Lilley *et al*., 2001). Fluorescent dyes (eg. Sypro Ruby) are equivalent in sensitivity to silver stain and have linear dynamic ranges of up to three orders of magnitude and pose no challenges to the subsequent sequencing technologies, they are also usually environmentally friendly, but tend to be expensive and require expensive equipment for visualizing the gels (Lilley *et al*., 2001; Brötz-Oesterhelt *et al*., 2005; Westermeier and Marouga, 2005). Conventionally Coomassie staining methods are employed due to the quantitative binding of the dye to proteins, lower costs, and good reproducibility, and the dye itself is easily removed from the

sample for mass spectrometry; however the corresponding disadvantages include longer staining times, lower sensitivity and narrow dynamic range (Westermeier and Marouga, 2005).

A proteomics approach to analyzing the physiological changes that organism undergoes during bioremediation studies provides valuable information into the expression and regulation of genes involved in bioremediation (Singh and Nagaraj, 2006). Several *Acinetobacter* sp. proteomes have been analyzed using a variety of proteomic technologies. Most often the soluble fraction of the cellular proteins is investigated, due to the complexities encountered with membrane proteins, (Pessione *et al*., 2003). However, an example of a membrane proteome study is that by Pessione *et al*. (2003). The authors investigated the induction of membrane proteins in *Acinetobacter radioresistens* S13 when exposed to aromatic substrates phenol and benzoate using 2-DE/MS. The proteins that were induced exclusively by the substrate, include:

i) Na^+/H^+ antiporter: whose function is likely to be regulation of intracellular pH,
ii) ABC type sugar transport system, involved in capsular polysaccharide translocation.

They also identified other proteins that were detected in acetate-grown but over-expressed in aromatic-grown cells. These include:

i) An outer membrane protein similar to an OmpA-like protein, described in the literature as "alasan",
ii) A trimeric porin of the PhoE family involved in facilitating the transport of anions;
iii) Two glycosyl transferases probably involved in capsules and/or lipopolysaccharide biosynthesis.

The same organism was utilized in another study by Mazzoli *et al*. (2010) who investigated those proteins, that are induced by aromatic compounds and which possess high isoelectric points (p*I* 6-11) using 2-DE/MS. Recalling earlier, that another of the major challenges in 2-DE investigations is that proteins with extreme molecular isoelectric points are often not seen in the proteome; the intention of these authors was to complete or complement the growing metabolic picture of this versatile organism. Some of the proteins they identified include: periplasmic proteases, chaperones,

enzymes catalyzing peptydoglycan biogenesis, proteins involved in outer membrane integrity, cell surface properties and cellular redox homeostasis. The authors also pointed out that the previous proteomic investigation focused on the acidic proteins in the p*I* range 4-7. Studies such as these that focus and compliment others with regards to individual microorganisms metabolism, are of great advantage to bioremediation studies as they help to complete the picture of how an organism utilizes and copes with stress associated with the use of various substrates (Kim *et al*., 2003).

Acinetobacter baumannii is another organism that has undergone proteomic investigations. In 2006, Marti *et al*. investigated the membrane proteome of this nosocomial pathogen using 2-DE/MS. Their study served as a platform for other studies into antimicrobial resistance demonstrating how proteomics can be used to determine new targets for antimicrobial agents, as the technology allows for the characterization of gene products in response to changing environmental and biological conditions (Marti *et al*., 2006). However, a more relevant study to the area of bioremediation using this organism was conducted by Soares *et al*. (2009). The authors looked at the cytoplasmic proteome of this organism in the aim of confirming results obtained via genetic analyses, that this organism possesses a versatile metabolism. The study investigated both cytoplasmic and membrane protein fractions from the cells and demonstrated the diverse nature of the *A. baumannii* proteome; Soares *et al*. (2009) divided this proteome into 16 functional groups. Their results also revealed that the most abundant membrane proteins were those proteins involved in the transport of different compounds (from amino acids to fatty acids). This contributes greatly to the understanding of the persistence of this organism in a wide range of environments, including hospital settings, since it reinforces the concept that *A. baumannii*, like other isolates from this genus, have an adaptable metabolism that is versatile enough to utilize the widest range of carbon sources (Soares *et al*., 2009).

In other bioremediation studies Kim *et al*. (2002) investigated aniline degradation using *Acinetobacter lwoffii* K24, and found that 20 proteins were aniline-induced, including: proteins corresponding to the *β*-ketoadipate pathway genes, malate dehydrogenase, putative hydrolase, ABC transporter, a subunit of amino group transfer and HHDD isomerase. In the case of organisms whose genomes have not been sequenced other proteomic technologies are required in order to identify their proteins of interest. The proteins were identified using N-terminal sequencing

followed by BLAST analysis. Kim *et al*. (2004) investigated the use of ESI-Q-TOF mass spectrometry for the de novo sequencing of the spots induced during growth of *Acinetobacter lwoffii* k24 on aniline as a sole source of carbon. Their study revealed that the use of ESI-Q-TOF MS improved the accuracy of protein identification and sequencing coverage from 2-25%. They concluded that this technology was a suitable tool for proteomic investigations into understanding bacterial physiology due to its high-throughput, reduced costs, improved sensitivity and speed as compared to the N-terminal sequencing technologies that were "rate-limiting for rapid analyses". Proteomic studies are essential to our understanding of microbial biodegradation, and the use of 2-DE technologies coupled to mass spectrometry, is a technology that is just as versatile as the organisms we wish to exploit to cleanup man-made disasters.

1.6 SCOPE OF THE PRESENT STUDY

In order to devise the most effective bioremediation strategy, it is imperative to intensively, and extensively characterize the catabolic genes, proteins and metabolites of microorganisms associated with the degradation of pollutants (Kim *et al*., 2007). Detailed characterization of bacterial biodegradation pathways at the genetic level has been achieved; however, there is a lack of information at the proteomic level (Kim *et al*., 2007). Catabolic pathways for many pollutants are complicated and the complexity of the enzymes involved means that the study of such pathways is difficult. Proteomics provides a suitable platform to facilitate the study of the relevant pathways involved in the breakdown of hydrocarbons. *Acinetobacter calcoaceticus* isolates LT1A and V2 were isolated and characterized in previous studies (Singh and Lin, 2008; Mandri and Lin, 2007) and their optimal growth requirements were established. These isolates were found to be effective hydrocarbon degraders. The genetic aspect of hydrocarbon degradation by these isolates has been investigated (Toolsi, 2008) and it was found that the isolates demonstrated interesting patterns of hydrocarbon utilization, possibly making use of alternative alkane hydroxylase systems. The purpose of this investigation therefore is to look at the protein expression patterns of these two isolates and attempt to elucidate mechanisms employed by these organisms in the breakdown of hydrocarbon substrates.

1.7 HYPOTHESIS

Acinetobacter sp. isolates V2 and LT1A make use of different strategies for the breakdown of hydrocarbon substrates.

1.8 OBJECTIVES

To investigate the hydrocarbon degrading ability of *Acinetobacter* sp. isolates V2 and LT1A using medium chain (C_{14}) hydrocarbon substrates

To investigate the hydrocarbon degrading ability of *Acinetobacter* sp. isolates V2 and LT1A using long chain (C_{28}) hydrocarbon substrates

To compare the hydrocarbon degrading abilities and corresponding protein expression patterns during growth on these hydrocarbon substrates for both isolates

1.9 AIMS

To investigate the hydrocarbon degradation potential of each isolate using medium and long chain hydrocarbons as a substrate

To analyze the protein expression patterns induced by growth on the hydrocarbon substrates for the two isolates using denaturing 1D SDS-PAGE and 2D-PAGE

To obtain sequences of proteins of interest using MALDI-TOF MS

To identify protein sequences by Mascot analysis

To compare the degradation abilities, in relation to protein expression patterns, of the two isolates

1.10 KEY QUESTIONS

Do the isolates utilize similar/different strategies for the breakdown of the hydrocarbon substrate?

Is there any difference between the utilization of medium versus long chain hydrocarbons between the two isolates?

CHAPTER TWO

PROTEIN EXPRESSIONS AND HYDROCARBON DEGRADATION ABILITIES OF *ACINETOBACTER* SP. V2 AND LT1A DURING GROWTH IN THE MEDIUM-CHAIN ALKANE, TETRADECANE (C_{14}) AS A CARBON SOURCE

2.1 INTRODUCTION

Acinetobacter as a genus have been described as being nutritionally versatile organisms with a range of substrates that can be used as sole carbon and energy sources matching that of the Pseudomonads (Abdel-El-Haleem, 2003; Barbe *et al*., 2004; Doughari *et al*., 2011). It has been stated that the lack of many genes involved in the utilization of carbohydrates by *Acinetobacter* sp. ADP1 implies that the genus has a very simplified sugar metabolism, confirming the results obtained from biochemical studies on the genus many years ago (Juni, 1978; Barbe *et al*., 2004). *Acinetobacter* spp. have adapted their lifestyles so as to improve their survival chances in even the harshest of environments, including hydrocarbon contaminated sites. Their cell surface polysaccharides (involved in surface attachment and colonization) are released into their environment whereby they form a complex with proteins, promoting the assimilation and uptake of hydrocarbons (Barbe *et al*., 2004; Kang and Park 2010). *Acinetobacter* spp. are perfectly suited to hydrocarbon degradation.

Acinetobacter sp. have numerous applications in the treatment of a range of hazardous wastes and the production of bio-products of economic importance (Abdel-El-Haleem, 2003). Of relevance to this study is that some *Acinetobacter* sp. have been found to be capable of utilizing a wide range of *n*-alkanes (C_{10}-C_{40}) as a sole source of carbon (Throne-Holst *et al*., 2007). The bacterial utilization of *n*-alkanes favours the use of shorter chains (greater than C_9) over the longer chain alkanes as they require less energy to process due to their increased solubility and accessibility to catabolic enzymes (Sugiura *et al*., 1997; Plohl *et al*., 2002; Hamamura *et al*., 2006; Nyssonen, 2009). However it is also accepted that the bioavailability and toxicity of *n*-alkanes depends on their chain length, since the shorter chains can act as solvents for cellular membranes and the longer chains contribute to the formation of oil films/slicks thus preventing the diffusion of gases and nutrients in the ecosystem (Plohl *et al*., 2002; Kloos *et al*., 2006). The way in which *Acinetobacter* sp. utilize these hydrocarbons shows the versatility of these organisms; there are multiple variations in the choice of enzymes or metabolic systems used amongst the genus (Ratajczak *et al*., 1998a). *Acinetobacter* sp. M-1, was shown to differentially induce two different alkane hydroxylase genes in response to the chain length of the hydrocarbon (Tani *et al*., 2001). The enzyme systems utilized for medium chain alkanes in some *Acinetobacter* sp. have been shown to involve the bacterial P450

oyxgenases (C_5-C_{16}), dioxygenase systems (C_{10}-C_{30}) or in some cases the alkane hydroxylase systems (C_5-C_{16}) (Das and Chandran, 2011).

An early investigation into *n*-alkane utilization by *Acinetobacter* sp. includes the study by Hanson and Desai (1996). The authors attempted a protoplast fusion between *Acinetobacter* sp. A3 and *Pseudomonas putida* DP99 in order to take advantage of the tetradecane-degrading ability (*Acinetobacter* sp. A3) and naphthalene degradation ability (*P. Putida* DP99) of these individual isolates. They were able to combine these metabolic characteristics and create one hybrid organism that possessed a degradative ability equal to or greater than the parent strains, that was capable of degrading two classes of hydrocarbons. The fusant that was created was found to be genetically stable for 6 months. This study shows that the properties of hydrocarbon degradation can be harnessed from this versatile organism and used to remediate pollutants comprising more than one class of hydrocarbons. It is no wonder that the genome sequence of *Acinetobacter* sp. DR1 was completed; its biotechnological applications are boundless (Jung *et al*., 2011, Kang *et al*., 2011). In 1997 Sugiura *et al*. investigated the crude-oil degradation ability of a known tetradecane degrading *Acinetobacter* isolate T4 that was isolated from the Pacific Ocean. Their investigation revealed that *Acinetobacter* was indeed capable of degrading the heavier hydrocarbon chains (from C_{14} onwards) present in different crude oils, but they found that the same compound in different crude oil samples was degraded by different degrees by the same isolate. From this they suggested that biodegradation of hydrocarbons was highly dependent on the bioavailability of the alkanes making up the specific crude oil type.

The use of a chemically defined medium comprising a single hydrocarbon substrate is commonly employed in the literature (Penet *et al*., 2004). Diesel oils, crude oils or petroleum fractions are accepted to be a complex substrates consisting of various concentrations of *n*-alkanes. Although the mixtures contain similar constituents, the abundance of each varies greatly (Penet *et al*., 2004; Hamamura *et al*., 2006; Zanaroli *et al*., 2010). Analyses of the proteomes resulting from growth on complex *n*-alkane substrates would result in complex degradative pathways due to the complexity of the substrates used and the wide array of enzyme systems that could be employed. Most often the degradation of the medium chain alkane, hexadecane, by *Acinetobacter* sp. is mentioned (Maeng *et al*., 1996; Koma *et al*., 2001; Bach *et al*., 2003; Ishige *et al*., 2002; Wentzel *et al*., 2007;

Jung *et al*., 2011; Manilla-Perez *et al*., 2010). Confusion surrounds the exact allocation of this alkane to a chain length category, as some authors refer to it as a medium chain alkane and others as a long chain alkane. For purposes of this discussion it shall be defined as a medium chain alkane bordering long chain alkane. In 1996, Maeng *et al*. mentioned that an *Acinetobacter* sp. strain ATCC 31012, a known Emulsan producer, utilized a dioxygenase enzyme to catalyze the initial step in hexadecane degradation. More recently, in 2011 Jung *et al*. found that a quorum sensing system plays an important role in hexadecane degradation in *Acinetobacter* sp. DR1. Other studies have shown that hexadecane can be used for wax ester production in *Acinetobacter* sp. strain M-1 (Ishige *et al*., 2002) and has been shown to encourage wax ester production in *A. baylyi* ADP1 and *Acinetobacter* sp. H01-N (Manilla-Perez *et al*., 2010). It has been suggested that *Acinetobacter* sp. RAG-1, when grown on hexadecane, utilizes its cell surface fimbriae to attach to hydrophobic surfaces such as those of the long chain alkanes and in so doing facilitate the uptake of the carbon source (Wentzel *et al*., 2007).

Few studies have investigated *Acinetobacter* sp. growth on tetradecane (C_{14}) specifically other than the ones already mentioned. In 2008 Yamahira *et al*. isolated a novel psychrotolerant, alkalitolerant bacterium designated *Acinetobacter* sp. strain Ths, from soil near a hot spring. Their isolate was found to be capable of degrading tetradecane as a sole carbon source at low temperatures and with high pH tolerances. The organism was found to grow on *n*-alkanes ranging from C_{13}-C_{30} at pH 9 and at 4°C. This was the first account of a hydrocarbon degrading organism acting under these conditions. More recently, Luckarift *et al*. (2011) investigated the biodegradation of medium-chain alkanes using a human-hair based adsorbent mat with *Acinetobacter venetianus* 2AW immobilized to its surface. The isolate produced a biosurfactant that aided in the dispersion of the complex composition of the hydrophobic compounds like used motor oil. The authors demonstrated an 85% removal of 1% tetradecane (C_{14}) within a 24 hour period. The mats themselves also contributed to the remediation process by sequestering the hydrocarbon substrates and facilitating the biodegradation of the hydrocarbon *in situ*. Their research demonstrated that the immobilization of these whole bacterial cells on the surface of these absorbent mats has practical applications for the remediation of oil contaminated waters.

Some of the main goals in the study of microbial ecosystem functioning for the purposes of environmental remediation are to attribute essential functions to certain members of the community and reveal cooperation and functional redundancies between its members (Benndorf *et al*., 2007). In identifying the roles individual microbial species have in removing contaminants from an environment, one can artificially create microbial populations to fill the various niches that arise in these polluted situations (Nyssonen, 2009). Microbial species that display alternative strategies for the breakdown of contaminants would be especially useful for this purpose as they could contribute metabolically to those areas where another organism could not (Nyssonen, 2009; Zanaroli *et al*., 2010). Most often researchers turn to nucleic acid based community assessments to determine the metabolic composition of its members; however a consequence of evolutionary and environmental pressures is that not all genes that may be present in an organism(s) are necessarily expressed, especially if the organism possesses 2 or more related genes (Smits *et al*., 1999; Callister *et al*., 2008). Since it is not always possible to verify the expression of these genes of interest due to time and cost factors a gap in our knowledge base exists (Callister *et al*., 2008).

The study of protein expression is a promising alternative to that of nucleic acid based research because proteins reflect the functionality of metabolic reactions and regulatory pathways directly (Benndorf *et al*., 2007). The presence/expression of mRNA does not directly relate to the activity of the encoded protein (Wilmes and Bond, 2006; Benndorf *et al*., 2007). The genome is a static entity, representing a set of instructions for all cellular functions and properties, whereas a proteome is a dynamic entity, with far more complex interactions that are critical for survival as a cell must constantly adjust its protein compositions to meet the challenges faced in different environments (Brötz-Oesterhelt *et al*., 2004). Proteomic technologies allow for the analysis of global changes in the cellular metabolism and give an indication of the response of a microorganism to the environmental stresses or stimuli and because they are the key structural and functional molecules making up a cell, the molecular characterization of proteomes is essential to completely understand biological systems (Beranova-Giogianni, 2003; Kim *et al*., 2003; Singh and Nagaraj, 2006). The transcriptome and proteome of an organism reflects its physiological status in response to a particular environmental condition. These approaches to understanding the physiological state of an organism should not be used as „stand-alone' technologies as a more integrated approach will provide a comprehensive understanding of any physiological activity within the microbial cell (Singh and Nagaraj, 2006).

A previous study (Toolsi, 2008) using the isolates V2 and LT1A investigated the involvement of *alkM, alkR, rubA, rubB, estB, lipA, lipB* and *xcpR* in the degradation of diesel, whereby the levels of gene expression were compared using real-time quantitative PCR. The results obtained in that study suggested that isolate V2 expressed a second hydroxylase gene after a 20 day period. This is not an uncommon occurrence since it is also seen in *Pseudomonas aeruginosa* PAO1 where two AlkB-related hydroxylases with similar substrate ranges are induced at different times within the growth period suggesting that the enzymes are different in some other, unknown aspect (Rojo, 2005). The expression of *alkR* and *xcpR* also revealed multiple product formations in isolate V2 as compared to LT1A. The real-time quantitative data indicates that isolates V2 and LT1A employ different strategies for the breakdown of hydrocarbon substrates at different points in the degradative process. The present study investigated the protein expression profiles of isolates V2 and LT1A in order to confirm or clarify the mechanisms by which these organisms break down hydrocarbons.

2.2 MATERIALS AND METHODS

2.2.1 *n*-ALKANE

The medium-chain alkane, tetradecane (C_{14}) (99%) (Sigma) was stored at 4 °C until required. Before use, the substrate was filtered through Whatman 25mm GD/X 0.2 µm membrane filters for sterilization.

2.2.2 BACTERIAL ISOLATES V2 AND LT1A

The known diesel, and used-engine oil degrading *Acinetobacter* isolates LT1A (Genbank accession number JN036552) and V2 (Genbank accession number JN036552) respectively, were obtained from the Department of Microbiology, University of Kwazulu Natal, Westville Campus. Pure cultures were streaked onto nutrient agar (Merck, Germany) and were incubated at 30 °C for 24 hours to obtain single colonies. These nutrient agar plates were stored at 4 °C for short-term usage. For long-term preservation pure colonies were inoculated into 2ml nutrient broth and were incubated at 30 °C for 16 hours at 160 rpm. One ml of this overnight broth culture was combined

with 1 ml sterile 40% glycerol stock solution and dispensed into 2 ml Eppendorf tubes and stored at -70 ^{o}C.

2.2.3 EXPERIMENTAL SETUP

The experiments were performed as described by Ganesh and Lin (2009) with modifications. A single colony of *Acinetobacter* sp. V2 and LT1A were each inoculated into 10 ml nutrient broth (Merck) and incubated at 30°C overnight (16 hours) at 160 rpm. The overnight cultures were centrifuged for 10 min at 10000 × *g* in a Beckman Coulter centrifuge (Avanti J-HC, Germany). The cell pellets were washed twice with Phosphate buffered saline (pH 7.6) and re-suspended in Bushnell Haas (BH) medium until OD_{600nm} was equivalent to 1. One ml of these bacterial inocula was added to separate 250 ml Erlenmeyer flasks containing 100 ml BH medium (Bushnell and Haas, 1941; Ganesh and Lin, 2009), pH 7.0 (Composition per litre: 1 g KH_2PO_4; 1 g K_2HPO_4; 1 g NH_4NO_3; 0.2 g $MgSO_4.7H_2O$; 0.05 g $FeCl_3$; 0.02 g $CaCl_2.2H_2O$). The flasks were supplemented with 0.1% sodium acetate to encourage microbial growth and incubated at 30°C at 160 rpm for 3 days (Ganesh and Lin, 2009). After culture growth, the flasks were spiked to a final concentration of 1% (v/v) filter sterilized tetradecane as a carbon source and grown at 30°C at 160 rpm for 20 days. Controls for the experiment comprised of cells grown for three days on sodium acetate alone under the same culture conditions and another control devoid of bacterial isolates was prepared to determine abiotic losses of the hydrocarbon.

2.2.4 DETERMINATION OF BACTERIAL GROWTH PATTERNS

Growth patterns of the isolates for the 20 day experimental period for each of the hydrocarbons, were obtained through the measurement of optical densities at 600 nm and total viable counts (cfu/ml) using the spread plate technique. Serial dilutions of a 1 ml sample from the culture medium from each of the flasks were made, and 0.1 ml of an appropriate dilution was plated onto nutrient agar (Merck) and incubated at 30°C for 24 hrs. Thereafter the plates were removed and the single colonies enumerated.

2.2.5 QUANTITATION OF HYDROCARBON DEGRADATION

The level of hydrocarbon degradation was determined using Gravimetric analysis as described by Ganesh and Lin (2009). In brief: 50 ml glass beakers were pre-weighed and the mass recorded. Samples were collected at set intervals during the 20 day experimental period. One hundred milliliters of the culture was transferred to a 250 ml separation funnel. The funnel contained two phases after gravimetric separation, the upper phase containing the hydrocarbon separated by an interface and the lower phase comprising the culture medium. The culture medium was extracted first for use in the enumeration assay, and for protein extraction. The hydrocarbon remaining in the separating funnel was extracted using 30 ml of an organic solvent, dichloromethane (Merck). This extract was passed through filter paper containing 10 g anhydrous sodium sulphate (Na_2SO_4) (Merck) to facilitate the removal of cellular debris and moisture. The extract was collected in the pre-weighed glass beakers and was left in the fume cupboard to allow for the evapouration of the dichloromethane. The beakers were then weighed. The percentage of hydrocarbon that is degraded was calculated using the following formula:

$$\% \text{ Hydrocarbon degraded} = \frac{\text{weight of hydrocarbon degraded}}{\text{original weight of hydrocarbon introduced}} \times 100$$

Where the weight of hydrocarbon degraded was determined as:
(weight of hydrocarbon + the beaker) - original weight of the beaker
(Ganesh and Lin, 2009).

2.2.6 PROTEIN EXTRACTION

Cells were harvested from the BH culture medium phase obtained during gravimetric analysis, using centrifugation (4°C, 10 min, 10000 × *g*) in a Beckman Coulter centrifuge (Avanti J-HC, Germany). The pellet was re-suspended in 10 ml PBS (pH 7.6) and washed three times discarding the supernatant following each centrifugation step. The final pellet was re-suspended in 10 ml PBS, aliquoted into 2 ml Eppendorf tubes and stored at -20°C. This is to be referred to as the culture

solution (Ganesh and Lin, 2011). Cell lysis using BugBuster® Master Mix Protein Extraction Reagent (Novagen®, Leuven, Belgium) was performed according to manufacturer's instructions using 2 ml of the culture solution. Twenty microlitres of Protease inhibitor cocktail (Complete mini, Roche Diagnostics, Germany) was added to the resulting protein solution.

2.2.7 PROTEIN QUANTIFICATION USING THE BRADFORD ASSAY (BRADFORD: 100-1500 mg/ml)

Protein concentrations were determined for all extractions. Bovine serum albumin (BSA) (Roche) of known concentrations was used as a standard to construct a standard curve. Protein measurements were performed as per the protocol of Bradford (1976) and modified as follows: One mililitre of Bradford reagent (Appendix I) was added to 20 µl of a suitably diluted (1/10) protein sample in a glass test tube, and vortexed. Samples and BSA standards were diluted using 0.15 M NaCl. A 1:50 ratio of sample to Bradford was maintained for both the BSA standard curve and the protein samples. After 15 minute incubation at room temperature, the samples were measured for absorbance at 595 nm using the Libra S12 spectrophotometer (BIOCHROM). The sample concentration was then estimated from the BSA standard curve (Appendix IID) and expressed as milligrams per mililitre (mg/ml). All experiments were repeated four times and averaged. (Appendix IIE).

2.2.8 ONE DIMENSIONAL SODIUM DODECYL SULPHATE POLY ACRYLAMIDE GEL ELECTROPHORESIS (1D SDS-PAGE)

The protocol of Ganesh and Lin (2009) was followed. In short: all proteins were diluted 1:1 v/v with SDS-PAGE sample buffer (2% SDS, 50 mM Tris-HCl at pH 6.8, 25% Glycerol, 0.01% Bromophenol blue (Saarchem, South Africa) as a tracking dye) to approximately 0.5 mg/ml (50 µg/100µl) in accordance with the protein assay data (Appendix IIE). The samples were vortexed briefly for homogenization and then denatured at 95°C in a water bath for 10 min. Thereafter the samples were centrifuged (10000 × *g* for 2 min) in a MSE Micro Centaur (Sanyo, USA) to clarify

the sample. Twelve percent SDS-PAGE gels were prepared as per the method of Laemmli (1970) and modified as per the protocol of Ganesh and Lin (2009) using the electrophoresis equipment illustrated in the Appendix. The SDS-PAGE gel were prepared by casting 25 ml of the 12% separating gel layer (8.2 ml double distilled H_2O, 10 ml 30% Acrylamide stock solution, 6.3 ml 1.5 M Tris-HCl (pH 8.8), 250 µl 10% sodium dodecyl sulphate, 250 µl 10% ammonium persulphate (Merck) (and 10 µl TEMED (Merck)). After polymerization and the decanting of the butanol : water (1:1 v/v) layer, 5 ml of the stacking layer (comprising: 3.4 ml double distilled H_2O, 830 µl 30% acrylamide stock solution, 630 µl 1 M Tris-HCl (pH 6.8), 50 µl 10% sodium dodecyl sulphate, 50 µl 10% ammonium persulphate and 5 µl TEMED) was prepared and cast over the separating gel. The gel was placed into an electrophoresis tank filled with 1 × Tris-Glycine-SDS running buffer (25 mM tris base, 250 mM glycine (pH 8.3), 0.1% SDS). Spectra™ Multicolor Broad range Protein ladder (Fermentas, Germany) was used as a reference to estimate molecular weights. Eighty microlitres of the diluted samples were then added into the remaining wells. All empty wells were filled with 80 µl sample buffer to avoid the distortion of bands. Electrophoresis was performed at room temperature for 17 hours at 40 V and 500 mA followed by 4 hours at 60 V and 500 mA unless otherwise indicated. The gel was then visualized following staining with Coomassie Blue (uniLAB) overnight, and destaining with the application of heat for 1-2 hours in a destaining solution comprising methanol: water (1:1 v/v) and 10 ml glacial acetic acid in a final volume sufficient to cover the gel. Images of the gels were scanned onto the computer using a HP Scanjet 4600.

2.2.9 TWO DIMENSIONAL POLYACRYLAMIDE GEL ELECTROPHORESIS (2D-PAGE)

All reactions were performed (in duplicate) using ReadyPrep 2-D Starter Kit (BIO-RAD, USA) following manufacturer's instructions comprising the following steps:

2.2.9.1 SAMPLE PREPARATION

The ReadyPrep™ 2-D cleanup kit (BIO-RAD, USA) was used to remove contaminants from the whole cell protein extracts, following manufacturer's instructions. The final protein pellet was re-

suspended in rehydration/sample buffer (comprising: 8 M urea, 2% CHAPS, 50 mM DTT, 0.2% Bio-Lyte 3/10 ampholyte, Bromophenol Blue BIO-RAD, USA) in a final volume of 195 µl. The rehydrated protein aliquot was then pipetted onto a rehydration tray, and a ReadyStrip IPG strip (11cm, pH 3-10) (BIO-RAD, USA), was placed over the solution containing the protein sample. This was followed by rehydration of the strip for 30-60 min and overlaying with mineral oil (Sigma). The strip was then rehydrated overnight at room temperature for 16 hours.

2.2.9.2 FIRST-DIMENSION ISO-ELECTRIC FOCUSING (IEF)

Following overnight rehydration, the strip was removed from the rehydration tray and placed onto a focusing tray atop wetted wicks (BIO-RAD, USA). The PROTEAN IEF cell (BIO-RAD, USA) was programmed to focus the ReadyStrip IPG strip at 8000 V for a total of 30000 V-hr. After IEF, the IPG strip was stored in a tray at -80°C until further use. The ReadyStrip IPG strip was prepared for the second dimension by equilibration. The first step involved the equilibration of the IPG strip in buffer containing 5 mM Tris-HCl (pH 8.8), 6 M urea, 2% SDS, 30% glycerol, and 1% DTT for 15 min. This was followed by a second equilibration in the same buffer supplemented with 2.5% iodoacetamide for 15 min. The IPG strip was then rinsed off with 1× Tris-glycine-SDS running buffer.

2.2.9.3 SECOND-DIMENSION SDS-PAGE

The ReadyStrip IPG strip was transferred onto an Any kD™ Criterion TGX precast gel (BIO-RAD, USA) and overlaid with 0.5% agarose in Laemmli buffer (BIO-RAD, USA). Five microlitres of BIO-RAD precision plus unstained protein molecular weight marker was added to the marker well. The gels were run for 45 min at 175 V, 500 mA, in 1× Tris-glycine-SDS running buffer in the Criterion Dodeca cell (BIO-RAD, USA). Following electrophoresis, the gels were removed from the cassettes and stained using Oriole™ Fluorescent gel stain (BIO-RAD, USA) following manufacturers instructions, in brief the gels were immersed in the staining solution and agitated in the dark for 90 min. The gels were transferred to water prior to imaging to prevent damage to the imaging equipment. They were then imaged using the ChemiDoc XRS gel documentation system (BIO-RAD, USA) under UV light.

2.2.9.4 IMAGE ANALYSIS AND SPOT EXTRACTION

Digital images of 2D-PAGE gels were analysed using PDQuest™ Advanced 2-D analysis software (version 8.0.1, BIO-RAD, USA). The images were processed for spot detection and background subtraction as per Ganesh and Lin (2011). The criteria for determining protein expression in response to hydrocarbon exposure were as follows: all proteins showing at least a two-fold decrease in intensity after staining were classified as down-regulated, and all proteins showing at least a two-fold increase in intensity after staining were classified as up-regulated (Geng and Lim, 2007). To allow for spot-to-spot comparisons of the gels, a match set was created that included all gel images within an experiment. The images were inverted or adjusted appropriately so as to account for excessive background staining and warped prior to analysis. For each match set, a standard (master) gel was created from the image within the match set that contained the maximum number of spots with an absence of streaking or other gel distortions. The master gel was denoted as the detection parameter gel. The PDQuest™ Advanced 2-D analysis software (version 8.0.1, BIO-RAD, USA) was used to normalize the spot quantities so as to remove variations in spot intensity caused by non-treatment effects. This normalized spot quantity was equal to the raw spot quantity expressed as a percentage of the total pixel quantity of all spots in the gel due to the presence of saturated spots in some images, as recommended by the software, PDQuest Advanced (Zheng *et al*., 2007; Ganesh and Lin, 2011).

Samples of protein extracts were sent for processing and sequence analysis at the proteomics facility at the University of the Western Cape. These samples were run on 12% 2D PAGE gels and stained with Coomassie Blue- spots of interest were then extracted (using SPOT CUTTER) and neutralized with 10mM NH_4HCO_3 and destained with 400 µL 50% acetonitrile in 10mM NH_4HCO_3. Following this, the gel pieces were dried in the SpeedVac concentrator before undergoing overnight digestion (37°C) using sequencing-grade trypsin (2 µg/ml Promega, USA) in 50 mM NH_4HCO_3. After rehydration with the trypsin solution, the spots were crushed and a few µL of 50 mM NH_4HCO_3 were added to prevent drying of the samples during the cleavage process. The peptides were extracted once with 100 µL of 50 mM NH_4HCO_3 for 30 min and twice with 100 µL 60% acetonitrile in 0.1% TFA for 30 min and the collected extracts were lyophilized (Wissing *et al*., 2000).

2.2.10 MALDI-TOF ANALYSIS OF PROTEINS

Lyophilized protein samples were sequenced using MALDI-TOF MS at the Proteomics Facility at the University of the Western Cape.

2.2.11 MASCOT ANALYSIS

Resulting protein sequences were subjected to MASCOT analysis followed by alignment to known sequences within the protein bank so as to determine the identity of the relevant proteins.

2.2.12 STATISTICAL ANALYSIS

All experiments, unless otherwise indicated, were performed in triplicate, and measurements are presented as mean ± standard deviation. Student t-tests (SPSS version 19) were used to examine the statistical significance between the hydrocarbon and non-hydrocarbon exposed cultures. Probability was set at 0.05 (Wilkinson, 1988). Correlation coefficients and spot match rates between control cultures and hydrocarbon exposed samples was determined using PDQuest™ Advanced 2D Analysis software (version 8.0.1, BIO-RAD).

2.3 RESULTS

2.3.1 TETRADECANE BIODEGRADATION ASSAY

The degradation profile of the *Acinetobacter* isolates V2 and LT1A during the course of the 20-day degradation assay is shown in Figure 2.1. Prior to the addition tetradecane (C_{14}), the isolates were grown on 0.1% sodium acetate to encourage microbial growth (Appendix Tables IIB, C). One day following hydrocarbon inoculation the bacterial population begins to increase (Figure 2.1). By day 5, C_{14} degradation reached 85% and 87% for V2 and LT1A respectively and the bacterial population remains relatively stable after day 5 showing no further increase. By day 20, both bacterial populations begin to drop as 90% of the hydrocarbon has been removed and very little

remains to sustain microbial numbers. This degradation was significant ($p<0.05$) for both V2 and LT1A in comparison to the abiotic control as was determined by the student t-test (Appendix Table IIIH). By day 20, 32% of the hydrocarbon loss was attributed to abiotic factors as seen in the abiotic controls in Figure 2.1. The degradation patterns for V2 and LT1A were comparable, and there was no significant difference ($p=0.454$) in their utilization of the hydrocarbon substrate.

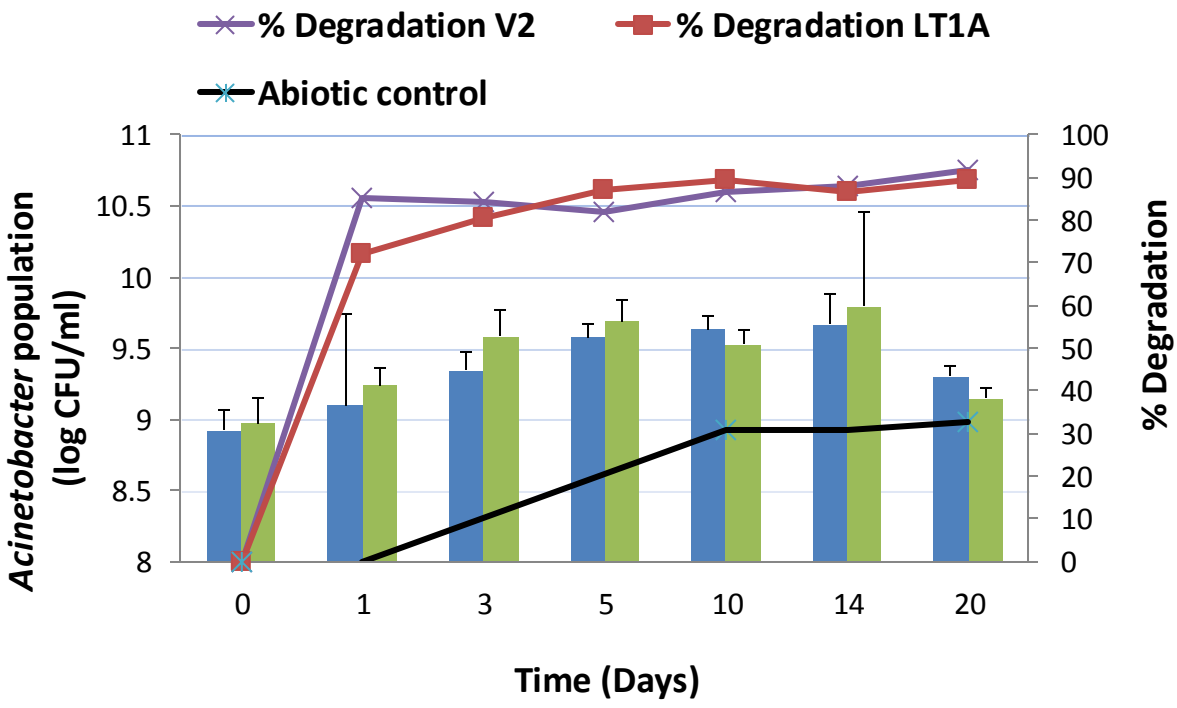

Figure 2.1 Degradation profile for *Acinetobacter* sp. V2 and LT1A grown in Bushnell Haas medium spiked with 1% Tetradecane (C_{14}) in relation to the abiotic control. The increase in microbial populations in relation to the % C_{14} degradation over 20 days is shown. Blue bars represent growth of V2, green bars represent growth of LT1A (*n*=3).

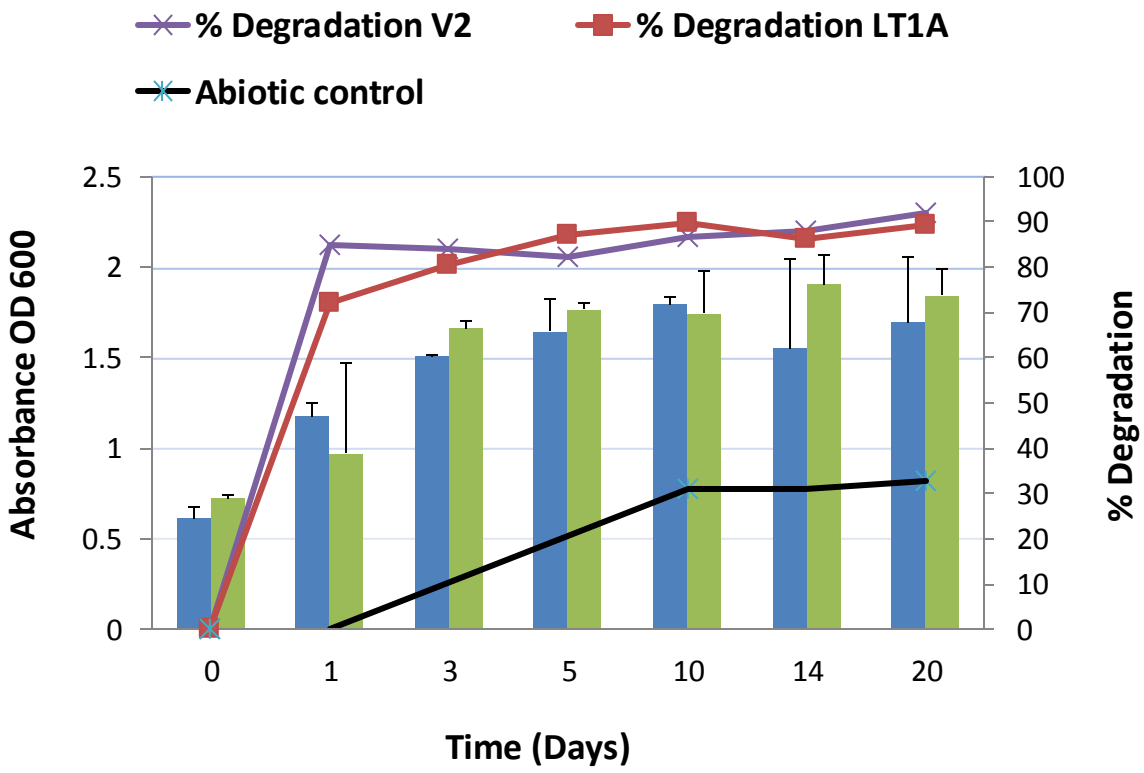

Figure 2.2 Degradation profile for *Acinetobacter* sp. V2 and LT1A grown in Bushnell Haas medium spiked with 1% Tetradecane (C_{14}), showing the microbial populations as determined spectrophotometrically at OD_{600nm} and the % C_{14} degradation over 20 days. Blue bars represent growth of V2, green bars represent growth of LT1A (*n*=3).

In Figure 2.2, the bacterial population as determined by optical density readings at OD_{600nm} increases from day 0 to day 3 where after it remains relatively stable. The difference in the interpretation of the bacterial population between Figures 2.1 and 2.2 can be seen on day 20, where actual plate count data shows the bacterial populations begin to decline, whereas OD readings show very little to no change in the population numbers at all. A bioemulsifier was seen flocculating within the medium during the degradation assay.

2.3.2.1 1D SDS-PAGE ANALYSIS WITH ACETATE AS THE SOLE CARBON SOURCE

The soluble proteins extracted from the isolates grown on sodium acetate as a sole carbon source (using the BugBuster Mastermix) were analyzed on a denaturing PAGE gel to serve as a control. Figure 2.3 illustrates the immediate differences in protein expressions that were observed for the two isolates when grown on sodium acetate for 3 days. It is apparent from this 1D SDS-PAGE gel that the organisms express different proteins during the breakdown and metabolism of sodium acetate, implying that from the onset they make use of different processes for the utilization of a carbon source. In some cases this could be a matter of possessing more than one isoform of a particular protein. The different coloured circles in Figure 2.3 point out the most obvious differences in protein expression. A visual inspection shows the following: The red circle corresponds to a protein (or combination of proteins) of approximately 37-38 kDa for V2, but LT1A expresses proteins that appear to be larger (~39-40 kDa). The green circle highlights the proteins expressed by V2 in the 35 kDa region that are slightly larger than the proteins of LT1A. The blue circle points to a case where for V2, two protein bands of approximately 23-24 kDa are observed as compared to LT1A which shows a single band of around 21-22 kDa. And then the yellow circle shows a similar scenario except in this case LT1A displays numerous bands in the 17-19 kDa region and V2 shows only two.

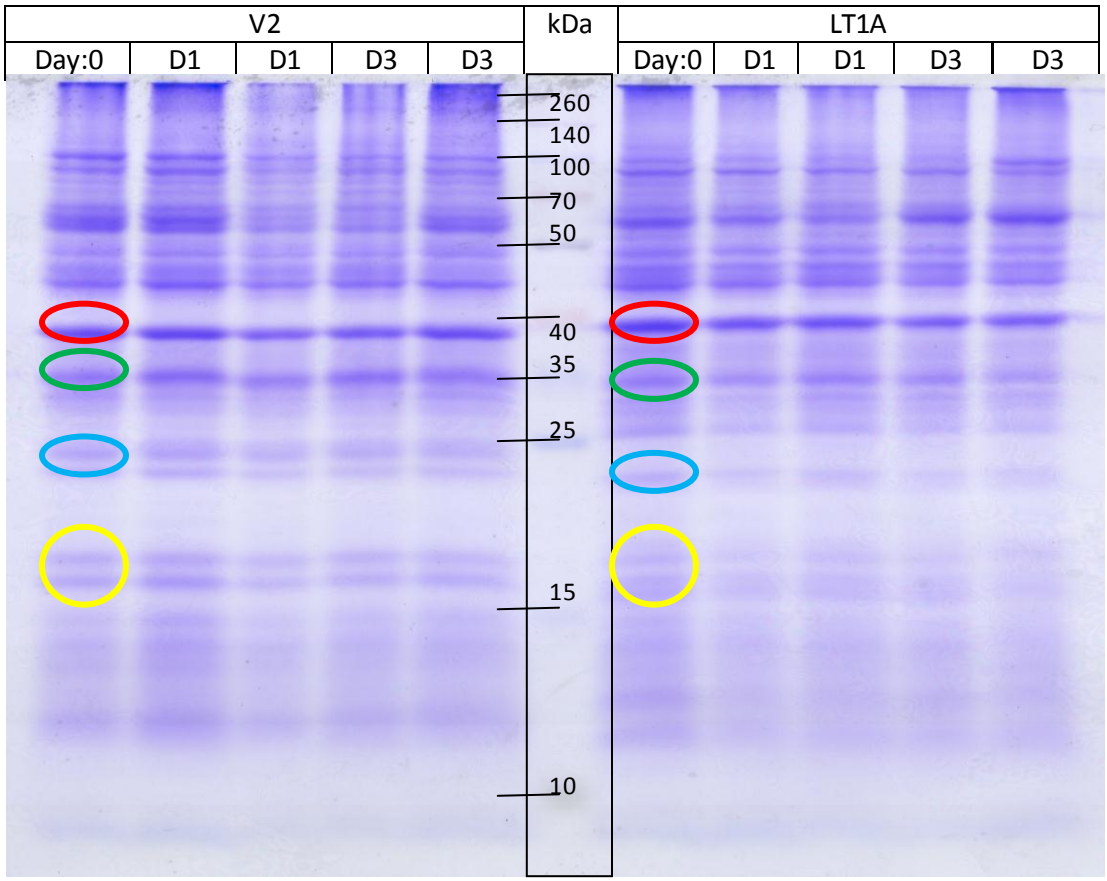

Figure 2.3 SDS-PAGE showing protein expression profiles of isolates V2 and LT1A when grown on sodium acetate as a sole carbon source for 3 days before tetradecane inoculation. Circled areas point out obvious differences in carbon source utilization.

2.3.2.2 1D SDS-PAGE ANALYSIS WITH TETRADECANE AS THE SOLE CARBON SOURCE

As shown in Figure 2.4 the isolates display different expression patterns to one another. Although the patterns are similar to that of the sodium acetate grown cells, a closer look reveals that there are at least 5 protein bands that show varying intensity as compared to day 0. The band A (~50 kDa) for organism LT1A shows a definite increase in intensity from day 0 to day 20, implying it is involved in the utilization of C_{14} to a greater extent than for sodium acetate; for organism V2 this

band remains unchanged. The band indicated by arrow B (~27 kDa) was not present for isolate V2 at day 0, but is upregulated (or expressed) from day 3 onwards. The proteins highlighted by arrow C (~100 kDa) show an increase in expression for both isolates from day 3 onwards. Arrow D (~29 kDa) indicates a protein (s) that is upregulated from day 3 onwards for isolate LT1A but which is present for V2 from day 0. From Day 3 for organism V2, proteins in the region marked by arrow E (~46 kDa) show an upregulation in response to tetradecane exposure; however for LT1A these proteins were active from day 0 implying they play some other metabolic role not limited to the use of tetradecane.

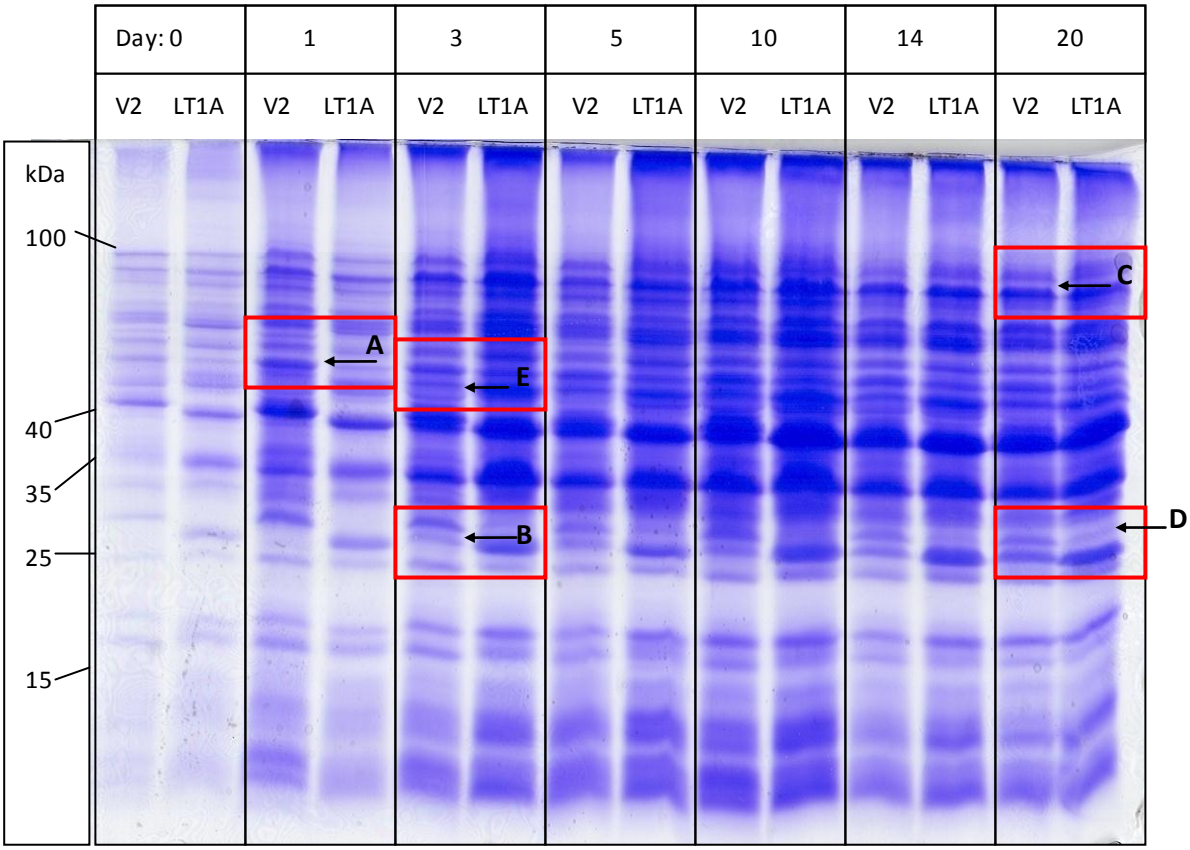

Figure 2.4 SDS-PAGE Protein expression profiles of *Acinetobacter* sp. isolates V2 and LT1A during growth in Bushnell Haas medium spiked with 1% Tetradecane (C_{14}) for 20 days. Some areas have been highlighted to point out obvious differences in protein expression

2.3.3 2D SDS-PAGE ANALYSIS

Figure 2.5 shows the protein expression patterns of *Acinetobacter* sp. V2 and LT1A during growth on tetradecane (C_{14}). Those proteins found in the soluble fraction of the cell extracts are represented by this Figure. A visual examination of the gel images reveals the following observations (In most cases, these are confirmed by the 2D master gel images obtained in Figures 2.7 and 2.8, as is pointed out by the histograms showing relative expression levels):

1. The spot indicated by A (~50 kDa, *p*I= 6) is down regulated from day 5 to 20 for organism V2, but is not detected for LT1A.
2. Spots marked by B (~45 kDa, *p*I=5.2) are present for organism V2 from day 5 to 20, but is once again not detected for LT1A.
3. Spot C (~36 kDa, *p*I= 6) shows consistent expression from day 5 to 20 for organism V2, and it is assumed that spot C corresponds to spot I (on LT1A gel image). The spot directly adjacent to spot C, denoted #, is not present for LT1A throughout the assay.
4. The protein spots in the region of D (~100 kDa), are very poorly detected in organism LT1A.
5. Spot E (~24 kDa, *p*I= 5.8) is upregulated for V2, but undergoes no change in LT1A, and is undetected on day 20.
6. Spot F (~17 kDa, pI=5.9) is not detected in V2 on day 10, but is present on days 5 and 20 and is present for LT1A on all 3 images.
7. Spot G (~11 kDa, *p*I=5.3) appears to show an increase in expression levels for organism V2 from day 5 to 20, but is constitutively expressed for LT1A, showing little to no change in expression.
8. Spots H and B refer to proteins in the same general area of the gels (~45 kDa, *p*I=5). In organism V2, there appear to be 3 proteins in this area, whereas for LT1A there seems to be only one. It is presumed that spot H corresponds to the middle spot in the row of 3 spots seen in B.
9. Spot J (~20 kDa, *p*I= 5) is absent in organism LT1A, but upregulated from day 5 to 20 for organism V2.
10. Spot K (~16 kDa, *p*I= 5.8) is adjacent to spot F, and is not detected in organism LT1A at all. This spot also lies directly in line with spot #. Many of the other proteins, expressed in very small quantities, are not seen on all the gel images and so will not be included in the analysis.

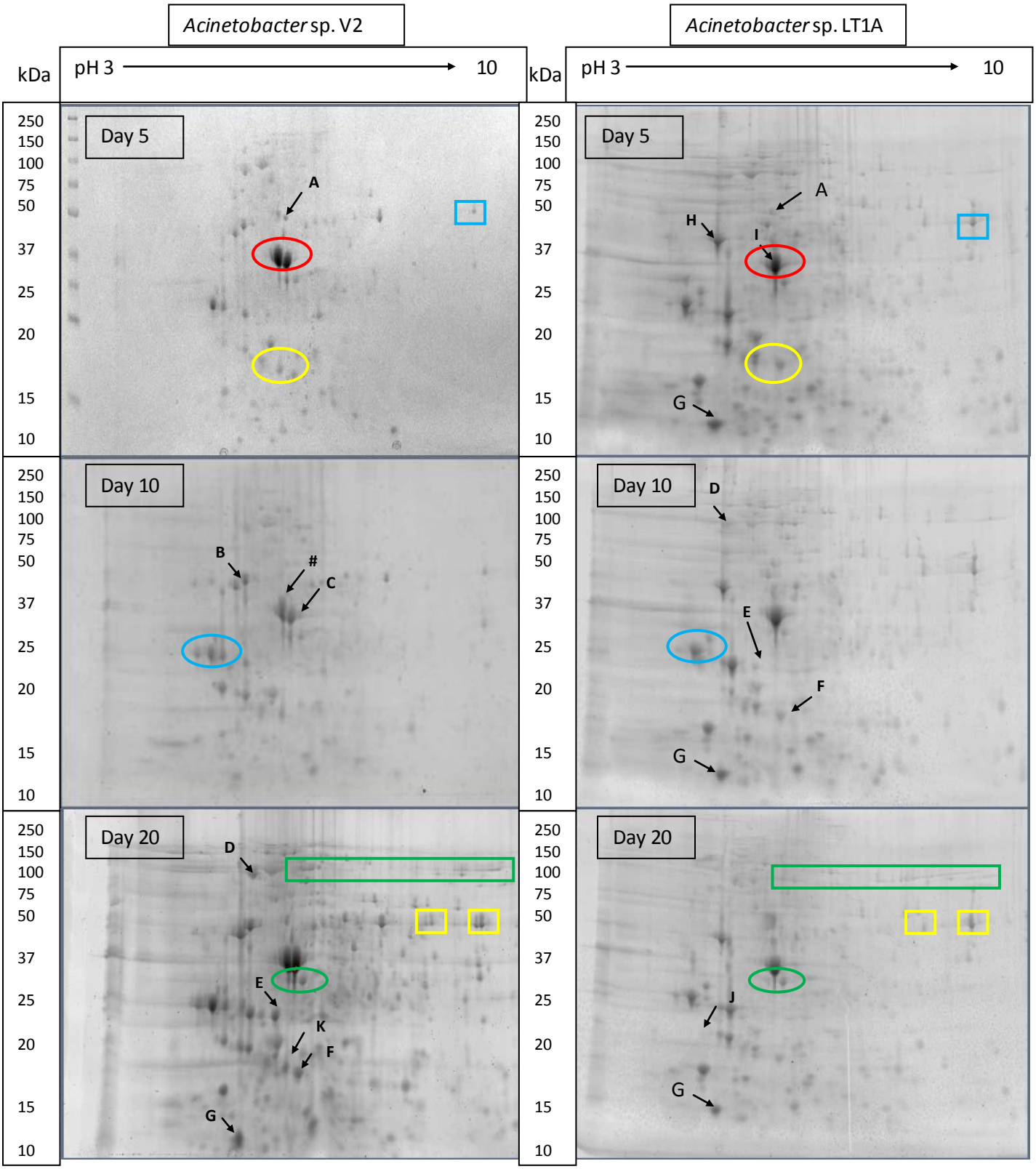

Figure 2.5 Selected 2D SDS-PAGE protein expression profiles of *Acinetobacter* sp. isolate V2 and LT1A. Spots to be discussed are indicated by arrows and are referred to by the corresponding letter (A, B, C, D etc.) or coloured shape.

The use of the BugBuster Master mix to lyse the bacterial cells achieved good results in terms of protein extraction as can be seen from the Oriole (BIORAD) stained 2D images (Figure 2.5 and Figure 2.6) that show that protein distribution occurs across a broad range of molecular weight regions and *p*I values. In Figure 2.6 it can be seen that the proteins of isolate V2 and LT1A are well distributed across the pH range of 3-10 with most proteins appearing in the pH 4-7 region suggesting that much of the *Acinetobacter* proteome is acidic. The proteins range in size from 150 to 10 kDa. As can be seen in Figure 2.6, majority of these 2 fold-up or down regulated proteins appear in the 20-40 kDa region, with very few proteins in the higher molecular weight areas (>100 kDa) especially for organism LT1A (Appendix Table IIF). Organism V2 displayed 70 proteins showing a 2 fold increase or decrease in expression, 26 of which were upregulated from day 0 to day 20. Organism LT1A displayed only 25 proteins, 14 of which were upregulated from day 0 to 20. The pH 3-10 IPG strips used to separate the protein samples ensured a good separation of all soluble proteins across the widest range possible so as to give the best representation of the proteomes of each isolate.

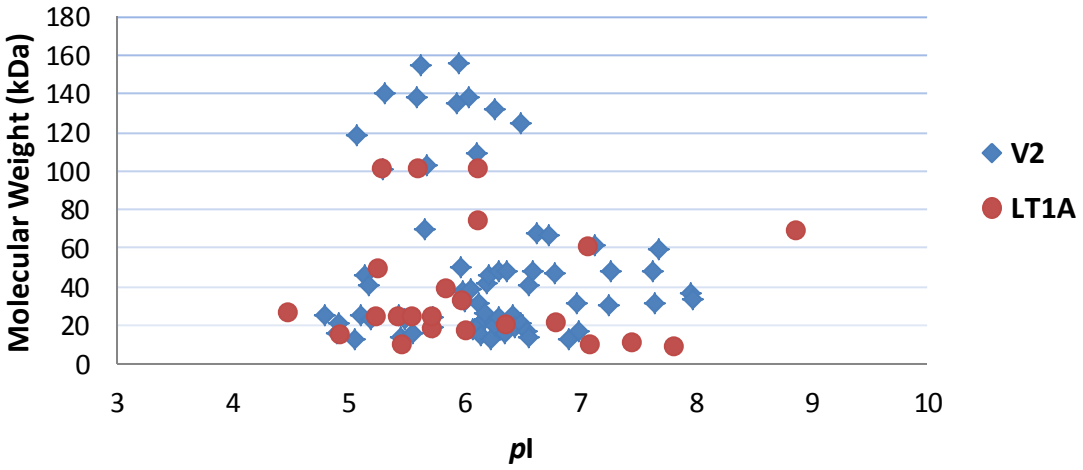

Figure 2.6 Spot distribution patterns in terms of molecular weight and *p*I (isoelectric point) for those proteins showing a 2-fold increase or decrease in expression levels for organisms V2 and LT1A from day 0 to day 20 as determined by PDQuest™ Advanced 2-D analysis software (version 8.0.1, BIO-RAD, USA).

Table 2.1 illustrates the qualitative analysis of the 2D gel images for isolates V2 and LT1A. The values depicted in the table represent averages for duplicate samples (n=2) (Appendix Table IIG). The correlation between the day 20 samples (master gel) and the day 0 and day 5 samples for organism V2 was low; however all other samples showed good correlation to the master gel with r values of 0.578, 0.605 and 0.757 obtained for days 10, 14 and 20 respectively. LT1A samples all showed a good correlation to the master gel (day 0) with r = 0.847, 0.754, 0.806, 0.776 and 0.714 for days 0, 5, 10, 14, 20 respectively. The match rates to member gels (match rate 1) and match rates to the master gel (match rate 2) were relatively low for both organisms corresponding to the low number of spots matched to the master using automated matching and manual corrections during analysis. The use of a cleanup kit resulted in good separation of the proteins with little to no streaking thus producing good 2D images for analyses.

The total spot numbers on the 2D gels were detected using PDQuest™ Advanced 2-D analysis software (version 8.0.1, BIO-RAD, USA), and the gels with the most spots and least background interference were chosen as the master gels and used for spot detection parameters as stated in section 2.2.9.4. A master gel containing all the spot attributes for each experimental set was created (Figures 2.7 and 2.8). The software was selected to normalized spot quantities based on the total pixel intensity within spot boundaries of Gaussian spots. This normalized spot quantity was equal to the raw spot quantity expressed as a percentage of the total pixel quantity of all spots in a gel (Ganesh and Lin, 2011) (Appendix Table IIH).

Table 2.1. Qualitative analysis of 2-DE separated proteins as determined using PDQuest ™ Advanced 2D analysis software for both *Acinetobacter* sp. isolates V2 and LT1A

Gel group	Spots (*n*=2)	No. of spots matched to master	Match Rate 1	Match Rate 2	Correlation Coefficient
Isolate V2					
C14 d0	149	58	39%	36%	0.212
C14 d5	96	48	52%	30%	0.471
C14 d10	103	44	40%	27%	0.578
C14 d14	142	55	40%	34%	0.605
***C14 d20**	127	91	70%	57%	0.757
Isolate LT1A					
***C14 d0**	87	66	74%	44%	0.847
C14 d5	148	58	40%	39%	0.754
C14 d10	143	58	44%	38%	0.806
C14 d14	186	70	39%	46%	0.776
C14 d20	186	64	36%	42%	0.714

*master gel

Match rate 1: no. of matched spots on gel, relative to member gel

Match rate 2: no. of matched spots on gel, relative to master gel

Correlation coefficient relative to master gel

Table 2.2 is to be used as an aid to interpret the data seen in the 1D and 2D images as it helps to relate the information obtained in the 1D image to the information that can be gathered from the 2D images. These findings have been visually interpreted from the gel images obtained and are presumptive observations to be used as a guide only. The differences in expression seen between the isolates grown on acetate as a sole carbon source can be related to the 2D images of the cells grown on C_{14} as they represent major differences in the way the organisms utilize carbon sources. These interpretations are then used to highlight areas of focus for the 2D analysis software as is seen in the next two Figures (2.7 and 2.8) that illustrate the master gel images for both isolates with margin graphs displaying the relative intensities of protein expression for the spots of interest.

Table 2.2. Visual analyses and interpretation of separated proteins of *Acinetobacter* sp. isolates V2 and LT1A on 1D and 2D gel images.

Approx. molecular weight (kDa) of bands/spots of interest	Notes about bands	Label in Figure 2.3 or 2.4 (1 D PAGE)	Notes about spots	Label in Figure 2.5 (2D PAGE)
Acetate as the sole carbon source				
~23-24	V2 has 3 bands in this region, LT1A has only 2	Blue circle	3 similar sized spots for V2 1 predominant spot for LT1A	Blue circle
~37-39	LT1A protein band in 39 V2 protein band in 37-38	Red circle	LT1A 1 main spot V2 has 2	Red circle
~34-37	LT1A protein band in 37 V2 protein band in 34	Green circle	V2 has 3 spots LT1A has only 2	Green circle
~18-19	V2 has two bands LT1A has 3	Yellow circle	V2 has 3 spots LT1A has 2 spots	Yellow circle
C14 as the sole carbon source				
~50	Increases in intensity from D0-20 for LT1A, no change in V2	Block A	Many spots in 50 kDa region, difficult to assign 1	Blue square
~27	Induced by C14 in V2, increases for LT1A	Block B	The closest match is to spot E	Arrow E
~100	Increases for both organisms up to day 20, greater extent V2	Block C	Spots poorly separated on some gels	Green rectangle
~29-30	Increases for LT1A up to day 20, but no change in V2	Block D	Hard to detect, may be comprised many small proteins or out of pH range	Not detectable
~46	Upregulated in V2, no change in LT1A	Block E	2 instances of V2 expressing 2 proteins of same size, LT1A expressing only 1	Yellow squares

Figures 2.9 and 2.10 represent the same master gel images seen in Figures 2.7 and 2.8, except that they highlight specific analysis sets created using PDQuest Advanced 2D image analysis software (BIORAD). These analysis sets were created to point out specific areas of interest within the protein expression profiles of each isolate as defined in Table 2.3. The analysis sets created offer an unbiased interpretation of the gel images using computer software.

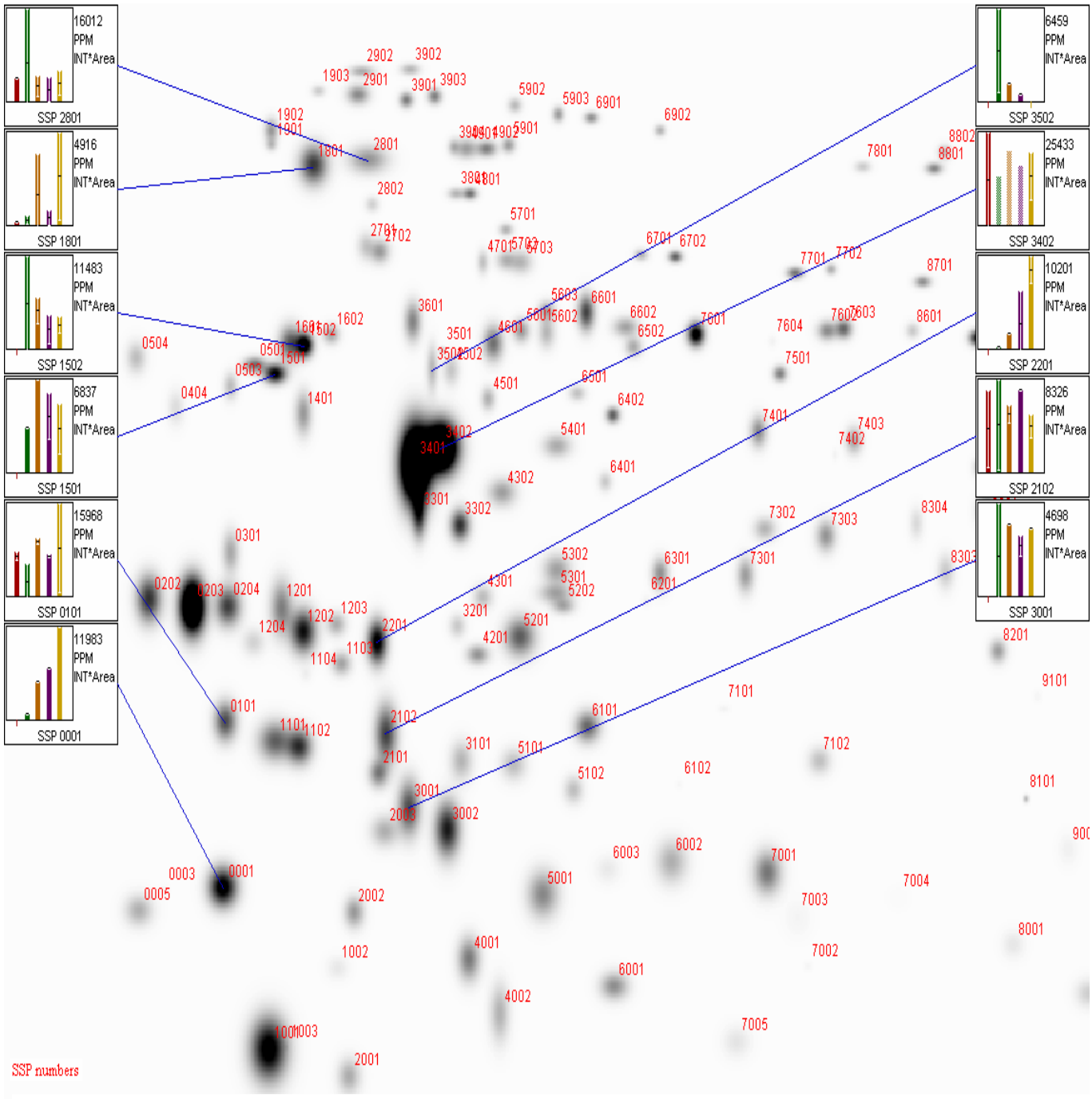

Figure 2.7 Master 2D PAGE image showing protein expression profiles of *Acinetobacter* sp. isolate V2. Margin graphs show relative expression for the specified spots as determined by PDQuest 2D advanced software (BIORAD). Spots are numbered in red. Normalization values determined by total density in gel image due to saturated spots present in some members of the experiment and Histogram Bars represent relative intensity of individual spots on set days: red (day 0), green (day 5), orange (day 10), purple (day 14), and yellow (day 20). Spot numbering and corresponding markers in Figure 2.5: Spot 3502: arrow A; spots 1501, 1502: arrows B, H; spot 3402: arrow C, I; Spots 1801, 2801: arrow D; spot 2201: arrow E; spot 3001: arrow F; spot 0001: arrow G; spot 0101: arrow J; and spot 2102: arrow K.

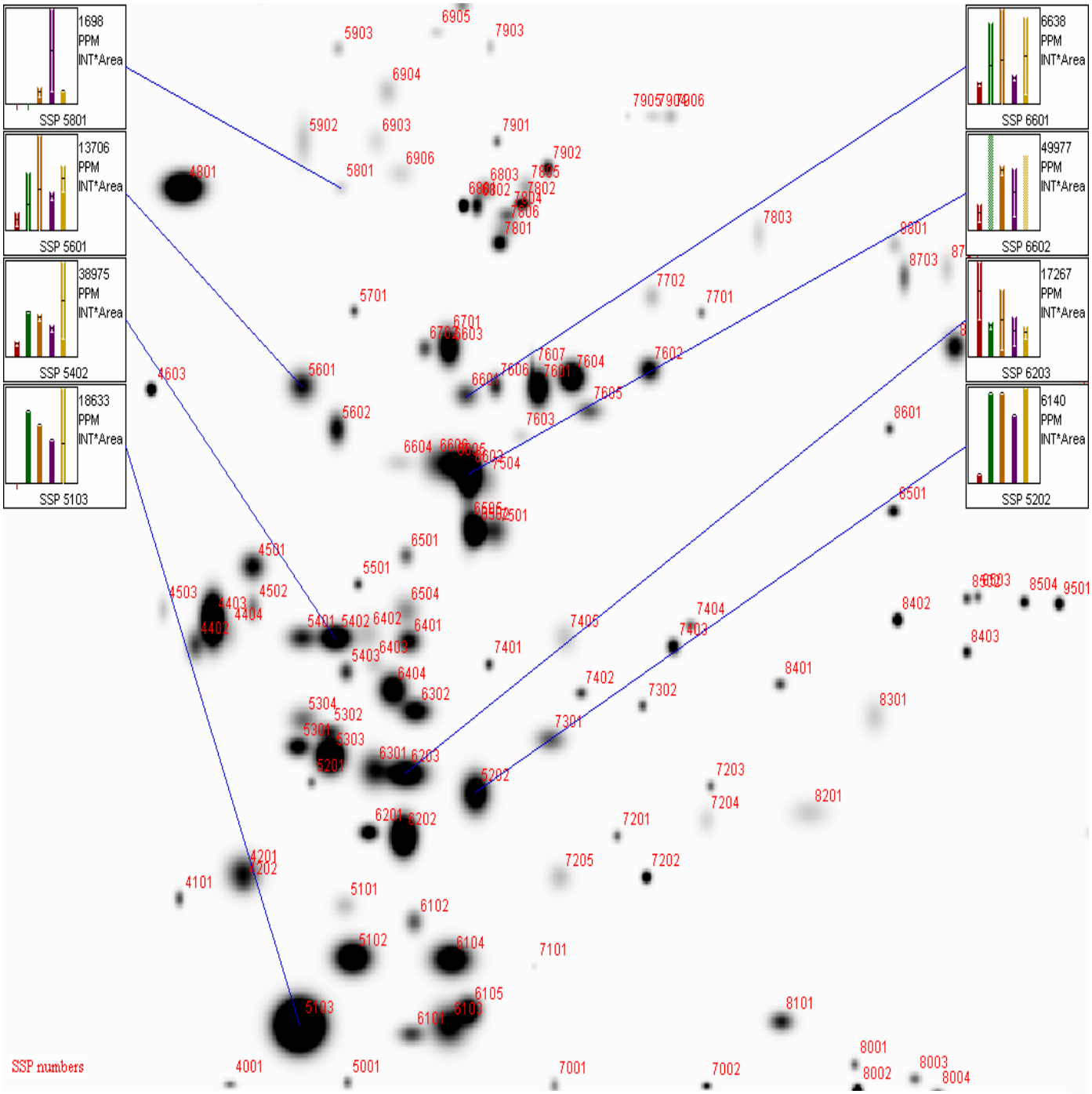

Figure 2.8 Master 2D PAGE image showing protein expression profiles of *Acinetobacter* sp. isolate LT1A. Margin graphs show relative expression for the specified spots as determined by PDQuest 2D Advanced software (BIORAD). Spots are numbered in red. Normalization values determined by total density in gel image due to saturated spots present in some members of the experiment (Raw data in appendix) and Histogram Bars represent relative intensity of individual spots on set days: red (day 0), green (day 10), orange (day 14), purple (day 20), and yellow (day 5). Spot numbering and corresponding markers in Figure 2.5**:** Spot 6601: arrow A; spot 5601: arrow B, H; spot 6602: arrow C, I; Spot 5801: arrow D; spot 5402: arrow E; spot 5202: arrow F; spots 5103: arrow G; and spot 6203: arrow K.

Spots showing differential expression between the isolates, based on samples run at the Proteomics facility at the University of the Western Cape, were sequenced (Appendix Table IV and Figure VC) and labeled accordingly in Figures 2.9 and 2.10. The exact locations of these sequenced proteins are based on assumptions and visual interpretations. These proteins were found to be similar between the degradation processes for both medium-and long-chain alkanes (Chapter 3) and are presumed to be involved in alkane degradation. Although more spots were selected for sequencing, they generated poor spectra and consequently gave no results. As shown in Table 2.3, very few spots were detected for each category. Those proteins that were upregulated 2-fold between days 0 and 20 are pointed out by the green cross. V2 showed 26 upregulated proteins, whereas LT1A displayed only 14. Qualitative analysis of those proteins absent/undetected on day 0 but present by day 5, as indicated by the blue crosses, revealed 7 and 11 proteins for V2 and LT1A, respectively. Those proteins that were not present/detected on day 0 but were present by day 20 are indicated by the green square. As expected, more proteins are seen as compared to the day 0-day 5 analysis set (blue crosses) with 19 and 22 proteins being detected for V2 and LT1A respectively. Only 7 protein spots were found to show a statistically significant change in expression from day 0 to day 5 for both isolates, and of these spots, only 6 were found to be specifically induced by C14.

Table 2.3. Overview of protein expression patterns for both *Acinetobacter* sp. Isolates V2 and LT1A, as determined by PDQuest 2D Advanced software (BIORAD)

Expression pattern	V2	LT1A	Analysis type*	Designation in Figures 2.9 and 2.10
	Number of spots			
2-fold or greater upregulated spots (Day 0-Day 20)	26	14	Quantitative	Green cross
C14 induced proteins (Day 0-Day 5)	7	11	Qualitative	Blue cross
C14 induced proteins (Day 0-Day 20)	19	22	Qualitative	Green square
Spots showing statistically significant change in expression (Day 0-Day 5)	7	7	Statistical (95%)	N/A
Statistically significant spots induced by C14 (Day 0-Day 5)	6	6	Boolean	N/A

*Definitions:
Quantitative: Spots whose quantity has increased or decreased "X-fold" (X: user determined)
Qualitative: Spots present in one gel image and absent from another, but showing a 10-fold expression level over the background
Statistical: Composed of spots that are significant based on student t-test with $p<0.05$
Boolean: Created by comparing 2 or more analysis sets
N/A: Not applicable

Due to the extensive costs involved, only 14 spots were selected for MALDI-TOF-MS sequencing across the tetradecane and octacosane assays (as illustrated in Table 2.4 and Table 3.3 in Chapter 3). Those spots chosen for sequencing were determined based on obvious changes in expression between the isolates, but that were similar to both assays. Of the spots that were sequenced, 4 spots (3402, 3401 from Figure 2.7 and 6602, 6606 from Figure 2.8 and circled in red on Figures 2.9, 2.10) represented „conserved hypothetical proteins'. These 4 proteins did show differences in expression between the isolates. They were induced from day 0 to day 5, showing at least a 2-fold increase in expression levels as indicated by Figures 2.9 and 2.10 (marked by the green crosses). In Figure 2.5 it was observed that the spots in the region marked by A (~36 kDa, *p*I= 6) show that on day 5 organism V2 possess 3 proteins as opposed to organism LT1A that expresses only 2 at this stage, it is possible that the proteins are isoforms that differ perhaps in their phosphorylation states. One of the isoforms was induced from day 0 to day 20 for organism V2, showing at least a 2-fold increase in expression levels as indicated in Figure 2.9 (marked by the green cross). Isolate LT1A showed an increase in expression in both of the isomeric forms of this protein (spots 6602 and 6606) as seen in Figure 2.10. It is unclear why one organism expressed a particular isoform over the other. These differences were apparent from the start of the experiment where the isolates were grown on sodium acetate as a sole carbon source as shown in Figure 2.3, suggesting that the 4 proteins play a central role in cellular metabolism not limited to growth on alkanes.

The other protein identified in the current investigation included a TonB-dependent receptor protein (spots 1801, 2801 from Figure 2.7 and 5801, 6906 from Figure 2.8 and circled in red on Figures 2.9, 2.10). This protein (spot 1801) showed a 2 fold increase in expression from day 0 to day 20 for organism V2 (as seen by the green cross in Figure 2.9). The analysis also revealed that for organism LT1A these proteins (spots 5801 and 6906) were induced from day 0 to day 20 as seen by the green cross and green square in Figure 2.10. Once again the differences in expression of this protein between the isolates is unclear, as the visual interpretation of the gel images in Figure 2.5 revealed, the area marked by the arrow D was very poorly detected for LT1A. Both organisms possess two possible spots that fit the profile of the TonB-dependent receptor protein as seen in Table 2.4.

Peptidyl-prolyl-cis-trans isomerase (rotamase) was detected for both organisms (spot 5101 in Figure 2.7 and spot 7301 in Figure 2.8 and circled in red on Figures 2.9, 2.10). For organism V2, it was

seen to be 2-fold upregulated from day 0 to day 20 as seen by the green cross in Figure 2.9. LT1A however showed no significant change in expression of this protein as observed in Figure 2.10. The last protein that was successfully sequenced was found to be a protein containing DUF1559. This protein was present in both isolates although to a greater extent for organism V2 (spot 6401 in Figure 2.7 and spot 7605 in Figure 2.8 and circled in red on Figures 2.9, 2.10) and it showed differential regulation throughout the incubation period, unfortunately the function of this protein is unknown.

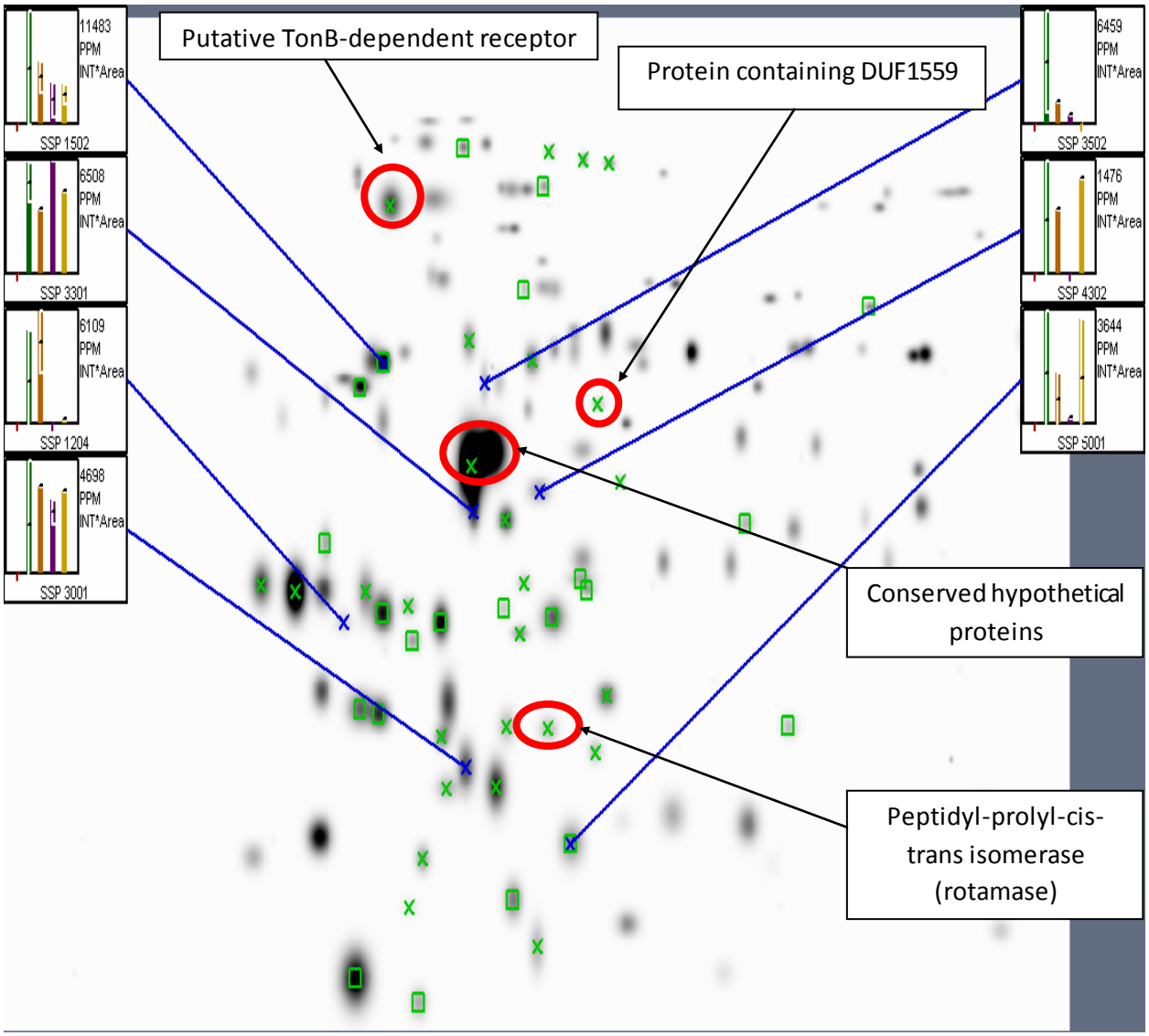

Figure 2.9 Master 2D PAGE image showing protein expression profile of *Acinetobacter* sp. isolate V2 with specific analysis sets displayed. Sequenced proteins are circled in red, and annotated. Margin graphs show relative expression of those proteins induced by C_{14} exposure as determined by PDQuest 2D Advanced software (BIORAD). Histogram Bars represent relative intensity of individual spots on set days: red (day 0), green (day 5), orange (day 10), purple (day 14), and yellow (day 20). Analysis sets represented by:

Green cross: Quantitative analysis of 2-fold upregulated proteins between days 0 and 20
Blue cross: Qualitative analysis of proteins induced by C_{14} from day 0 to day 5
Green square: Qualitative analysis of hydrocarbon induced proteins from day 0 to day 20

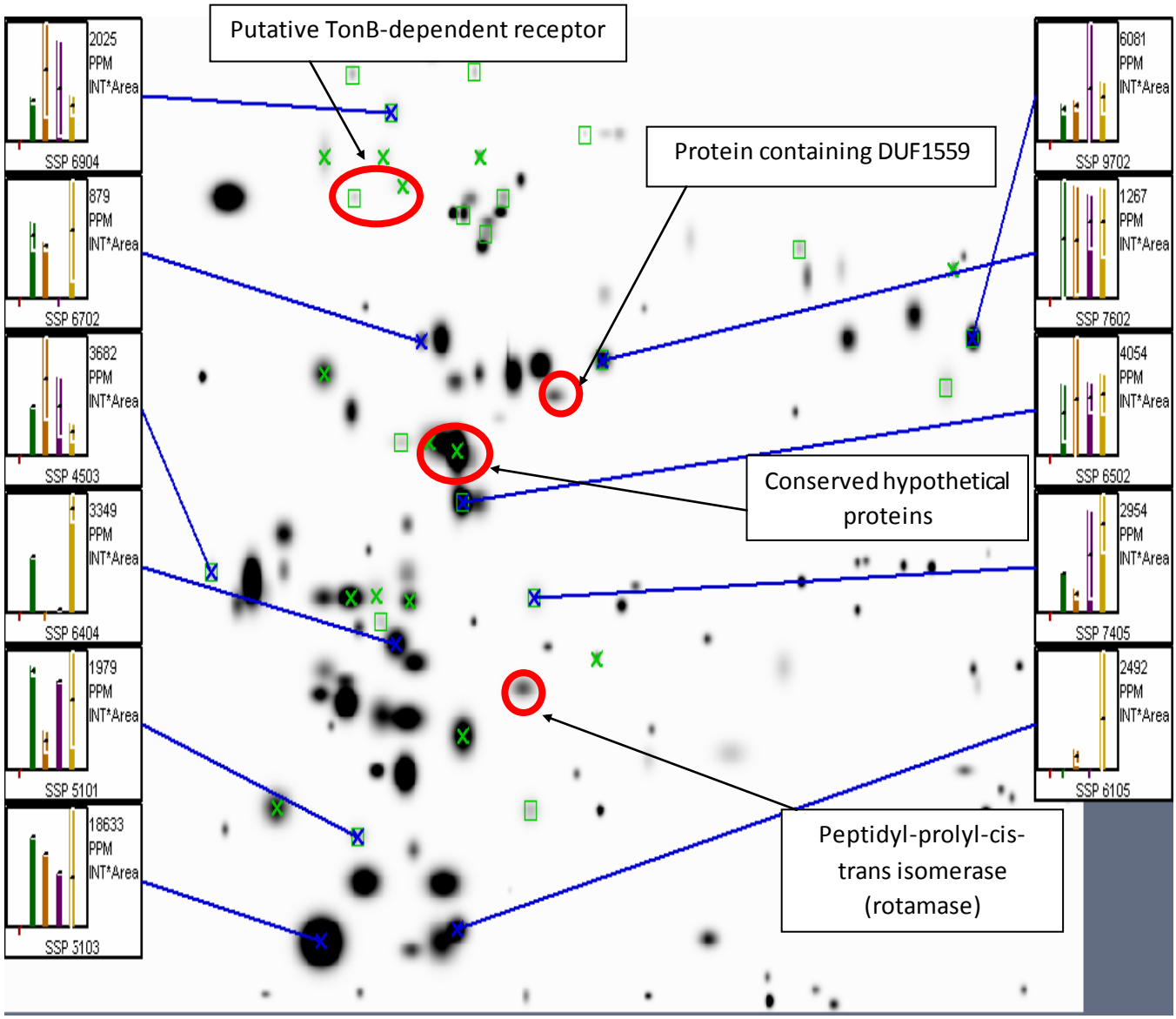

Figure 2.10 Master 2D PAGE image showing protein expression profile of *Acinetobacter* sp. isolate LT1A with specific analysis sets displayed. Sequenced proteins are circled in red, and annotated. Margin graphs show relative expression of those proteins induced by C_{14} exposure as determined by PDQuest 2D Advanced software (BIORAD). Histogram Bars represent relative intensity of individual spots on set days: red (day 0), Green (day 10), orange (day 14), purple (day 20), and yellow (day 5). Analysis sets represented by:

Green cross: Quantitative analysis of 2-fold upregulated proteins between days 0 and 20
Blue cross: Qualitative analysis of proteins induced by C_{14} from day 0 to day 5
Green square: Qualitative analysis of hydrocarbon induced proteins from day 0 to day 20

Table 2.4. Identities and functions of sequenced proteins

Spot no.		Identity	Function in cell
Figure 2.7	**Figure 2.8**		
3401, 3402	6602, 6606	Conserved hypothetical proteins	Proteins that lack homology to well-characterized proteins but whose gene product has significant similarity to a gene from another species; a protein that may possess unique functions, or be responsible for completing an as of yet incompletely verified pathway
1801, 2801	5801, 6906	TonB-dependent receptor protein	Transport of large hydrophilic molecules like vitamin B12 and iron-siderophores into the cells, most likely playing a role in iron sequestration
1501	7301	Peptidyl-prolyl-cis-trans isomerase (rotamase)	Plays a role in catalyzing the cis to trans isomerization of certain polypeptides for the folding of proteins
6401	7605	Protein containing DUF1559	Unknown

2.4 DISCUSSION

Studies that have investigated the degradation of medium-chain *n*-alkanes by *Acinetobacter* sp. have been extensively investigated from a molecular perspective, and current developments in molecular and sequencing technologies has accelerated research into bacterial biodegradative pathways at the genetic level (Ratajczak *et al*., 1998a; van Hamme *et al*., 2003; Diaz, 2004). *Acinetobacter* as a genus is highly rated in its ability to degrade hydrocarbons (70.6%-82%), and has since gained a lot of interest for the remediation of hydrocarbon contaminated environments, and the production of enzymes with biotechnological applications (Abdel-El-Haleem, 2003; Mandri and Lin, 2007; Singh and Lin, 2008; George-Okafor *et al*., 2009, Jung *et al*., 2011, Kang *et al*., 2011). *Acinetobacter* sp. isolates V2 and LT1A are capable of degrading hydrocarbon substrates, ranging from complex substrates such as diesel and used engine oil to the simpler substrate medium-chain alkane tetradecane (C_{14}) used in this study (Mandri and Lin, 2007; Singh and Lin, 2008; Toolsi, 2008). C_{14} degradation reached 85% and 87% for V2 and LT1A respectively by day 5. Studies by Plohl *et al*. (2002) demonstrated that rapid degradation

of medium-chain alkanes occurs after the first 5 days of incubation which can be attributed to the exponential phase of growth. But it is noted that the time taken for adaptation of bacteria to new carbon sources varies from minutes to days (Ballihaut *et al*., 2004). The *Acinetobacter* isolate A3 used in the study by Hanson and Desai (1996) achieved 77% degradation of the initial 0.5% v/v C_{14} concentration by day 5. Luckarift *et al*. (2011) found that the *Acinetobacter venetianus* 2AW immobilized on an adsorbent mat could achieve 85% removal of the initial 1% C_{14} concentration within a 24 hour period. The rapid degradation of the hydrocarbon substrate by isolate V2 and LT1A has been observed in previous work (Mandri and Lin, 2007; Singh and Lin, 2008; Toolsi, 2008) and further confirms the ability of these organisms to break down hydrocarbon substrates. The large amount of C_{14} lost to abiotic causes can be attributed to the volatile nature of tetradecane which has been seen in other studies (Hanson and Desai, 1996). The isolates achieved similar rates of hydrocarbon usage, as there was no significant difference in their patterns of hydrocarbon degradation (Appendix Table IIIH). This suggests that whatever strategy the isolates employ for carbon usage, they are remarkably similar in their efficiency.

In both enumeration experiments the bacterial population was seen to increase in relation to an increase in degradation of the hydrocarbon substrate, as shown in Figures 2.1 and 2.2. This result is expected as the bacteria utilize the hydrocarbon as both a carbon and energy source. The most consistent results for the enumeration of the bacterial population were obtained by enumeration on nutrient agar as optical density readings varied from actual colony counts on nutrient agar, especially by day 20. This can be attributed to a number of causes: The lower sensitivity of turbidimetry is consistent with other studies that have shown the limitations of the method in that it is unable to detect cell concentrations less than 10^7 cells/ml and is only linear between 10^7-10^9 cells/ml (Rattanasomboon *et al*., 1999). Different stress factors can affect the relationship between the OD and the cell count of microorganisms by lowering the cell viability (Francois *et al*., 2005; Reichert-Schwillinsky *et al*., 2009); cell shape can be affected by the hydrocarbon substrate (Kato *et al*., 2009); and data represented by plate counts can be misleading as it is not always certain that a colony arise from a single bacterial cell, as some cells are known to clump (Rattanasomboon *et al*., 1999). The production of Emulsan is also suspected to have complicated readings. Therefore it is accepted that the relationship between optical density and plate count data is complex (Reichert-Schwillinsky *et al*., 2009) and these two methods should be used in conjunction with one another so as to give the best representation of microbial growth.

Tetradecane is a hydrophobic substrate and thus relatively inaccessible to microbial cells. In order for this insoluble material to be utilized as a substrate it has to be incorporated into the cell so that the hydrocarbon oxidizing enzymes can come into contact with it. This can be achieved by direct contact or pseudosolubiliztion of the compound (Kaplan *et al*., 1987; Ballihaut *et al*., 2004); Bioemulsifiers increase the rate of both of these processes (Kaplan *et al*., 1987; Ballihaut *et al*., 2004). Isolates V2 and LT1A are known to produce an emulsan/ bioemulsifier (Toolsi, 2008). Emulsan, in general, is a bioemulsifier that plays an important role in degradation of hydrocarbon substrates for *Acinetobacter* sp. (Bach *et al*., 2003). It stabilizes oil-water emulsions of a variety of hydrophobic compounds (Bach *et al*., 2003). This Emulsan-like material produced by isolates V2 and LT1A was seen in the culture medium during growth on C_{14}. Emulsan is comprised of polysaccharides and proteins, and very little is known about the protein component of this bioemulsifier (Bach *et al*., 2003). What is understood however is that the release of emulsan from the cell surface is mediated by an esterase with a molecular mass of approximately 34.5 kDa in *Acinetobacter venetianus* RAG-1 (Bach *et al*., 2003). Kim *et al*. (2003) found that the esterase from in *Acinetobacter lwoffi* I6C-1 is approximately 37.5 kDa and is found in the very basic *p*I region of 9.1. The production of bioemulsifiers is dependent on the carbon source used as a growth substrate, as some bacteria favour certain carbon sources over others (Okoro, 2011). In the case of Alasan produced by *Acinetobacter radioresistens*, citrate is preferred over acetate as the carbon source for bioemulsifier activity (Navon-Venezia *et al*., 1995). It is presumed then, that the isolates V2 and LT1A would have produced an emulsan-like compound during the initial stages of growth on acetate, so the synthesis of emulsan would not be detected on the 1D SDS PAGE gels as it would also be present for growth on tetradecane. However, it is expected that the intensity of the bands represented by the cell surface esterase should increase in intensity from day 0 to day 20. A reason that the esterase was not detected on the 2D gel images may be due to the predicted isoelectric point (*p*I value) that is very basic and as was seen, not many protein spots were found in this region of the gels. And as previously revealed by Toolsi (2008), the esterase does not necessarily play a role in alkane degradation as no correlation between its expression and alkane degradation was found.

Bacteria in the current investigation were initially grown on sodium acetate as a sole carbon source prior to the inoculation of the hydrocarbon substrate to increase microbial numbers sufficiently in order to degrade the hydrocarbon. In Figure 2.3, it was shown that isolates V2 and LT1A made use of different protein systems for growth from the onset. Microbial metabolism facilitates the conversion of acetate into acetyl CoA which is fed into the glyoxylate cycle/Tricarboxylic acid cycle (Cozzone, 1998; Fischer *et al*., 2008; Paul *et al*., 2011); the conversion of acetate to acetyl CoA is an energy demanding step (Fischer *et*

al., 2008). It has been seen that for some organisms, the glyoxylate bypass is favoured over the Tricarboxylic acid cycle (TCA cycle) when acetate is used as a carbon source. One of the tell tale signs that this has occurred is to look at the expression of isocitrate dehydrogenase, an enzyme that is bypassed in the TCA cycle for the glyoxylate shunt; which is expected to show a decrease in expression levels. Unfortunately this cannot be detected in the proteome maps of either organism, since they were only grown on acetate (or the relevant carbon source) so there is no other proteome map of cells grown on an alternative carbon source to serve as a comparison. Juni (1978) first reported that *Acinetobacter* has two NADP-linked isocitrate dehydrogenases with molecular weights of 90 and 360 kDa respectively; the larger isomer comprised a tetramer of the smaller one. The isocitrate dehydrogenase enzyme from *Acinetobacter calcoaceticus* RUH2202 is approximately 82.8 kDa (Dadssi and Cozzone, 1990) and *Acinetobacter* ADP1 possesses two differentially regulated isocitrate dehydrogenases but lacks (or was undetected in the study by Barbe *et al*., 2004) malate synthase A. Malate synthase (~ 75 kDa in *Acinetobacter calcoaceticus* (Munir *et al*., 2002) and isocitrate lyase (~ 59.3 kDa in *Acinetobacter calcoaceticus* RUH2202 (Dadssi and Cozzone, 1990) and 64 kDa in *Acinetobacter calcoaceticus* B4 (Hoyt *et al*., 1991) are two other enzymes involved in the glyoxylate bypass that are expected to show an increase in expression levels. Due to the large sizes (between 60-80 kDa) of isocitrate dehydrogenase, malate synthase and isocitrate lyase, they cannot be presumptively detected on the 2D gel images, as these regions had very few, resolved proteins showing any changes in expression.

It is expected that certain proteins should be upregulated in response to growth on hydrocarbons since their emulsification and assimilation would require additional proteins to those required for growth on acetate alone. It is known that alkane utilization involves many other proteins, which would be involved in other cellular processes such as chemotactism, membrane transport systems, stress responses and cell to cell communication amongst others (Ballihaut *et al*., 2004). It is also expected that some proteins should be expressed in response to the change in environmental conditions within the medium and others should be repressed based on carbon catabolite repression favouring carbon chains of different lengths (Fischer *et al*., 2008). These proteins may not necessarily be visible on a one dimensional PAGE gel as a band on a one dimensional gel is most likely a combination of proteins of a similar size, but which posses different *p*I values. Proteins especially sensitive to carbon catabolite repression includes the protein encoded by the *alk*S gene in *Pseudomonas putida* GPo1 (Fischer *et al*., 2008), the regulator of the *alk*B1GHJ operon. This protein is approximately 98.1 kDa in *Alkanivorax borkumensis* SK2 (Sabirova *et al*., 2006) but is not detected in *Acinetobacter* ADP1, which instead has a different regulatory protein, AlkR (Ratajczak *et al*., 1998b). *Alk*R expression was previously investigated through real-time PCR

analysis with isolates V2 and LT1A when grown on diesel (Toolsi, 2008). The results from that study suggested that isolate V2 possessed two genes, namely *alk*R1 and *alk*R2 that encoded transcription regulators for *alk*M2 and *alk*M1 genes respectively. These regulators were expressed at specific time periods, in accordance with the respective hydroxylase genes (*alk*R2 was expressed from day 5 to 15, and *alk*R1 expressed from day 15 to 60). This finding had been observed by another author, Tani *et al*. (2001). The *alk*R1 gene from V2 was comparable to the *alk*R gene of LT1A (Toolsi, 2008). The gene product of *alk*R is predicted to be approximately 34.6 kDa in size for *Acinetobacter* ADP1 based on the corresponding nucleotide sequence in the Swiss-Prot data base. Unfortunately, no protein (of any significance) is detected on the 2D gel images in Figure 2.5 within this molecular weight region.

Ratajczak *et al*. (1998b) stated that there are 5 essential proteins required for alkane utilization in *Acinetobacter* sp. ADP1, these comprise: AlkM (alkane hydroxylase), rubA (rubredoxin), rubB (rubredoxin reductase), AlkR (alkane hydroxylase regulator), and xcpR (a protein involved in the general secretory pathway during alkane degradation). The expression of *xcp*R, *rub*A and *rub*B genes in *A. calcoaceticus* is known to be constitutive (Ratajczak *et al*., 1998b; Toolsi, 2008). The *xcp*R gene was found to exhibit multiple product formations for organism V2 as compared to LT1A in a previous study (Toolsi, 2008). The xcpR protein of *Acinetobacter* ADP1 has been found to be 68% similar to the amino acid sequence of the xcpR protein of *Pseudomonas aeruginosa* (Parche *et al*., 1997; Busch *et al*., 1999). The xcpR protein in *Acinetobacter baumannii* is predicted to be approximately 55 kDa, and in *Acinetobacter* sp. ADP1 approximately 49.5 (Swiss-Prot database). There are several proteins within the 50 kDa regions in Figure 2.5 that show an increase in expression from days 5 to 20, however, the lack of further information about the xcpR proteins in the literature, and lack of sequence data obtained in this study, makes it difficult to presumptively assign any of these spots this identity.

The rubredoxin and rubredoxin reductase proteins of *Acinetobacter* are constitutively expressed with xcpR, so there expression is expected to correlate with that of xcpR. The predicted protein sizes are 42.46 kDa (rubredoxin reductase, Swiss-Prot database) and 6.2 kDa (rubredoxin, Swiss-Prot database) for *Acinetobacter* sp. ADP1. Protein in the regions marked by arrows B and H (spots 1501, 1502 in Figure 2.7; 5601 in LT1A Figure 2.8) in Figure 2.5 could represent rubredoxin reductase proteins, as these are known to be acidic proteins and the molecular weights do correspond. The previous study by Toolsi, (2008), found that rubredoxin reductase gene expression could not be detected due to low expression levels. The small size of the rubredoxin protein means it is easily over-looked in both the 1D and 2D gel

images due to the nature of the polyacrylamide content that does not allow for good separation of small proteins. In the study by Toolsi (2008), rubredoxin gene expression was detected and was found to be independent of an alkane substrate. The rubredoxin and rubredoxin reductase enzymes, although necessary for alkane utilization, are also involved in other electron transfer reactions (Ratajczak *et al.*, 1998b), and detecting changes in their expression is difficult without sequence data.

The final remaining „essential' gene required for alkane utilization in *Acinetobacter* sp. is the *alk*M gene encoding an alkane hydroxylase. This *alk*M gene is related to *alk*B of *Pseudomonas putida* GPo1 (van Beilen *et al.*, 2003). The alkM protein of *Acinetobacter* sp. ADP1 is predicted to be 46.76 kDa and in *Acinetobacter baumannii*, 46.39 kDa (Swiss-Prot database). Table 2.2 shows that there were 2 separate instances within the 46 kDa region of the 2D gel images that demonstrated a difference in the number of proteins expressed by V2 as compared to LT1A. What was pointed out by the yellow squares is that V2 expresses 4 proteins of the same molecular weight, but differing *p*I values, and LT1A expresses only 2. But without adequate sequence data, the identities of these proteins can only be speculated. In the study by Toolsi (2008), isolate V2 was found to possess two *alk*M genes, designated *alk*M1 and *alk*M2, it was also noted in that study that V2 only expressed the *alk*M gene after 15 days when grown on diesel, suggesting that some other alkane hydroxylase system was in operation prior to day 15. The expression of *alk*M in LT1A revealed only one product, and was found to be down-regulated during the course of the investigation (Toolsi, 2008). Due to the complex substrate (diesel) used in the 2008 study (Toolsi, 2008), it is difficult to predict that one or more enzyme systems were involved in its degradation; the multitude of different carbon chain lengths that make up diesel, serve as substrates for a variety of enzymes at different time points. From the results from 2D PAGE in this study and RT-PCR in the previous study (Toolsi, 2008), *Acinetobacter* isolates V2 and LT1A utilize different strategies for hydrocarbon degradation.

The presence of dioxygenase or cytochrome P450 enzymes are possible alternative systems that could account for medium-chain *n*-alkane degradation activity in these isolates, as it has been noted to occur in other *Acinetobacter* spp. (Das and Chandran, 2011). The dioxygenase enzyme of *Acinetobacter* sp. M-1 was reported to be comprised of two subunits of approximately 64 kDa (Sakai *et al.*, 1996; Maeng *et al.*, 1996). Cytochrome P450 in *Acinetobacter* sp. EB104 has a predicted molecular weight of 56 kDa (Maier *et al.*, 2001). The cytochrome P450 from *Bacillus megaterium* (P450 BM-3) comprises a hydroxylase domain of approximately 64 kDa and a reductase domain of approximately 54 kDa in a single polypeptide

chain (Glieder *et al*., 2002). The identities of the sequenced proteins for isolates V2 and LT1A were assigned based on the highest scores obtained in the Mascot database search. One of the proteins was assigned the identity of a conserved hypothetical protein, however it also obtained a lower score for its similarity to a PAH dioxygenase subunit from an uncultured bacterium. More information is required in this aspect, but there is the possibility that some form of dioxygenase enzymes is present in these isolates.

Of the proteins that were successfully sequenced, no alkane hydroxylase components were detected. This does not preclude their presence in the experiment, since four of the sequenced spots represented „conserved hypothetical proteins'. These are proteins that lack homology to well-characterized proteins but whose gene product has significant similarity to a gene from another species (Elias *et al*., 2006). Although not particularly useful in this study, it is suggested that they "may possess unique functions, or be responsible for completing an as of yet incompletely verified pathway" (Elias *et al*., 2006). These four proteins, most likely isoforms, did show differences in expression between the isolates but it is unclear why one organism expressed a particular isoform over the other. These differences were apparent from the start of the experiment where the isolates were grown on sodium acetate as a sole carbon source, suggesting that the four proteins play a central role in cellular metabolism not limited to growth on alkanes. The other proteins identified in the current investigation included a TonB-dependent receptor protein. As shown in Table 2.4, these proteins transport large hydrophilic molecules like vitamin B12 and iron-siderophores into the cells (Hearn *et al*., 2008); most likely playing a role in iron sequestration (Chakraborty *et al*., 2007). Presumably this iron may play a role in the activation of the alkane substrates as it is required by the alkane hydroxylase enzyme amongst other enzymatic reactions in the cell (Rojo, 2005; Chakraborty *et al*., 2007). The reason for the allocation of 2 spot numbers instead of 1, is that the gel distortions and some other factors, have contributed to misalignment of some of the gels during the analysis, and since the identity of these spots is being inferred from their location on another gel, it cannot be said with certainty which of these 2 spots encodes the receptor protein (Appendix VB). Peptidyl-prolyl-cis-trans isomerase (rotamase) plays a role in catalyzing the cis to trans isomerization of certain polypeptides for the folding of proteins (Orozco *et al*., 1993). Although it showed differential expression between the isolates, it is involved in other cellular processes and cannot be linked to growth on alkane substrates. A protein containing DUF1559 was also found to be present in both isolates although to a greater extent for organism V2 unfortunately the function of this protein is unknown.

The small protein spots observed on all the gels, may encode proteins of some significance to this study, but were overlooked due to their low expression levels and not considered for sequencing purposes. Some

other smaller proteins were also chosen for sequencing, but resulted in poor spectra and consequently gave no results (Appendix Table IV and Figure VB). The low expression levels observed does not necessarily mean that these proteins were not involved in alkane degradation, as it is most likely that the cells only require small amounts of the proteins, especially those with high specific activity, as part of an energy conservation mechanism. As is evident in the literature, a major disadvantage with the use of 2DE as an analysis tool is the inherent reproducibility issues that are encountered with its use. These issues come about as a result of several factors that may account for the variations in protein spot detection, numbering and quantification noted in this chapter, but will be discussed in the next chapter.

Without sequence data of relevance to alkane degradation, and the general lack of protein data in the available databases, no conclusions can be made about the mechanisms these isolates employ for medium-chain alkane degradation. What can be stated though is that from the onset, the organisms employ different strategies for carbon utilization. And until there is a technology equivalent to PCR to amplify target proteins, large amounts of sample will be required to completely analyze and characterize proteins of interest (Herbert *et al*., 2001).

CHAPTER THREE

PROTEIN EXPRESSIONS AND HYDROCARBON DEGRADATION ABILITIES OF *ACINETOBACTER* SP. V2 AND LT1A DURING GROWTH ON LONG-CHAIN ALKANE, OCTACOSANE (C_{28}) AS A CARBON SOURCE

3.1 INTRODUCTION

Long chain alkanes are sometimes referred to as the paraffin waxes of crude oils, and consist of those *n*-alkanes with chain lengths greater than C_{16} that are in a solid state at ambient temperature (Tani *et al*., 2001; Wentzel *et al*., 2007). Widespread use of hydrocarbons as energy sources and the associated transport of such compounds have resulted in an increasing risk of environmental pollution (Throne-Holst *et al*., 2007; Sheppard *et al.*, 2011). The accidental release of oil into the environment poses many challenges to clean-up efforts, especially for the long chain hydrocarbon components of the oil that are less volatile and tend to persist (Wentzel *et al*., 2007; Binazadeh *et al*., 2009). Their limited bioavailability means they are hardly biodegraded by microbes as compared to shorter chain alkanes (Koma *et al*., 2001). These solid alkanes are not only a problem in oil-spill contaminated areas, as they also pose challenges in oil storage reservoirs where they cause clogging of pipes as well as problems during the transport and processing of crude oils (Throne-Holst *et al*., 2007). As the crude oil is pumped to the surface from its reservoir, the change in temperature and pressure causes the wax-like hydrocarbons present within it, to precipitate out and form deposits on the oil retrieval systems (Sood and Lal, 2007). These deposits are expensive to mechanically or chemically remove and they cost oil companies both in time and money (Sood and Lal, 2007). More relevant to our everyday lives, is the contamination of the environment with car engine oil which comprises base oils and additives; the base oil consists mainly of hydrocarbons with chain lengths between C_{16}-C_{36} (Koma *et al*., 2001). Very rarely do these waste oils get recycled or disposed of properly and little attention is paid to long chain alkanes contaminating the environment in this way (Koma *et al*., 2001).

Wax-like alkanes are also naturally synthesized by plants, algae and other organisms, and it is well known that they serve as carbon sources for a variety of bacteria (Smits *et al*., 2002; Piccolo *et al*., 2010). Taking advantage of this property, one could utilize biological remediation/removal methods which would be an economically viable option to clean up areas contaminated with a wide range of alkanes, including the long chain alkanes (Wang *et al*., 2006; Sood and Lal, 2007). Bacterial biodegradation of long chain alkanes is also considered to be a useful strategy for the recovery of oil from storage reservoirs since it results in the removal of the heavier oil components

leaving the valuable shorter chains in tact (van Beilen *et al*., 2003; Binazadeh *et al*., 2009); It also aids in the viscosity reduction of diesel and jet fuels (van Beilen *et al*., 2003).

The microbiology of alkane biodegradation has been studied, with many novel hydrocarbonoclastic bacterial isolates being described (Wentzel *et al*., 2007; Piccolo *et al*., 2010). There has also been an improvement in our understanding of long-chain alkane metabolism due to the in-depth characterization of the genes and associated enzyme systems involved. However this understanding is limited to few strains in the genera of *Acinetobacter* and *Pseudomonas* and only for alkanes up to C_{16} (Feng *et al*., 2007); the identity of the enzymes involved in the oxidation of long chain alkanes ($>C_{16}$) in most cases is still to be solved (Van Beilen and Funhoff, 2007; Wentzel *et al*., 2007; Piccolo *et al*., 2010). The exact mechanisms of long chain alkane degradation are complicated by the fact that they are often solids. This makes the isolation of mutant strains lacking certain genes very difficult in PCR-based studies (van Beilen and Funhoff, 2007). Enzyme based assays have also been unsuccessful (Tani *et al*., 2001) possibly due to the fact that a) these long chain alkanes are not soluble in water, b) the hydroxylase component is suspected to be unstable, and c) the activity of the membrane bound hydroxylase enzymes is limited by substrate mass transfer (Tani *et al*., 2001; Smits *et al*., 2002).

The complicated nature of enzyme diversity, overlapping functions of the enzymes and poorly understood regulatory pathways results in a very complex picture of long chain *n*-alkane metabolism in *Acinetobacter* spp. amongst others (Sakai *et al*., 1996; Tani *et al*., 2001; van Beilen and Funhoff, 2007). Long chain alkanes up to C_{32} are known to support the growth of *Rhodococcus* isolates, however the enzyme systems involved with this organism are unknown (van Beilen and Funhoff, 2007). *Pseudomonas fluorescens* on the other hand has been found to utilize an alkane hydroxylase that is yet to be characterized (Smits *et al*., 2002; van Beilen and Funhoff, 2007). *Pseudomonas aeruginosa* strain WatG was found to degrade C_{36} and C_{40} in a medium containing crude oil (Hasanuzzaman *et al*., 2007). The authors found that their isolate degraded these long chain alkanes better when they were combined in a medium containing crude oil and suspected that the crude oil solubilized the long chain alkanes making them available to the microbes for degradation. The authors did not look at the mechanism behind the degradation, but suggested that *P. aeruginosa* strains possess a third type of alkane hydroxylase for long chain alkane degradation.

Biochemical analysis revealed that *n*-alkane degradation by *Acinetobacter* sp. strain ODDK71 was carried out via the terminal oxidation pathway; however the authors did not investigate the specific enzymes involved in the utilization of *n*-hexadecane (Koma *et al.*, 2001). In most cases the mechanism of long chain alkane degradation remains a mystery.

Sood and Lal (2008) discovered a novel thermophilic hydrocarbonoclastic bacterium that was capable of effective degradation of paraffin wax deposits in oil wells and tubing. *Geobacillus kaustophilus* TERI NSM was found to degrade these paraffin waxes in conditions of low nutrients and high temperatures and was found to selectively degrade the long chain components leaving the valuable shorter chains in tact. This organism according to the authors is a good candidate for the treatment of oil wells with paraffin deposition problems. Feng *et al*. (2007) also described a thermophillic bacillus isolated from a deep oil reservoir in China. *Geobacillus thermodenitrificans* NG80-2 was found to grow between 45°C and 73°C and could use long-chain alkanes ranging between C_{15}-C_{36}. This organism made use of a long chain alkane monooxygenase, LadA that was found to be a key-component in alkane degradation. This enzyme has potential to be used as part of an effective treatment in bioremediation of oil polluted environments and biocatalytic processes, given its stability at high temperatures. According to Wang *et al.* (2006), thermophillic hydrocarbonoclastic organisms have several advantages in the bioremediation of hydrocarbon pollutants in that the elevated temperatures that they thrive in, result in an increase in the solubility of the hydrocarbons, decrease in their viscosity, enhanced diffusion and transfer of the long chain alkanes from solid to liquid phase making them more accessible to the cells.

Another Gram-positive organism, isolated by Piccolo *et al.* (2010) is the novel *Gordonia* sp. SoCg that was found to be capable of degrading a wide range of long chain alkanes ranging from dodecane (C_{12}) to hexatriacontane (C_{36}), a substrate range that included the solid *n*-alkanes. The study involved the cloning and sequencing of the *alk* locus. They observed functional expression of the cloned genes in heterologous hosts (unable to utilize *n*-alkanes) and *Gordonia alkB* disruption mutants revealed the role of an actinobacterial di-iron non-heme integral-membrane alkane hydroxylases in long chain alkane degradation. Interestingly the authors also found that their isolate utilized other electron transport systems, other than the rubredoxin and rubredoxin reductase containing complex.

Several *Acinetobacter* strains are known to degrade long chain alkanes with paraffin wax like properties (Maeng *et al.*, 1996; Sakai *et al.*, 1996; Koma *et al.*, 2001; Tani *et al.*, 2001; Bihari *et al.*, 2007; Mandri and Lin, 2007; Sood and Lal, 2008; Throne-Holst *et al.*, 2007). *Acinetobacter* sp. strain M-1 is known to degrade long chain alkanes from C_{20}-C_{44} (Maeng *et al.*, 1996; Sakai *et al.*, 1996; Tani *et al.*, 2001). In 1996, Sakai *et al.* validated the existence of the Finnerty pathway in *Acinetobacter* sp. M-1 isolate growing on long chain alkanes C_{16}, C_{20} and C_{30}. The Finnerty pathway postulates that *n*-alkanes are converted to an acid via the formation of an alkyl-hydroperoxide and it is accepted to be a non-conventional pathway for alkane oxidation (Maeng *et al.*, 1996). Sakai *et al.* (1996) showed that their isolate utilized the Finnerty pathway by stating that: i) *n*-alkane monooxygenase activity was not detected, ii) fatty alcohol dehydrogenase activities were low, iii) NAD(P)H-dependent fatty aldehyde reductase activity was found and iv) they also detected the reaction intermediate *n*-alkyl-hydroperoxide. They purified a flavoprotein found to be the alkane oxidizing enzyme and assumed it was a dioxygenase enzyme involved in the Finnerty Pathway. The results of the study by Tani *et al.* (2001) revealed that strain M-1 had two genes encoding alkane hydroxylases. The authors proposed a mechanism for the utilization of long chain, and very long chain hydrocarbons. The model they constructed shows that strain M-1 controls alkane hydroxylase activity in response to the chain length of the substrate; that is, the alkane hydroxylase component of the oxidizing complex, represented by AlkMa (very long chain alkanes) or AlkMb (long chain alkanes), is switched. The remaining components of this complex remain unchanged, that is, the rubredoxin and rubredoxin reductase components are constitutively expressed. But they did not investigate this on a proteomic or enzymatic level. Another isolate, *Acinetobacter* sp. strain DSM 17874 was capable of growing on *n*-alkanes ranging from C_{10}-C_{44} (Throne-Holst *et al.*, 2007). The authors found that their strain possessed at least one more enzyme system in addition to the flavin-binding monooxygenase (encoded by the *almA* gene) through the use of *almA*-deficient mutants that could still grow on alkanes C_{20}-C_{24}. The *almA* gene represented the first cloned gene for an enzyme that is involved specifically in the degradation of long chain *n*-alkanes (>C_{30}); however, *Acinetobacter* sp. RAG-1, *Acinetobacter* sp. M-1 and *Acinetobacter baylyi* ADP1 have all been shown to contain genes homologous to *almA* (Wentzel *et al.*, 2007). Bihari *et al.* (2007) isolated an *Acinetobacter haemolyticus* strain AR-46 that was capable of degrading alkanes between the C_{12}-C_{35}. The interesting findings from their study were that their isolate possessed a very unusual adherence strategy involving the utilization of thicker fimbriae to attach to the alkane droplets. The attachment was so strong that it prevented the cells from being separated from the substrate, even with intensive centrifugation. The isolate was also found to possess only

one alkane hydroxylase gene with high similarity to that of *Acinetobacter* sp. M-1 but that was activated by more than one substrate.

The long chain alkane octacosane (C_{28}) is not commonly used as a substrate for monitoring long-chain alkane degradation. The most relevant study available in the literature that looks at *Acinetobacter* sp. growing on the long chain alkane octacosane was that of Lal and Khanna (1996). The authors used biochemical analyses to trace the pathway of C_{28} oxidation by isolate S30 and found that it utilized a terminal oxidation pathway, resulting in the formation of octacosanol, but they did not look at the specific proteins or enzyme systems involved. Amongst *Acinetobacter* sp. there are a range of enzyme systems that can be used for the breakdown of long chain alkanes, implying that there are complex regulatory mechanisms governing the activation of certain enzymes over others and that there is still much to learn about this versatile organism. This chapter investigates the protein expression profiles of isolates V2 and LT1A during growth on the long-chain alkane, octacosane (C_{28}), with the intention of identifying the mechanisms used for long-chain alkane degradation by the *Acinetobacter* sp. isolates.

3.2 MATERIALS AND METHODS

3.2.1 *n*-ALKANE

The long chain alkane, Octacosane (C_{28}) (99%) was purchased from Sigma and stored at room temperature until required. The substrate was carefully measured out and added to the Bushnell Haas liquid medium and autoclaved for sterilization before use. Hereafter, the flask was stored at 4 ^{o}C until required.

3.2.2 BACTERIAL ISOLATES V2 AND LT1A

As per section 2.2.2

3.2.3 EXPERIMENTAL SETUP

As per section 2.2.3 except with the following modifications: One ml of these bacterial inocula was added to separate 250 ml Erlenmeyer flasks containing 50 ml Bushnell Haas medium, pH 7.0. The flasks were supplemented with 0.1% sodium acetate and incubated at 30°C at 160 rpm for 3 days (Ganesh and Lin, 2009). After culture growth, the flasks were supplemented with a further 50 ml BH medium containing 0.5 g octacosane as a carbon source and grown at 30°C at 160 rpm for 20 days. Controls for the experiment comprised of cells grown for three days on sodium acetate alone under the same culture conditions and another control devoid of bacterial isolates was prepared to determine abiotic losses of the hydrocarbon.

3.2.4 DETERMINATION OF BACTERIAL GROWTH PATTERNS

As per section 2.2.4

3.2.5 QUANTITATION OF HYDROCARBON DEGRADATION

The level of hydrocarbon degradation was determined using Gravimetric analysis as described in section 2.2.5 with Hexane (Merck) as the organic solvent to extract C_{28}.

3.2.6 PROTEIN EXTRACTION

As per section 2.2.6

3.2.7 PROTEIN QUANTIFICATION USING THE BRADFORD ASSAY (BRADFORD: 100-1500 mg/ml)

As per section 2.2.7

3.2.8 ONE DIMENSIONAL SODIUM DODECYL SULPHATE POLY ACRYLAMIDE GEL ELECTROPHORESIS (1D SDS-PAGE) ANALYSIS

As per section 2.2.8 Except: Gel running conditions: 500mA, 140V, 4 hours

3.2.9 TWO DIMENSIONAL POLY ACRYLAMIDE GEL ELECTROPHORESIS (2D-PAGE)

As per section 2.2.9

3.2.10 MALDI-TOF ANALYSIS OF PROTEINS

As per section 2.2.10

3.2.11 MASCOT ANALYSIS

As per section 2.2.11

3.2.12 STATISTICAL ANALYSIS

As per section 2.2.12

3.3 RESULTS

3.3.1 OCTACOSANE BIODEGRADATION ASSAY

The degradation profiles of the *Acinetobacter* isolates V2 and LT1A during the course of the 20-day degradation assay are shown in Figure 3.1. As in Chapter 2, prior to the addition of the hydrocarbon substrate octacosane (C_{28}), the isolates were grown on 0.1% sodium acetate to encourage microbial growth (Appendix Tables IIIB and IIIC). Figure 3.1 shows that bacterial growth on C_{28} was much slower than that of C_{14} (refer to Figure 2.1 in Chapter 2), only beginning to

increase substantially by day 5. C_{28} degradation reached 14% and 18% for V2 and LT1A respectively by day 5, with a corresponding increase in bacterial numbers. The bacterial population was relatively unstable after day 5 showing a drop in number on day 10 and only a slight increase on day 14. By day 20 both bacterial populations begin to drop. From day 10 fluctuations in the C_{28} degradation were observed, with organism V2 achieving a 36% degradation opposed to the 19% achieved by LT1A. But by day 20, both isolates had degraded approximately 35-37% C_{28}. This degradation was significant ($p<0.05$) for both V2 and LT1A in comparison to the abiotic control as was determined by the student t-test (Appendix Table IIH). By day 20, only 3% of the hydrocarbon loss was attributed to abiotic factors as seen in the abiotic control (Figure 3.1). The degradation patterns for V2 and LT1A were comparable, and there was no significant difference ($p=0.533$) in their utilization of the hydrocarbon substrate. Both isolates were noted to produce an Emulsan-like material during the process of degradation, which was seen to flocculate within the medium. A large standard deviation was observed during the octacosane degradation assay, especially on day 14 as is seen in Figure 3.1. In Figure 3.1 the bacterial populations are seen to decrease at day 20 as was observed on plate counts, however for the optical density readings at 600 nm, the populations were seen to increase on day 20 (Appendix Figure IIIA).

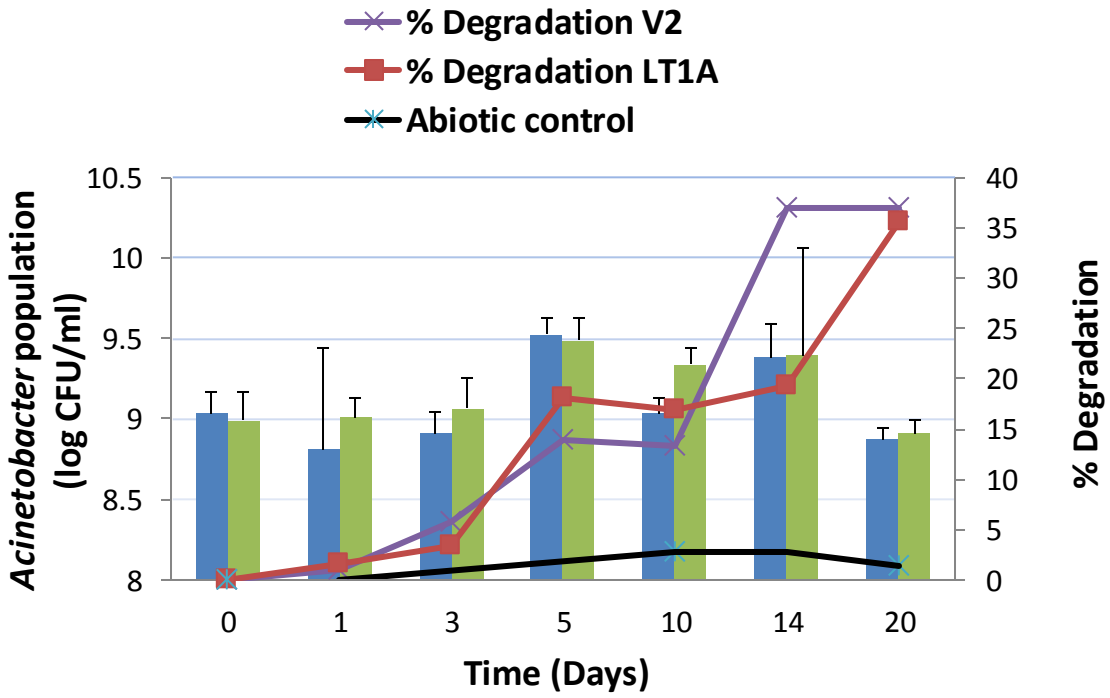

Figure 3.1 Degradation profile for *Acinetobacter* sp. V2 and LT1A grown in Bushnell Haas medium spiked with 0.5% Octacosane (C_{28}),in relation to the abiotic control. The increase in microbial populations in relation to the % C_{28} degradation over 20 days is shown. Blue bars represent growth of V2, green bars represent growth of LT1A (n=3).

3.3.2 1D SDS-PAGE ANALYSIS

Figure 3.2 illustrates the protein expression patterns of isolates V2 and LT1A when grown on octacosane for 20 days. This 1D SDS-PAGE gel image reveals that the organisms do not have many differences in protein banding patterns as compared to C_{14} (chapter 2 section 2.2.2). Areas of interest are pointed out by arrows A, B and C. Arrow A (80-90 kDa) corresponds to a protein (or combination of proteins as mentioned in Chapter 2) expressed by isolate V2 and not LT1A when grown on 0.1% sodium acetate 3 days prior to C_{28} inoculation. As was seen with tetradecane, the isolates utilize different proteins from onset. Arrow B highlights protein(s) in the 60 kDa (approximately) region that was present for both isolates between days 5 to 14 but was not detected on day 0 or day 20. Arrow C (25 kDa) points to a protein that was not present (or was not detected) on day 10 for both isolates, possibly indicating some shift in metabolism.

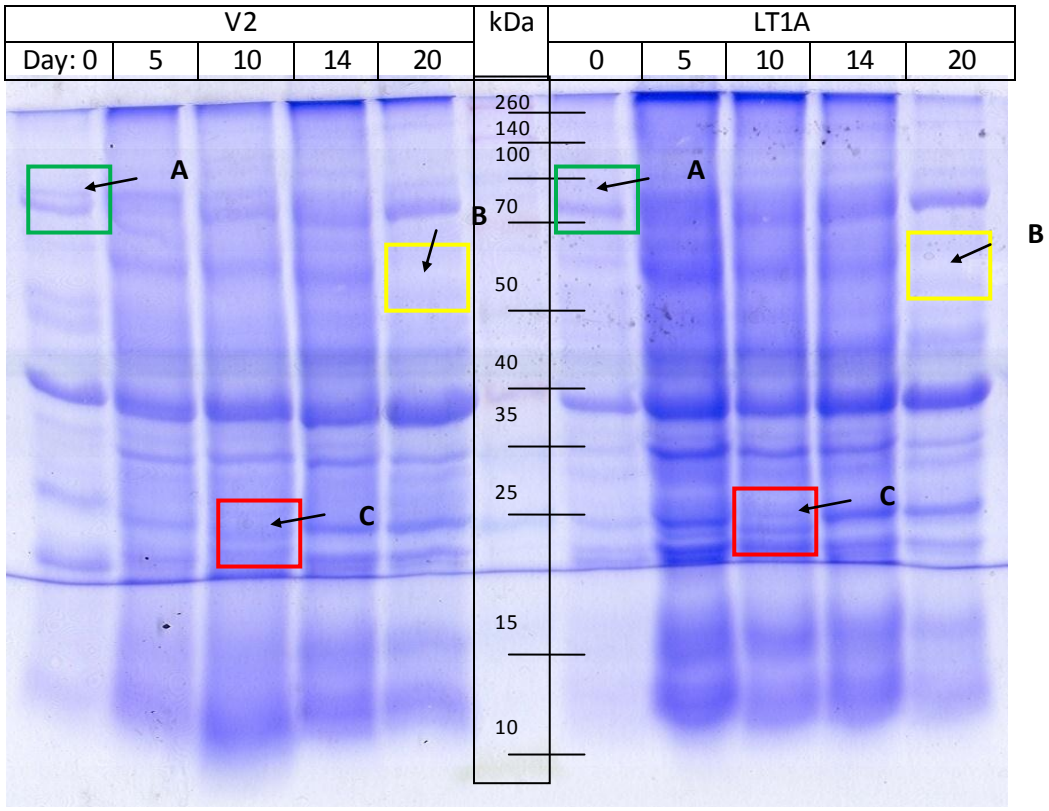

Figure 3.2 SDS-PAGE showing protein expression profiles of isolates V2 and LT1A when grown on Octacosane (C_{28}) Highlighted areas A, B, C indicate differences or similarities in protein expression. Day 0 represents the protein profiles of the organisms following growth on acetate 3 days prior to C_{28} inoculation.

3.3.3 2D SDS-PAGE ANALYSIS

Figure 3.3 shows the protein expression pattern of *Acinetobacter* sp. V2 and LT1A during growth on octacosane (C_{28}). The protein spots obtained represent those proteins found in the soluble fraction of the cell extracts. This series of images show that the proteins of isolate V2 and LT1A are well distributed across the pH range of 3-10 with most proteins appearing in the pH 4-7 region confirming what was seen in Chapter 2, that much of the *Acinetobacter* proteome is acidic. The proteins range in size from 10 to 100 kDa and very few proteins seen in the higher molecular weight regions. A visual examination of the gel images reveals the following observations:

1. The spots in the region marked A (~36 kDa, *p*I= 6) show that on day 5 organism V2 possess 3 proteins as opposed to organism LT1A that expresses only 2 at this stage. However, by day 20, organism LT1A has activated the expression of another protein, at which point it appears both isolates have the same proteins being expressed in this region as pointed out by the arrows labeled G.
2. The protein marked B (~26 kDa, *p*I= 5) is present for both organisms but appears to be required by V2 to a greater extent than for LT1A where it is weakly expressed.
3. Protein marked C (~24 kDa, *p*I= 5.8) is present for both organisms, but appears to be down regulated from day 5 to day 10 in V2, and remains unchanged in LT1A.
4. The protein in D (~20 kDa, *p*I= 5.4) is upregulated in both organisms from day 5 to 20 and corresponds to the spot marked E in Figure 2.6 (Chapter 2).
5. Spot E (~34 kDa, *p*I= 6.2) is present from day 5 to day 10, but is not detected for either organism on day 20.
6. Spot F (~45 kDa, *p*I= 5.2) is only present for organism V2. This spot corresponds to spot B in Figure 2.5 and the same observations were made with C_{14}.
7. The area pointed out by spot H (~18-20 kDa, pI= 5.5) and the red squares in the other images, is an area where the main differences in expression can be seen. On day 5, this area has very different patterns for both organisms, where LT1A appears to express 2 proteins, whereas V2 shows very poor expression of about 4 proteins in the same area. But by day 20, both isolates have similar patterns within this region.
8. The area marked by arrow I (~100 kDa, pI= 5.5) is very poorly expressed by both organisms.

9. Arrow J (~22 kDa, pI= 5.8) points to a protein spot that is down regulated in organism LT1A, from day 5 to 10, and does not appear in organism V2.
10. Spots K (~19 kDa) and L (~20 kDa) in the pH region of about 5.4 for organism LT1A, are upregulated from day 5 to 10, but then down regulated by day 20. These spots do not appear for organism V2.

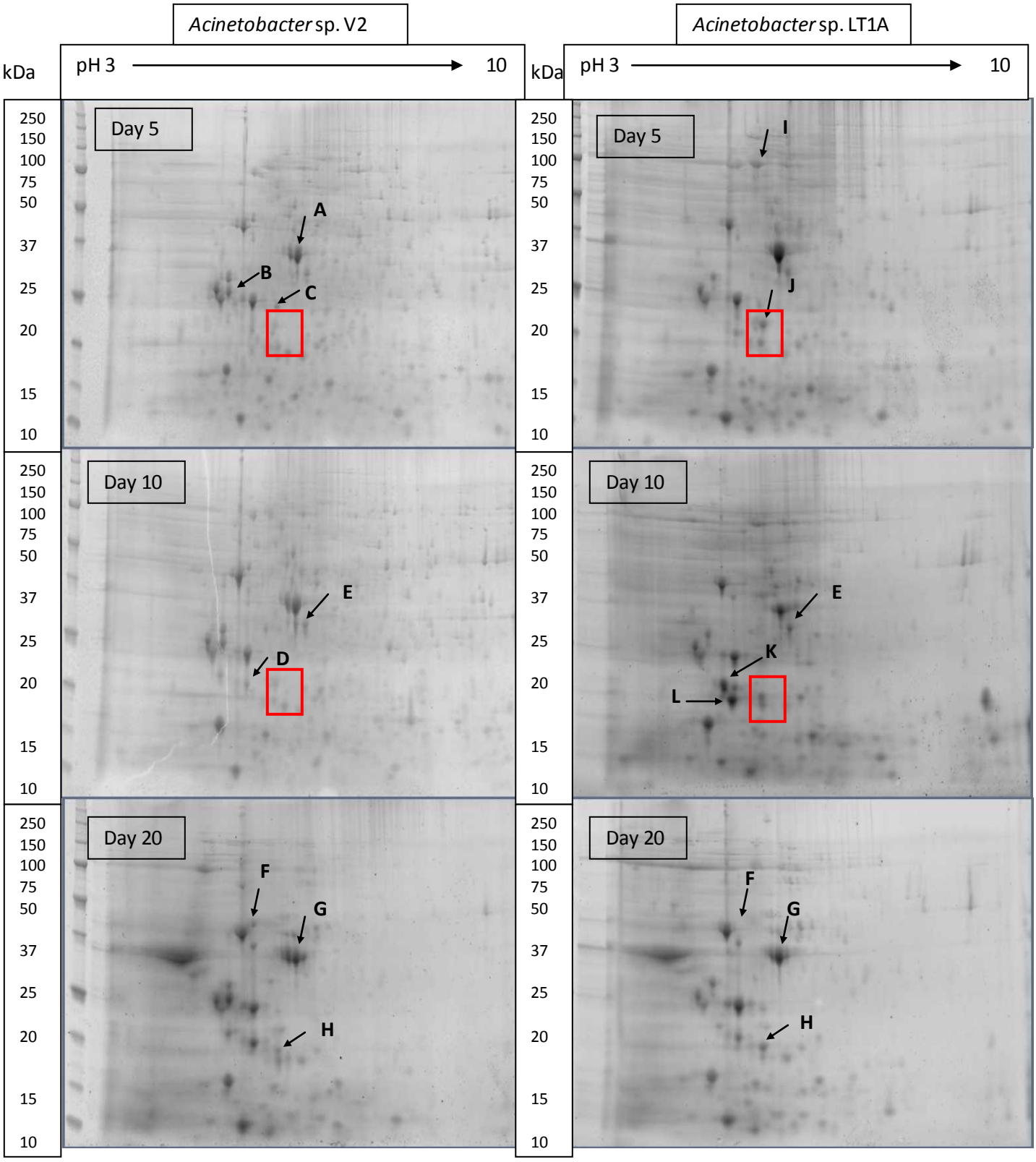

Figure 3.3 Selected 2D SDS-PAGE protein expression profiles of *Acinetobacter* sp. isolate V2 and LT1A. Spots to be discussed are indicated by arrows and are referred to by the corresponding letter (A, B, C, D etc.) or coloured shape.

Once again, the use of the BugBuster Master mix to lyse the bacterial cells achieved good results in terms of protein extraction as can be seen from the Oriole (BIORAD) stained 2D images (Figure 3.3) and Figure 3.4 that show that protein distribution occurs across a broad range of molecular weight regions and *p*I values between 4 and 9. As can be seen, majority of these up or down regulated proteins appear in the 20-60 kDa region, with very few proteins in the higher molecular weight areas (<100 kDa) especially for organism LT1A (Appendix Table IIIE). Organism V2 displayed 38 proteins showing a 2 fold increase or decrease in expression, 15 of which were upregulated from day 0 to day 20. Organism LT1A displayed only 27 proteins, 18 of which were upregulated from day 0 to 20. Once again, the pH 3-10 IPG strips used to separate the protein samples ensured a good separation of all soluble proteins across the widest range possible so as to give the best representation of the proteomes of each isolate as was observed in Chapter 2.

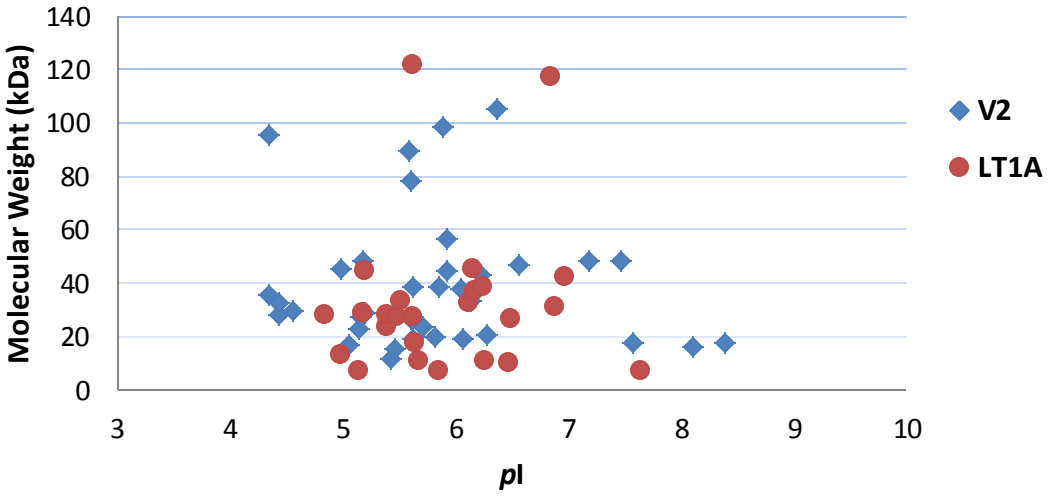

Figure 3.4 Spot distribution patterns in terms of molecular weight and *p*I (isoelectric point) for those proteins showing a 2-fold increase or decrease in expression levels for organisms V2 and LT1A from day 0 to day 20 as determined by PDQuest™ Advanced 2-D analysis software (version 8.0.1, BIO-RAD, USA).

Table 3.1 illustrates the qualitative analysis of the 2D gel images for isolates V2 and LT1A. The values shown in the table represent averages for duplicate samples (n=2) (Appendix table IIIF). The correlation between the day 5 sample (master gel) and the day 0, 5 and 14 samples for organism V2 was low, while day 10 and day 20 samples showed good correlation to the master gel with r values = 0.595 and 0.58 respectively. All LT1A samples showed a good correlation to the master gel (day 5) with r values of 0.862, 0.555, 0.776 and 0.622 obtained for days 5, 10, 14 and 20

respectively, with a poor correlation obtained for day 0. The match rates to member gels (match rate 1) and match rates to the master gel (match rate 2) were relatively low for both organisms corresponding to the low number of spots matched to the master using automated matching and manual corrections during analysis as was seen for chapter 2 results. The use of a cleanup kit resulted in good separation of the proteins with little to no streaking thus producing good 2D images for analyses. The total spot numbers on the 2D gels were detected using PDQuest™ Advanced 2-D analysis software (version 8.0.1, BIO-RAD, USA), and the gels with the most spots and least background interference were chosen as the master gels and used for spot detection parameters as stated in section 2.2.9.4. A master gel containing all the spot attributes for each experimental set was created (Figures 3.6 and 3.7). The software was selected to normalize spot quantities based on the total pixel intensity within spot boundaries of Gaussian spots. This normalized spot quantity was equal to the raw spot quantity expressed as a percentage of the total pixel quantity of all spots in a gel (Ganesh and Lin, 2011) (Apppendix Table IIIG).

Table 3.1. Qualitative analysis of 2-DE separated proteins as determined using PDQuest ™ Advanced 2D analysis software for both *Acinetobacter* sp. isolates V2 and LT1A

Gel group	Spots (*n*=2)	No. of spots matched to master	Match Rate 1	Match Rate 2	Correlation Coefficient
Isolate V2					
C28 d0	90	51	56%	18%	0.433
***C28 d5**	180	157	84%	57%	0.379
C28 d10	174	102	58%	37%	0.595
C28 d14	177	93	53%	34%	0.477
C28 d20	228	129	57%	47%	0.58
Isolate LT1A					
C28 d0	108	59	54%	29%	0.461
***C28 d5**	140	123	84%	61%	0.862
C28 d10	165	100	67%	50%	0.555
C28 d14	138	94	69%	47%	0.776
C28 d20	131	74	56%	37%	0.622

*master gel

Match rate 1: no. of matched spots on gel, relative to member gel

Match rate 2: no. of matched spots on gel, relative to master gel

Correlation coefficient relative to master gel

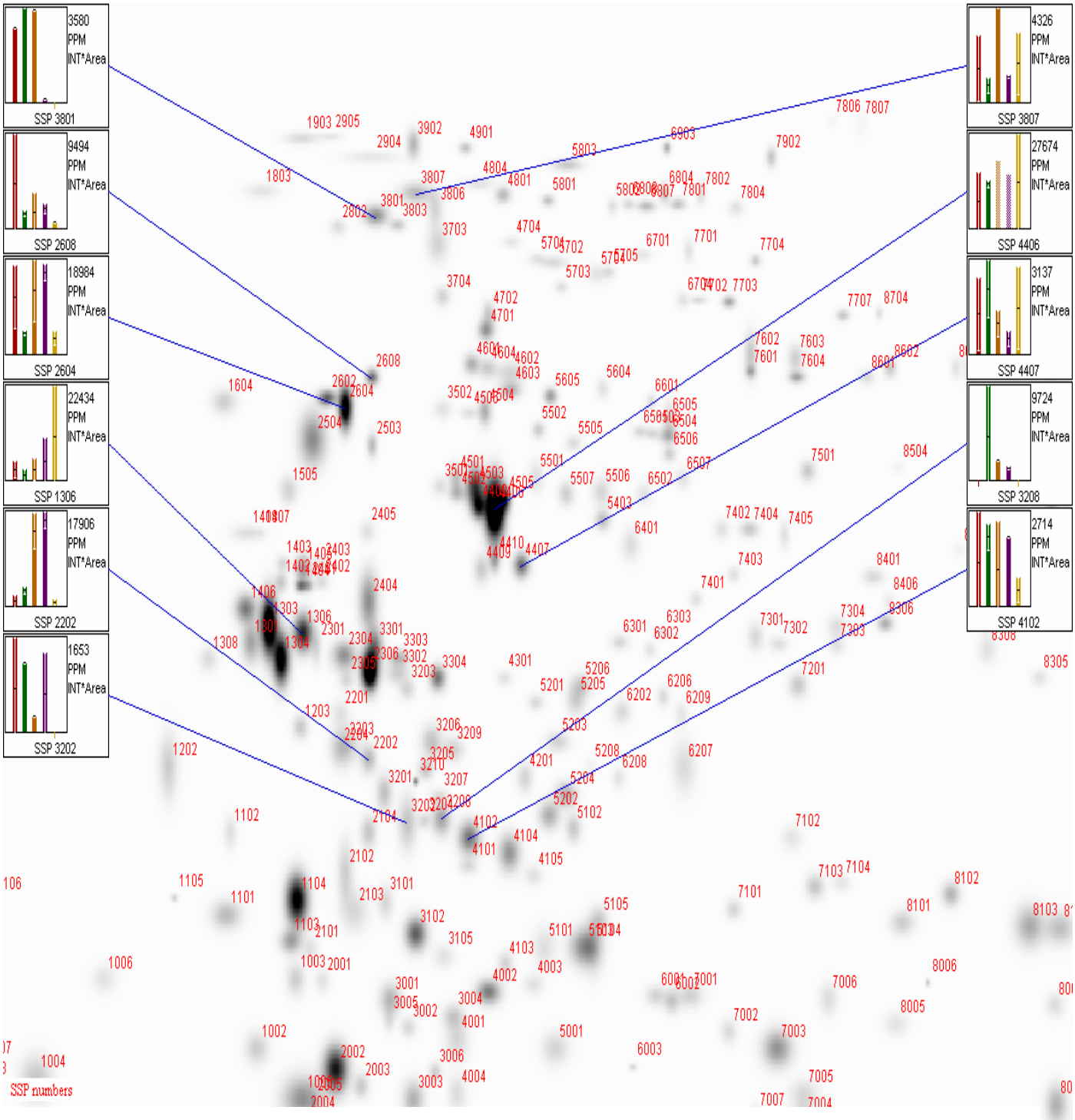

Figure 3.5 Master 2D PAGE image showing protein expression profiles of *Acinetobacter* sp. isolate V2. Margin graphs show relative expression for the specified spots as determined by PDQuest 2D advanced software (BIORAD). Spots are numbered in red. Normalization values determined by total density in gel image due to saturated spots present in some members of the experiment and Histogram Bars represent relative intensity of individual spots on set days: red (day 5), green (day 10), orange (day 14), purple (day 20), and yellow (day 0). Spot numbering and corresponding markers in Figure 3.4: 4406: arrow A and G; 1306: arrow B; 3304: arrow C; 2202: arrow D; 4407: arrow E; 2608: arrow F; 4102: arrow H.

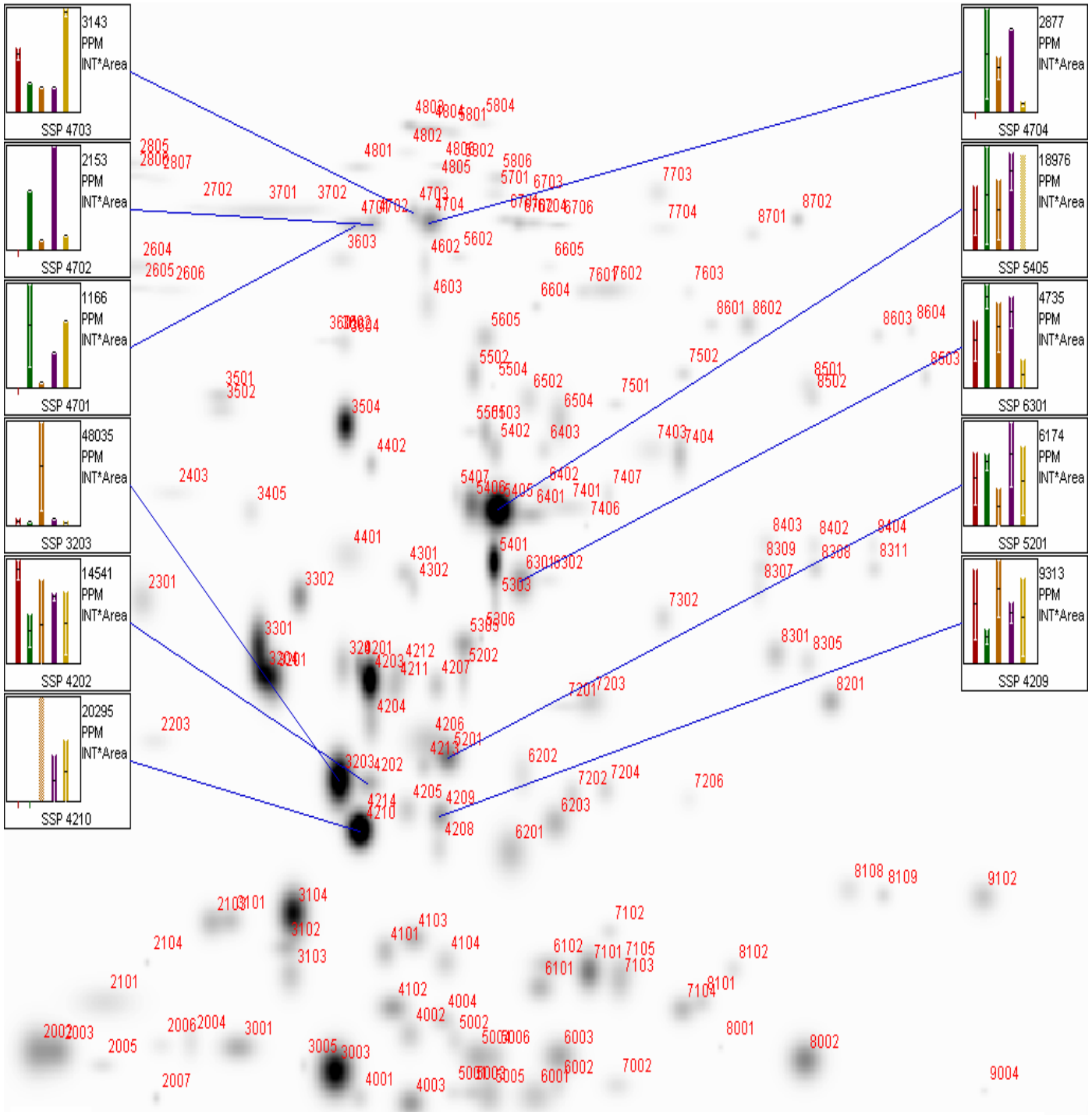

Figure 3.6 Master 2D PAGE image showing protein expression profiles of *Acinetobacter* sp. isolate LT1A. Margin graphs show relative expression for the specified spots as determined by PDQuest 2D Advanced software (BIORAD). Spots are numbered in red. Normalization values determined by total density in gel image due to saturated spots present in some members of the experiment (Raw data in appendix) and Histogram Bars represent relative intensity of individual spots on set days: red (day 0), green (day 5), orange (day 10), purple (day 14), and yellow (day 20). Spot numbering and corresponding markers in Figure 3.4: 6301: arrow E; 5405: arrow G; 5201: arrow H; 4701, 4702, 4703, 4704: arrow I; 4209: arrow J; 3203: arrow K; 4210: arrow L.

In most cases, the visual observations of Figure 3.4 are confirmed by the 2D master gel images obtained in Figures 3.5 and 3.6, as is pointed out by the histograms showing relative expression levels. Figures 3.7 and 3.8 represent the same master gel images seen in Figures 3.5 and 3.6, except that they highlight specific analysis sets created using PDQuest Advanced 2D image analysis software (BIORAD). These analysis sets were created to point out specific areas of interest within the protein expression profiles of each isolate as defined in Table 3.2. The analysis sets created offer an unbiased interpretation of the gel images using computer software. Table 3.2 shows that few spots were detected for each category as was seen in Chapter 2. Those proteins that were upregulated 2-fold between days 0 and 20 are pointed out by the green cross. These are proteins most likely involved in long chain alkane degradation, as well as other cellular processes related to growth. Gel images for V2 showed 15 upregulated proteins, whereas LT1A displayed 18. Qualitative analysis of those proteins absent/undetected on day 0 but present by day 5 (indicated by the blue crosses) revealed 50 and 30 proteins for V2 and LT1A respectively. These are proteins most likely to be involved in the adaptation to long chain-alkane degradation. Those proteins that were not detected on day 0 but were present by day 20 are indicated by the green square. As expected, more proteins are seen as compared to the day 0-day 5 analysis set (blue crosses) with 55 being detected for V2, but unexpectedly LT1A shows fewer proteins, with only 17 protein spots being detected between days 0 and 20. Sixty-four protein spots were found to show a statistically significant change in expression from day 0 to day 5 for isolate V2, and of these spots, only 19 were found to be specifically induced by C_{28}. LT1A displayed only 19 spots with statistically significant changes in expression between days 0 and 5, and of these, only 9 were induced by the long chain alkane substrate. Spots showing differential expression between the isolates, based on samples run at the Proteomics Research group at the University of the Western Cape, were sequenced (Appendix Table IV and Figure VC). These are labeled accordingly in Figures 3.7 and 3.8. The exact locations of these sequenced proteins are based on assumptions and visual interpretations from the results obtained in Chapter 2. These proteins were found to be similar between the degradation processes for both medium and long chain alkanes and presumed to be involved in alkane degradation. Although more spots were selected for sequencing, they generated poor spectra and consequently gave no results.

Table 3.2. Overview of expression patterns for both *Acinetobacter* sp. Isolates V2 and LT1A, as determined by PDQuest 2D Advanced software (BIORAD)

Expression pattern	V2	LT1A	Analysis type*	Designation in Figures 3.7 and 3.8
	Number of spots			
2-fold or greater upregulated spots (Day 0-Day 20)	15	18	Quantitative	Green cross
C28 induced proteins (Day 0-Day 5)	50	30	Qualitative	Blue cross
C28 induced proteins (Day 0-Day 20)	55	17	Qualitative	Green square
Spots showing statistically significant change in expression (Day 0-Day 5)	64	19	Statistical (95%)	N/A
Statistically significant spots induced by C28 (Day 0-Day 5)	19	9	Boolean	N/A

*Definitions:
Quantitative: Spots whose quantity has increased or decreased "X-fold" (X: user determined)
Qualitative: Spots present in one gel image and absent from another, but showing a 10-fold expression level over the background
Statistical: Composed of spots that are significant based on student t-test with $p<0.05$
Boolean: Created by comparing 2 or more analysis sets
N/A: Not applicable

Due to the extensive costs involved, only 14 spots were selected for MALDI-TOF-MS sequencing across the tetradecane and octacosane assays (Table 3.3). Those spots chosen to be sequenced were determined based on obvious changes in expression between the isolates, but that were similar to both assays. Of the spots that were sequenced, 4 spots (4406, 4502 from Figure 3.5 and 5405, 5406 from Figure 3.6 and circled in red on Figures 3.8, 3.9) represented 'conserved hypothetical proteins'. These 4 proteins did show differences in expression between the isolates. As shown in Figure 3.4, the results show that organism V2 expressed 3 proteins on day 5 (in the region marked by A, ~36 kDa, *p*I= 6) as opposed to organism LT1A that expresses only 2 at this stage. It is possible that the proteins are isomers that differ perhaps in their phosphorylation states. They were induced from day 0 to day 5 for organism V2, showing at least a 2-fold increase in expression levels as indicated by Figures 3.7 (marked by the green crosses). Isolate LT1A showed an increase in expression of one of the isomeric forms of this protein (spot 5405) as shown Figure 3.6, but its expression relative to day 0 was not significantly different; consequently it was not detected by the software as seen in Figure 3.8. It is unclear why one organism expressed a particular isoform over the other as was seen with Chapter 2. As stated in Chapter 2, these differences were apparent from the start of the experiment where the isolates were grown on sodium acetate as a sole carbon source,

suggesting that the 4 proteins play a central role in cellular metabolism not limited to growth on alkanes.

The other proteins identified in the current investigation included a TonB-dependent receptor protein (spots 3801, 3807 from Figure 3.5 and 4701, 4702, 4703, 4704 from Figure 3.6 and circled in red on Figures 3.7, 3.8). Although no differences in expression relative to day 0 were observed for organism V2 (as seen in Figure 3.7) the analysis revealed that for organism LT1A it was induced from day 0 to day 5 as seen by the blue crosses in Figure 3.8. Once again the reason for the differences in expression of this protein between the isolates is unclear. The resolution of the gel images by the arrow I (~100 kDa, *p*I= 5.5) was very poor for both isolates. LT1A has 4 protein spots that fit the profile of the TonB-dependent receptor protein as seen in Table 3.3. The reason for the allocation of 4 spot numbers instead of 2, is that the gel distortions and some other factors, have contributed to misalignment of some of the gels during the analysis, and since the identity of these spots is being inferred from their location on another gel, it cannot be said with certainty which of these 4 spots encodes the receptor protein (Appendix VB).

The last protein sequenced, encoded a peptidyl-prolyl-cis-trans isomerase (rotamase). This protein (spots 5102, 5202, and 5204 in Figure 3.5and spots 6203, 7202, and 7204 in Figure 3.6 and circled in red on Figures 3.7, 3.8) although showing differential expression between the isolates, is unfortunately involved in other cellular processes and cannot be linked to growth on alkane substrates. Organism V2 has one protein in this region that shows a 2-fold increase in expression from day 0 to day 20, as seen by the green cross in Figure 3.7. LT1A has one protein within this area that was induced from day 0 to day 5, as seen by the blue cross in Figure 3.8. A protein containing DUF1559 was also found to be present in both isolates (spots 6503, 6504, 6506 in Figure 3.5 and spots 7403, 7404 in Figure 3.6 and circled in red on Figures 3.7, 3.8) and it showed differential regulation throughout the incubation period. For organism V2, it was found to be induced between days 0 and 5 as marked by the blue crosses in Figure 3.7 and for LT1A it was found to display a 2-fold increase in expression between days 0 and 20 (Figure 3.8). Unfortunately the differences in expression cannot be explained, as the function of this protein is unknown.

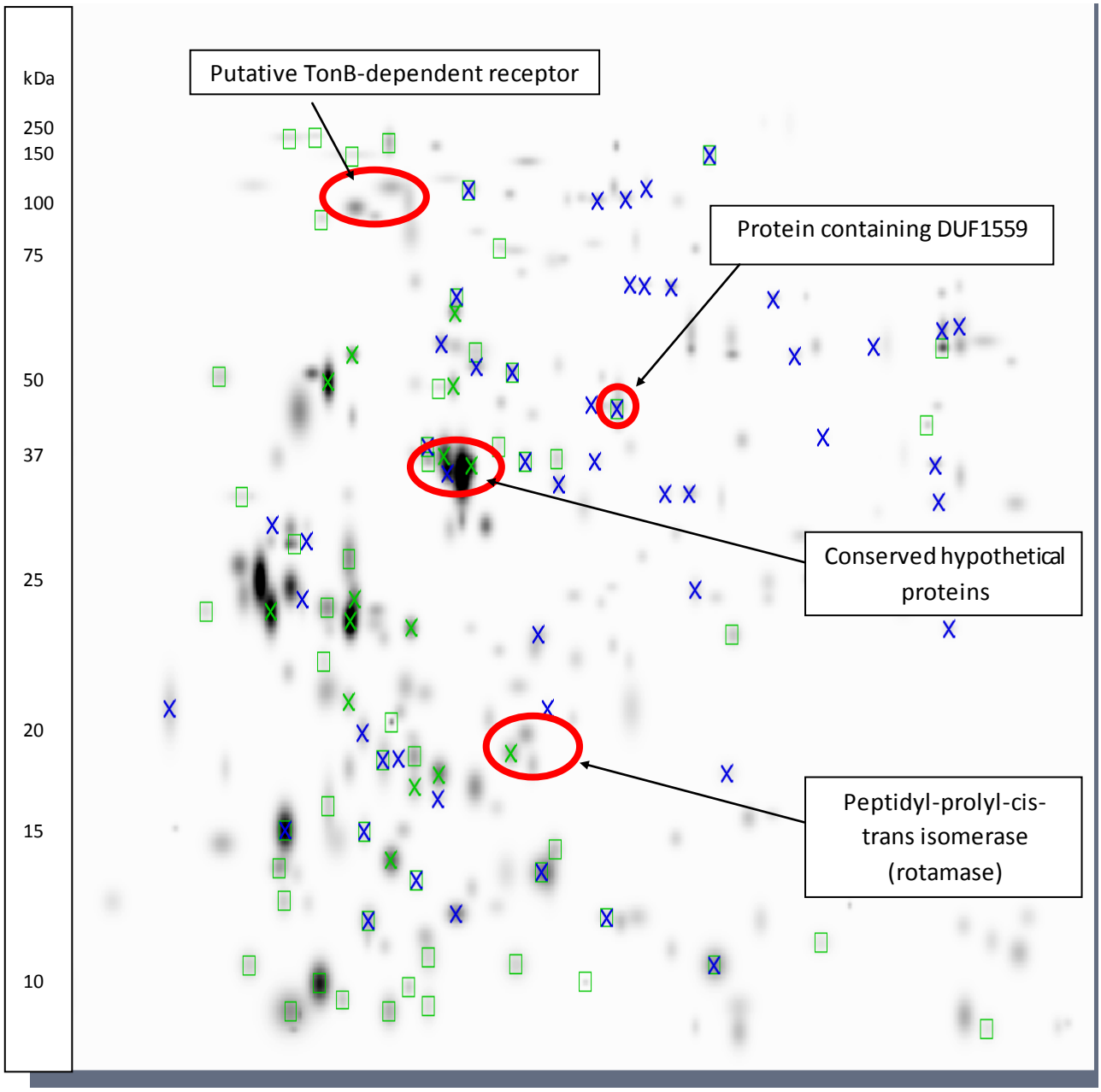

Figure 3.7 Master 2D PAGE image showing protein expression profile of *Acinetobacter* sp. isolate V2 with specific analysis sets displayed. Sequenced proteins are circled in red, and annotated. Analysis sets represented by:

Green cross: Quantitative analysis of 2-fold upregulated proteins between days 0 and 20
Blue cross: Qualitative analysis of proteins induced by C_{28} from day 0 to day 5
Green square: Qualitative analysis of hydrocarbon induced proteins from day 0 to day 20

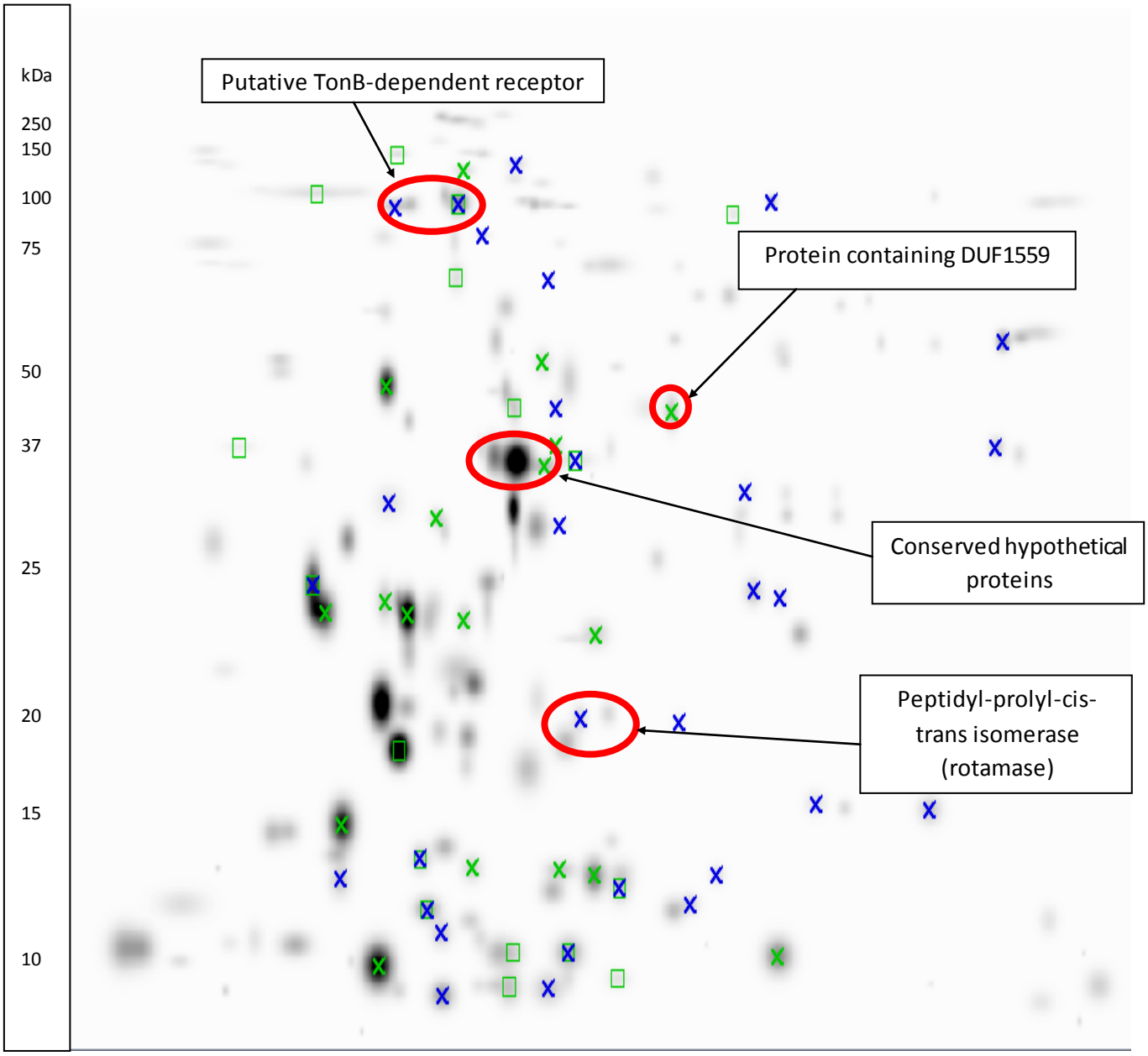

Figure 3.8 Master 2D PAGE image showing protein expression profile of *Acinetobacter* sp. isolate LT1A with specific analysis sets displayed. Sequenced proteins are circled in red, and annotated. Analysis sets represented by:

Green cross: Quantitative analysis of 2-fold upregulated proteins between days 0 and 20
Blue cross: Qualitative analysis of proteins induced by C_{28} from day 0 to day 5
Green square: Qualitative analysis of hydrocarbon induced proteins from day 0 to day 20

Table 3.3. Identities and functions of sequenced proteins

Spot no.		Identity	Function in cell
Figure 3.5	**Figure 3.6**		
4406, 4502	5405, 5406	Conserved hypothetical proteins	Proteins that lack homology to well-characterized proteins but whose gene product has significant similarity to a gene from another species; a protein that may possess unique functions, or be responsible for completing an as of yet incompletely verified pathway
3801, 3807	4701, 4702, 4703, 4704	TonB-dependent receptor protein	Transport of large hydrophilic molecules like vitamin B12 and iron-siderophores into the cells, most likely playing a role in iron sequestration
5102, 5202, 5204	6203, 7202, 7204	Peptidyl-prolyl-cis-trans isomerase (rotamase)	Plays a role in catalyzing the cis to trans isomerization of certain polypeptides for the folding of proteins
6504, 6506, 6503	7404, 7403	Protein containing DUF1559	Unknown

3.4 DISCUSSION

Bacterial oxidation of *n*-alkanes is known to occur naturally in both soil and water; it plays a major role in the geochemical recycling of oil originating from natural or accidental spills (Smits *et al*., 2002; Van Beilen *et al*., 2003). The microbial biodegradation of alkanes was established a century ago (Van Beilen *et al*., 2003) and to this day serve as important bioremediation agents. For example, Gram positive and Gram negative bacterial isolates have been employed on an industrial scale for the degradation of oil (Bihari *et al*., 2007). In particular, *Acinetobacter* species have been used for the break down of the long-chain components of crude oil (Bihari *et al*., 2007). The rapid biodegradation of long-chain alkanes is desirable for bioremediation of oil contaminated areas and for enhanced oil recovery (Binazadeh *et al*., 2009). A better understanding of the enzyme systems

and regulatory mechanisms involved in long-chain alkane degradation will have huge implications for oil spill cleanups, removal of wax deposits in oil systems and other oil related issues.

In laboratory studies the *n*-alkanes pose challenges for alkane degradation in that they are immiscible with water, and tend to form a layer at the surface of the liquid medium, making it difficult for microbes to come into contact with, and degrade the substrate (Koma *et al.*, 2001; Wentzel *et al.*, 2007; Binazadeh *et al.*, 2009). A true reflection of the microbes' ability to degrade long chain alkanes would be for them to degrade these most persistent wax-like alkanes. In this study, the *Acinetobacter* sp. isolates V2 and LT1A demonstrated the ability to degrade octacosane, a solid, wax-like alkane in a liquid medium. The degradation of the longer chain alkane C_{28}, was much slower than that of C_{14} (Chapter 2) and appeared to have a lag phase of about 3-5 days before the compound was utilized and microbial numbers increased, as was seen in Figure 3.1. The longer period of time for bacterial adaptation to this carbon source is understandable, as it is accepted that it is an energy demanding and stress-inducing process both for the uptake, and breakdown of this very insoluble material (Lal and Khanna, 1996; Marino, 1998; Jung *et al.*, 2011). The very long-chain alkanes are known to be resistant to microbial degradation (Bagherzadeh-Namazi *et al.*, 2008). Microbial adaptation to the new carbon source would require some change in physiology such as a change in the metabolic functions required for hydrocarbon uptake amongst others (Ballihaut *et al.*, 2004). One of the major changes may have been the production of the Emulsan-like bioemulsifier, by both isolates. As mentioned in Chapter 2, the isolates produce a biosurfactant that plays an important role in the solubilization of hydrocarbon compounds. This biosurfactant would have been especially important in the case of C_{28} degradation since it was the most inaccessible carbon source the isolates were exposed to; and it has been shown that the critical, growth-limiting factor in biodegradation studies is the bioavailability of the long-chain alkane substrate (Lal and Khanna, 1996).

The percentage degradation of C_{28} for both isolates was significant when compared to the abiotic control (Appendix Table IIIH). And there was no significant difference in the alkane utilization between the isolates suggesting that their strategies for long chain alkane degradation are rather similar. It has been reported that the efficiency of the long chain alkane hydroxylase system decreases with an increase in chain length (Piccolo *et al.*, 2010). On this note, both isolates achieved approximately 35-37% degradation of the initial 0.5% (w/v) C_{28} by day 20 with slight fluctuations being observed on day 10 (Figure 3.1). The fluctuations can be attributed to the nature

of the substrate, which has a very fine crystalline structure that after autoclaving was noted to form clusters that resembled flakes of plastic that floated on the surface of the medium (Appendix VA). Although every precaution was taken to minimize variability in the substrate from one experiment to another, it is still most likely to have some effect on the observed fluctuations in degradation patterns. In the literature, studies involving C_{28} degradation by *Acinetobacter* spp. specifically are rare. The study by Marino (1998) found that out of all the isolates used, the two *Acinetobacter* spp. were unable to grow on paraffin wax as a sole source of carbon. In the study by Lal and Khanna (1996) their isolate, *Acinetobacter calcoaceticus* S30, utilized about 70% of the intitial 0.26% (w/v) C_{28} concentration within 40 hours. The higher bacterial inoculum size of 5% as opposed to the 1% used in the current study, may have contributed to the faster degradation rate seen with their isolate, but what is noticed is that the amount of C_{28} degraded by the end of both studies is comparable, taking into account the initial starting concentrations. In the study by Bagherzadeh-Namazi *et al.* (2008), octacosane was used as an index for biodegradation of used engine oil; *Pseudomonas* sp. was capable of degrading 51% of the initial 0.5% C_{28} inoculum within 100 hours. The increased degradation rate can be attributed to the fact that the C_{28} substrate was solubilized in hexane prior to addition to the culture medium. This solubilization would have greatly improved the degradation process due to the improved accessibility of the substrate to microbial degradation. However, this method of solubilization may not be practical from a biotechnological point of view.

Fluctuations in bacterial numbers were observed throughout the study, both with optical density readings and with plate count data (Appendix Figure IIIA and Figure 3.1 respectively). The differences between plate count data and optical density (OD) readings have already been discussed in Chapter 2. The presence of the fine crystals of the C_{28} substrate, in addition to the Emulsan, can also affect the OD readings. These crystals were suspended throughout the shake flask cultures during the incubation period and are likely to have interfered with light absorption and deflection resulting in elevated and irregular cell counts. For the plate count data (Figure 3.1) it was observed that by day 20 both bacterial populations were seen to drop. The drop in microbial numbers can be due to a number of factors such as the build up of intermediates; and the depletion of micronutrients in the shake flasks as it is well known that microbial metabolism and growth depends on adequate supplies of essential macro- and micro-nutrients (Thomas, 1996). Cellular accumulation of the insoluble material can also have a detrimental effect on the cells (Marino, 1998). Other fluctuations in bacterial growth patterns may be related to shifts in metabolism during growth on the long-chain

hydrocarbon substrate. These shifts were noted on the 1D SDS PAGE gel in the ~60 kDa region on day 20 and ~25 kDa regions on day 10 (Figure 3.2) but were not detected on the 2D PAGE images for both isolates. These changes are possibly not detected on the 2D gels because a band on a 1D gel can be comprised of more than one protein of the same molecular weight. As seen in Figure 3.3, the 60 kDa region of the 2D gel images was poorly visualized for both isolates. There are several proteins in the 20-25 kDa region (marked with the red blocks) of the 2D gel images in Figure 3.3 that showed certain changes in expression on day 10, particularly for LT1A. Unfortunately the identity of these proteins is unknown; their molecular weights do not correspond to any of the alkane hydroxylase components discussed in Chapter 2.

Abiotic losses of the C_{28} substrate were low (~3%) compared to C_{14}, and probably not due to volatilization. Long-chain alkanes in general are very stable substrates that tend to resist degradation and persist in the environment (Okoh, 2006; Feng *et al*., 2007; Rios *et al*., 2007). It is known that solid alkanes tend to clump together, reducing the surface area available for microbial degradation and contributing to slower growth rates (Marino, 1998). Abiotic losses and fluctuations in the % degradation (Figure 3.1) are most likely due to the extraction process and cellular accumulation of the substrate in some cases (Lal and Khanna, 1996). C_{28} when extracted with hexane, forms fine crystals that tend to 'climb' up the sides of the beaker as the hexane is evapourated (Appendix V). Even during the extraction process small amounts of crystals were lost as the hexane rapidly dissipated, leaving the crystals adhered to the separating funnel, containing anhydrous sodium sulphate, and other apparatus that came into contact with the hexane-octacosane phase (Appendix V). Although the losses do not dramatically affect the results, future attempts at degradation studies using octacosane, should take this into account.

A comparison of C_{14} and C_{28} utilization by the isolates can be drawn using Table 2.3 (Chapter 2, pg 53) and Table 3.2 (pg 83). From these tables it can be seen that for both isolates, more proteins were induced from day 0 to day 5 for the C_{28} assay as compared to the C_{14} assay. Implying that there are more proteins involved in the utilization and adaptation to growth on long chain alkanes as compared to the shorter chain alkanes. It could also be a function of protein concentration, as the carbon rich substrate C_{28} may have contributed to increased protein production and hence greatly improved the number of proteins that could be detected in the 2D gel images. Figures 2.6 (Chapter

2, pg 47) and Figure 3.4 (pg 78), illustrate that the protein distributions are slightly different for both organisms when comparing C_{14} and C_{28} utilization: more proteins are 2 fold up or down regulated, in the larger molecular weight regions (>100 kDa) for the C_{14} assay, as compared to the C_{28} assay for organism V2. The same cannot be said for LT1A, which appears to show a greater concentration of proteins in the lower molecular weight regions (<40 kDa) for the C_{14} assay as compared to the C_{28} assay. Without the identities of these proteins, it is difficult to suggest why this may have occurred.

Ratajczak *et al*. (1998a) suggested that alkane degradation is not uniform in different *Acinetobacter* strains, as some strains are shown to grow on medium-chain and long-chain alkanes utilizing cytochrome P450 enzymes (Hamamura *et al.*, 2001); whereas *Acinetobacter* sp. strain M-1 is known to employ a dioxygenase for long chain alkane degradation. It is acknowledged that reports on bacterial cytochrome P450 enzymes involved in alkane degradation are scarce (Van Beilen *et al*., 2003); *Acinetobacter calcoaceticus* EB104 was reported to possess a P450 enzyme involved in alkane degradation that showed very little similarity to other P450 enzymes and was estimated to be approximately 52-53.6 kDa (Maier *et al*., 2001). The cytochrome P450 enzymes are generally soluble proteins that act on alkanes between C_5-C_{16} (Das and Chandran, 2011). For the purposes of this study, the presence and activity of the cytochrome P450 enzymes can be ruled out, as the substrate range of the P450 has not been reported to include the very long chain alkanes such as octacosane (C_{28}). Also, as mentioned in Chapter 2, very few proteins of any significance were detected within this molecular weight region. More appropriately, the alkane dioxygenases are capable of degrading alkanes ranging from C_{13} to C_{44} in *Acinetobacter* sp. strain M-1(Maeng *et al*., 1996; Ratajczak *et al*., 1998; Hamamura *et al*., 2001). The dioxygenase of the *Acinetobacter* sp. strain M-1 comprises two identical subunits of 64 kDa (Maeng *et al*., 1996; Sakai *et al*., 1996). Sakai *et al*. (1996) validated the existence of the Finnerty pathway in *Acinetobacter* sp. M-1 isolate growing on long-chain alkanes C_{16}, C_{20} and C_{30}. Subsequently, *Acinetobacter* strain M-1 has also been shown to make use of three alkane dioxygenases assumed to be involved in the oxidation of those alkanes that are slightly dissolved into the cytosol or inclusion bodies in the cell (Maeng *et al*., 1996b; Tani *et al*., 2001). Reportedly, one of the three enzymes isolated by Maeng *et al.* (1996b) preferentially oxidized the solid *n*-alkane, C_{24}. The dioxygenase enzymes do not require rubredoxins or NAD(P)H and are thought to contain Cu^{2+} (Van Hamme *et al*., 2003). Although there are no significant proteins within this molecular weight region for either of the isolates, the

presence of this enzyme system cannot be ruled out completely. Of all the alkane hydroxylase systems known to occur in *Acinetobacter* spp. the dioxygenase enzyme system is the most fitting for C_{28} degradation.

CHAPTER FOUR

CONCLUSIONS AND FUTURE PERSPECTIVES

The identification of proteins involved in the process of alkane degradation would aid in the development of a suitable bioremediation strategy based on the biochemical and physiological responses of microorganisms to the contaminant (Ballihaut *et al*., 2004). The current investigation attempted to correct the lack of information related to alkane degradation by the *Acinetobacter* genus, and a major objective was to confirm the observations made in a previous study that investigated the functional expression of a series of genes involved in alkane degradation using isolates V2 and LT1A using real-time PCR. The C_{14} and C_{28} degradation abilities of both isolates were comparable as there was no significant difference in the alkane degradation abilities of both isolates as determined using gravimetric analysis. In both the C_{14} and C_{28} assays the isolates achieved a significant reduction in the alkane substrate as compared to the abiotic control. This suggests that whatever protein systems the isolates employ, they are similar in efficiency. One dimensional-SDS PAGE indicated that the isolates made use of different protein systems for the break down of sodium acetate, implying that from the onset their proteomes were different. Analysis of the 2D-SDS PAGE gel images revealed that more proteins were required for the utilization of the long chain alkane (C_{28}) as compared to the medium chain alkane (C_{14}) for both isolates. There was a clear difference in protein expression patterns between the isolates.

A major disadvantage with the use of 2DE as an analysis tool is the inherent reproducibility issues that are encountered with its use. These issues come about as a result of several factors; those pertaining specifically to the experiment at hand include: the loss of protein sample during entry into the IEF gel, loss of protein sample during the cleanup procedure, the efficiency of transfer from the first to second dimension and possibly protein loss during staining (Garbis *et al*., 2005; Berth *et al*., 2007). Other factors are related to image acquisition and analysis with 2DE image analysis software that allow bias to be introduced through manual matching for example (Challapalli *et al*., 2004). Unfortunately, the influence of human bias cannot be avoided since many of the software programs over-look weakly expressed proteins when manual spot matching is not used in the

analysis (Challapalli *et al*., 2004; Biron *et al*., 2006). These factors can account for the variations in protein spot detection, numbering and quantification noted in both Chapters 2 and 3 as is seen from the results in Tables 2.1 and 2.3 (Chapter 2, pgs 49, 55) and Tables 3.1, 3.2 and 3.3. These issues with 2DE analysis can also account for the "lack of" proteins in the higher molecular weight regions, as observed on the 2DE gel images for both isolates during the C_{14} and C_{28} assays. Larger proteins are known to be excluded from the IEF strips during rehydration (Lower *et al*., 2005). It must also be remembered that those proteins with low copy numbers (low concentrations within the cell) are unlikely to be visualized on 2D gels (Graham *et al*., 2007). What can be suggested for the improvement of future investigations, is that larger sample sizes (biological replicates) need to be run, in order to improve the accuracy of observations (through the elimination of false-positives), reduce gel to gel variation and effects of gel artifacts; a minimum of 3 replicates per biological sample is preferred (Garbis *et al*., 2005; Biron *et al*., 2006). And until there is a technology equivalent to PCR to amplify target proteins, large amounts of sample will be required to completely analyze and characterize proteins of interest (Herbert *et al*., 2001; Marko-Varga, 2004).

Despite the disadvantages with its use, proteomic analyses have demonstrated their usefulness in studying the alteration of protein expression in microbial cells, under different environmental conditions (Ballihaut *et al*., 2004). The study by Feng *et al.* (2007) highlights the important role that proteomics and genomics play in gaining a near-complete understanding of the metabolism of biotechnologically important organisms. Graham *et al*. (2007) stated that reliable and detailed genomic information is required in order to realize the full potential proteomics could have in understanding microbial cellular processes. "*Measurements at the mRNA level are fraught with uncertainty, since the presence and abundance of a particular type of mRNA do not necessarily indicate a similar presence and abundance of the corresponding protein*" (Nisar *et al*., 2004).

Although no alkane hydroxylase components were detected for either of the alkane substrates, it cannot be ruled out that they may have been present, and that larger sample volumes of these enzymes and proteins of interest are needed in order to increase their chances of detection and identification (Nisar *et al*., 2004). It is also possible that other protein systems may have been present, but as stated, they may have been present in such small quantities to have been overlooked. And until there is a technology equivalent to PCR to amplify target proteins, large amounts of

sample will be required to completely analyze and characterize proteins of interest (Herbert *et al*., 2001; Marko-Varga, 2004). Thus far this investigation can only demonstrate the need for more studies at the proteomic level. A great deal of proteins of interest may have been overlooked due to the nature of their cellular location and the next investigation should consider the insoluble subproteome of the isolates. Future investigations should also focus on larger sample sizes (replicates) to reduce variation in spot detection and quantification. Genomic sequencing of the isolates will shed light on the genetics and biochemistry of alkane metabolism in these *Acinetobacter* sp. isolates. The biochemical aspects of dioxygenase detection in isolates V2 and LT1A should be considered for future studies since one of the proteins sequenced had some similarity to a PAH dioxygenase.

Those procedures that contribute to the loss of low abundance proteins and mis-representaiton of the bacterial proteome need to be refined. It is accepted that there is not one universal protein extraction/solubilization procedure for all bacteria and cell fractions that would result in visualization of the complete proteome (Garbis *et al*., 2005; Kim *et al*., 2005), so it is suggested then that the proteome should be considered in different compartments using the technique most applicable to that protein group/type, and then looked at as a whole (Garbis *et al*., 2005; Kim *et al*., 2005). More directed protein extraction procedures need to be considered for future attempts at alkane related proteomic studies. The protein extraction procedure using BugBuster mastermix may have been insufficient for the extraction of the integral membrane proteins such as the alkane hydroxylases, proteins involved in fatty acid oxidation as well as some transport and receptor proteins (Sabirova *et al*., 2006; Singh and Nagaraj, 2006; Graham *et al*., 2007). As stated by Pieper *et al*. (2009), it is a challenge to profile low abundance proteins that possess several transmembrane domains. Larger sample sizes (gel replicates) should be prepared for future investigations, as the variability and error introduced by analyzing only two replicates per sample needs to be avoided (Garbis *et al*., 2005).

The genome and proteome of an organism are tightly connected; without the genome sequence, one cannot identify the proteins within the proteome via Mass spectrometry (MS) technologies (Hecker *et al*., 2008). Genomic sequencing of the specific isolates used in this study will provide a more

detailed explanation as to what enzymes these organisms possess. Based on the genome sequence, the enzymes can be cloned into expression vectors to improve their production, and in so doing, allow for the identification and characterization of these biotechnologically valuable products. It is clear that isolates V2 and LT1A are good candidates for biotechnological applications; their abilities to degrade a wide range of substrates, including the wax-like long-chain alkanes highlights their versatility for bioremediation. The findings from the current study do confirm what was seen in the study by Toolsi (2008) in that even though the isolates achieved comparable rates of hydrocarbon utilization, they did so using different protein and enzyme systems. These differences were not limited to alkane utilization alone, as growth on sodium acetate as a sole carbon source generated the same conclusions.

REFERENCES

Abbott, B. J., A. I. Laskin and C. J. McCoy. 1973. Growth of *Acinetobacter calcoaceticus* on ethanol. Journal of Applied Microbiology. **25**: 787-792.

Abdel-El-Haleem, D. 2003. *Acinetobacter*: environmental and biotechnological applications. African Journal of Biotechnology. **2**: 71-74.

Al-Mutairi, N., A. Bufarsan, and F. Al-Rukaibi. 2008. Ecorisk evaluation and treatability potential of soils contaminated with petroleum hydrocarbon-based fuels. Chemosphere. **74**: 142-148.

Alonso-Gutiérrez, J., M. Teramoto, A. Yamazoe, S. Harayama, A. Figueras, and B. Novoa. 2011. Alkane-degrading properties of *Dietzia* sp. H0B, a key player in the Prestige oil spill biodegradation (NW Spain). Journal of Applied Microbiology. **111**: 800-810.

Andreoni, V., and L. Gianfreda. 2007. Bioremediation and monitoring of aromatic-polluted habitats. Applied Microbiology and Biotechnology. **76**:287-308.

Atlas, R. M. 1995. Petroleum biodegradation and oil spill bioremediation. Marine Pollution Bulletin. **31**: 178-182.

Bach, H., Y. Berdichevsky, and D. Gutnick. 2003. An exocellular protein from the oil-degrading microbe *Acinetobacter venetianus* RAG-1 enhances the emulsifying activity of the polymeric bioemulsifier emulsan. Applied and Environmental Microbiology. **69**: 2608-2615.

Bagherzadeh-Namazi, A., S. A. Shojaosadati, and S. Hashemi-Najafabadi. 2008. Biodegradation of used engine oil using mixed and isolated cultures. International Journal of Environmental Resources. **2**: 431-440.

Baldi, F., N. Ivosevic, A., Minacci, M. Pepi, R. Fani, V. Svetlicic and V. Zutic. 1999. Adhesion of *Acinetobacter venetianus* to Diesel Fuel Droplets Studied with In Situ Electrochemical and Molecular Probes. Applied and Environmental Microbiology. **65**: 2041-2048.

Ballihaut, G., B. Klein, P. Goulas, R. Duran, P. Caumette, and R. Grimaud. 2004. Analysis of the adaptation to alkanes of the marine bacterium *Marinobacter hydrocarbonoclasticus* sp. 17 by two dimensional gel electrophoresis. Aquatic Living Resources. **17**: 269-272.

Barbe, V., D. Vallenet, N. Fonknechten, A. Kreimeyer, S. Oztas, L. Labarre, S. Cruveiller, C. Robert, S. Duprat, P. Wincker, L. N Ornston, J. Weissenbach, P. Marlière, G. N Cohen and C. Médigue. 2004. Unique features revealed by the genome sequence of *Acinetobacter* sp. ADP1, a versatile and naturally transformation competent bacterium. Nucleic Acids Research. **32**: 5766-5779.

Benndorf D., G. U. Balcke, H. Harms and M. von Bergen. 2007. Functional metaproteome analysis of protein extracts from contaminated soil and groundwater. The ISME Journal. **1**: 224-234.

Bento, F. M., F. A. O. Camargo, B. C. Okeke, and W. T Frankenberger. 2005. Comparitive bioremediation of soils contaminated with diesel oil by natural attenuation, biostimulation and bioaugmentation. Bioresource Technology. **96**: 1049-1055.

Beranova-Giorgianni, S. 2003. Proteome analysis by two-dimensional gel electrophoresis and mass spectrometry: strengths and limitations. Trends in Analytical Chemistry. **22**: 273-281.

Berth, M., M. Frank, K. Markus, and B. Jörg. 2007. The state of the art in the analysis of two-dimensional gel electrophoresis images. Applied Microbiology and Biotechnology. **76**: 1223-1243.

Berthe-Corti, L., and S. Fetzner. 2002. Bacterial metabolism of *n*-alkanes and ammonia under oxic, suboxic and anoxic conditions. Acta Biotechnology. **22**: 299-336.

Bihari, Z, A. Pettko-Szandtner, G. Csanadi, M. Balázs, P. Bartos, P. Kesserű, I. Kiss and I. Mécs. 2007. Isolation and characterization of a novel *n*-alkane-degrading strain, *Acinetobacter haemolyticus* AR-46. Zeitschrift für Naturforschung. **62**: 285-295.

Binazadeh, M., I. A. Karimi and Z. Li. 2009. Fast biodegradation of long chain n-alkanes and crude oil at high concentrations with *Rhodococcus* sp. Moj-3449. Enzyme and Microbial Technology. **45**:195-202.

Biron, D. G., C. Brun, T. Lefevre, C. Lebarbenchon, H. D. Loxdale, F. Chevenet, J. Brizard, and F. Thomas. 2006. The pitfalls of proteomics experiments without the correct use of bioinformatics tools. Proteomics. **6**: 5577-5596.

Bradford, M. M. 1976. A rapid and sensitive method for the quantitation of microgram quantities of protein utilizing the principle of protein-dye binding. Analytical Biochemistry. **72**: 248-254.

Brötz-Oesterhelt, H. J. E. Bandow, and H. Labischinski. 2005. Bacterial proteomics and its role in antibacterial drug discovery. Mass Spectrometry Reviews. **24**: 549-565.

Busch, S., C. RosenplÄnter, and B. Averhoff. 1999. Identification and characterization of ComE and ComF, two novel pilin-like competence factors involved in natural transformation of *Acinetobacter* sp. starin BD413. Applied and Environmental Microbiology. **65**: 4568-4574.

Bushnell, D. L., and H. F. Haas. 1941. The utilization of certain hydrocarbons by microorganisms. Journal of Bacteriology. **41**: 653–673.

Callister, S. J., L. A. McCue, J. E. Turse, M. E. Monroe, K. J. Auberry, **R. D. Smith, J. N. Adkins, and M. S. Lipton.** 2008. Comparative bacterial proteomics: Analysis of the core genome concept. PLoS ONE **3**(2): e1542. Doi:10.1371/journal.pone.0001542.

Camarena, L., V. Bruno, G. Euskirchen, S. Poggio, and M. Snyder. 2010. Molecular mechanisms of ethanol-induced pathogenesis revealed by RNA-sequencing. PLoS Pathogens. **6** (4): e1000834. Doi:10.1371/journal.ppat.1000834.

Chakraborty, R., E. Storey and D. van der Helm. 2007. Molecular mechanism of ferricsiderophore passage through the outer membrane receptor proteins of *Escherichia coli*. Biometals. **20**: 263-274.

Challapalli, K. K., C. Zabel, J. Schuchhardt, A. M. Kaindl, J. Klose, H. Herzel. 2004. High reproducibility of large-gel two-dimensional electrophoresis. Electrophoresis. **25**: 3040-3047.

Choi, J. S., D. S. Kim, J. Lee, S. J. Kim, S. I. Kim, Y. H. Kim, J. Hong, J. S Yoo, K. H. Suh, and Y. M. Park. 2000. Proteome analysis of light-induced proteins in *Synechocystis* sp. PCC 6803: identification of proteins separated by 2D-PAGE using N-terminal sequencing and MALDI-TOF MS. Molecules and cells. **10**: 705-711.

Cozzone, A. J. 1998. Regulation of acetate metabolism by protein phosphorylation in enteric bacteria. Annual Review of Microbiology. **52** : 127-164.

Dadssi, M., and A. J. Cozzone. 1990. Evidence of Protein-tyrosine kinase activity in the bacterium *Acinetobacter calcoaceticus*. Journal of Biological Chemistry. **265**: 20996-20999.

Das, N., and P. Chandran. 2011. Microbial degradation of petroleum hydrocarbon contaminants: an overview. Biotechnology Research International. Doi:10.4061/2011/941810.

De Souza, G. A., and H. Wiker. 2009. The impact of proteomic advances on bacterial gene annotation. Current Proteomics. **6**: 84-92.

Diaz, E. 2004. Bacterial degradation of aromatic pollutants: a paradigm of metabolic versatility. International Microbiology.**7**: 173-180.

Doughari H. J., P. A. Ndakidemi, I. S. Human and S. Benade. 2011. The ecology, biology and pathogenesis of *Acinetobacter* sp.: An Overview. Microbes and Environments. **26**: 101-112.

Elias, D. A., M. E. Monroe, R. D. Smith, J. K. Fredrickson, and M. S. Lipton. 2006. Confirmation of the expression of a large set of conserved hypothetical proteins in *Shewanella oneidensis* MR-1. Journal of Microbiological Methods. **66**: 223-233.

Feng, L., W. Wang, J. Cheng, Y. Ren, G. Zhao, C. Gao, Y. Tang, X. Liu, W. Han, X. Peng, R. Liu, and L. Wang. 2007. Genome and proteome of long-chain alkane degrading *Geobacillus thermodenitrificans* NG80-2 isolated from a deep-subsurface oil reservoir. Proceedings of the National Academy of Sciences of the United States of America. **104**: 5602-5607.

Fischer, R., F. S. Bleichrodt and U. C. Gerischer. 2008. Aromatic degradative pathways in *Acinetobacter baylyi* underlie carbon catabolite repression. Microbiology. **154**: 3095-3103.

Francois, K., F. Devlieghere, A. R Standaert, A. H. Geeraerd, I. Cools, J. F. Van Impe and J. Debevere. 2005. Environmental factors influencing the relationship between optical density and cell count for *Listeria monocytogenes*. Journal of Applied Microbiology. **99**: 1503-1515.

Fulekar, M. H., and J. Sharma. 2008. Bioinformatics applied in bioremediation. Innovative Romanian Food Biotechnology. **2**: 28-36.

Ganesh, A., and J. Lin. 2009. Diesel degradation and biosurfactant production by Gram positive isolates. African Journal of Biotechnology. **8**: 5847-5854.

Ganesh, A., and J. Lin. 2011. Comparisons of protein extraction procedures and quantification methods for the proteomic analysis of Gram-positive *Paenibacillus* sp. strain D9. World Journal of Microbiology and Biotechnology. **27**: 1669-1678.

Garbis, S., G. Lubec and M. Fountoulakis. 2005. Limitations of current proteomics technologies. Journal of Chromatography A. **1077**: 1-18.

Geiβdorfer, W., R. G. Kok, A. Ratajczak, K. J. Hellingwerf, and W. Hillen. 1999. The genes *rub*A and *rub*B for alkane degradation in *Acinetobacter* sp. strain ADP1 are in an operon with *est*B, encoding and esterase, and *oxy*R. Journal of Bacteriology. **181**: 4292-4298.

Geng, A., and L. Lim. 2007. Proteome analysis of the adaptation of a phenol-degrading bacterium *Acinetobacter* sp. Edp3 to the variation of phenol loadings. Chinese Journal of Chemical Engineering. **15**:781-787.

George-Okafor, U., F. Tassie, and F. Muotoe-Okafor. 2009. Hydrocarbon degradation potentials of indigenous fungal isolates from petroleum contaminated soils. Journal of Physical and Natural Sciences. **3**: 1-6.

Glieder, A., E. T. Farinas, and F. H. Arnold. 2002. Laboratory evolution of a soluble, self-sufficient highly active alkane hydroxylase. Nature Biotechnology. **20**:1135-1139.

Görg, A. 2000. Advances in 2D gel techniques.Trends in Biotechnology. **18**: 3-6.

Görg, A., C. Obermaier, G. Boguth, A. Harder, B. Scheibe, R. Wildgruber, and W. Weiss. 2000. The current state of two-dimensional electrophoresis with immobilized pH gradients. Electrophoresis. **21**:1037-1053.

Graham, R. L. J., C. Graham, and G. McMullan. 2007. Microbial proteomics: a mass spectrometry primer for biologists. Microbial Cell Factories. Doi: 10.1186/1475-2859-6-26.

Greenwood, P. F., S. Wibrow, S. J. George, and M. Tibbett. 2009. Hydrocarbon biodegradation and soil microbial community response to repeated oil exposure. Organic Geochemistry. **40**: 293-300.

Gutnick, D. L. and E. Rosenberg. 1977. Oil tankers and pollution: A microbiological approach. Annual Reviews in Microbiology. **31**: 379-396.

Hamamura, N., C. M. Yeager, and D. J. Arp. 2001. Two distinct monooxygenases for alkane oxidation in *Nocardioides* sp. Strain CF8. Applied and Environmental Microbiology. **67**: 4992-4998.

Hamamura, N., S. H. Olson, D. M. Ward, and W. P. Inskeep. 2006. Microbial population dynamics associated with crude-oil biodegradation in diverse soils. Applied and Environmental Microbiology. **72:** 6316–6324.

Hanson, K. G., and A. J Desai. 1996. Intergeneric protoplast fusion between *Acinetobacter* sp. A3 and *Pseudomonas putida* DP99 for enhanced hydrocarbon degradation. Biotechnology Letters. **18**:1369-1374.

Hanson, K., G. Vikram, C. Kale, and A. J. Desai. 1994. The possible involvement of cell surface and outer membrane proteins of *Acinetobacter* sp. A3 in crude oil degradation. FEMS Microbiology Letters. **122:** 275-280.

Hara, A., K. Syutsubo, and S. Harayama. 2003. *Alcanivorax* which prevails in oil-contaminated seawater exhibits broad substrate specificity for alkane degradation. Journal of Environmental Microbiology. **5**: 746- 753.

Harrison, A. B., M. B. Ripley, R. K. Dart, W. B. Betts and A. J. Wilson. 2000. Effect of protein hydrolysate on the degradation of diesel fuel in soil. Enzyme and Microbial Technology. **26**: 388-393.

Hasanuzzaman, M., A. Ueno, H. Ito, Y. Ito, Y. Yamamoto, I. Yumoto and H. Okuyama. 2007. Degradation of long-chain *n*-alkanes (C36 and C40) by *Pseudomonas aeruginosa* strain WatG. International Biodeterioration and Biodegradation. **59**: 40–43.

Head, I. M., D. M. Jones and W. F. M. Rolling. 2006. Marine microorganisms make a meal of oil. Nature Reviews. **4**: 173-182.

Hearn, E. M., D. R. Patel, and B. van den Berg. 2008. Outer-membrane transport of aromatic hydrocarbons as a first step in biodegradation. Proceedings of the National Academy of Sciences. **105**: 8601-8606.

Hecker, M., H. Antelmann, K. Büttner, and J. Bernhardt. 2008. Gel-based proteomics of Gram positive bacteria: A powerful tool to address physiological questions. Proteomics. **8**: 4958-4975.

Heiss-Blanquet, S., Y. Benoit, C. Marechaux, and F. Monot. 2005. Assessing the role of alkane hydroxylase genotypes in environmental samples by competitive PCR. Journal of Applied Microbiology. **99**: 1392-1403.

Herbert, B. R., J. L. Harry, N. H. Packer, A. A. Gooley, S. K. Pedersen, and K. L. Williams. 2001. What place for polyacrylamide in proteomics? Trends in Biotechnology. **19** suppl.:S3-S9.

Hoyt, J. C., K. E. Johnson and H. C. Reeves. 1991. Purification and characterization of *Acinetobacter calcoaceticus* Isocitrate lyase. Journal of Bacteriology. **173**: 6844-6848.

Ishige, T., A. Tani, K. Takabe, K. Kawasaki, Y. Sakai and N. Kato. 2002. Wax ester production from *n*-alkanes by *Acinetobacter* sp. Strain M-1: ultrastructure of cellular inclusions and role of Acyl Coenzyme A reductase. Applied and Environmental Microbiology. **68**: 1192-1195.

Issaq, H. J., and T. D. Veenstra. 2008. Two-dimensional polyacrylamide gel electrophoresis (2D-PAGE): advances and perspectives. Biotechniques. **44**: 697-700.

Jung, J., J. Baek and W. Park. 2010. Complete Genome sequence of diesel-degrading *Acinetobacter* sp. DR1. Journal of Bacteriology. **192**: 4794-4795.

Juni, E. 1978. Genetics and physiology of *Acinetobacter*. Annual Reviews Microbiology. **32**: 349-371.

Kang, Y., and W. Park. 2010. Protection against diesel oil toxicity by sodium chloride-induced exopolysaccharides in *Acinetobacter* sp. Strain DR1. Journal of Bioscience and Bioengineering. **109**: 118-123.

Kang, Y., J. Jung, C. Jeon, and W. Park. 2011. *Acinetobacter oleivorans* sp. nov. is capable of adhering to and growing on diesel-oil. The Journal of Microbiology. **49**: 29-34.

Kaplan, N., Z. Zosim, and E. Rosenberg. 1987. Reconstitution of emulsifying activity of *Acinetobacter calcoaceticus* BD4 Emulsan by using pure polysaccharide and protein. Applied and Environmental Microbiology. **53**: 440-446.

Kato, T., A. Miyanaga, S. Kanaya, and M. Morikawa. 2009. Alkane inducible proteins in *Geobacillus thermoleovorans* B23. BMC Microbiology. **9**: 60-69.

Kerr, R. A. 2010. Gulf spill Big but not enormous, yet. Science Insider news article. Accessed from [http://news.sciencemag.org/scienceinsider/2010/05/gulf-spill-big-but-not-enormous-.html] on 28/05/2010.

Kim, D., K. F. Chater, K. Lee, and A. Hesketh. 2005. Effects of growth phase and the developmentally significant *bldA*-specified tRNA on the membrane-associated proteome of *Streptomyces coelicolor*. Microbiology. **151**: 2707-2720.

Kim, E. A., J. Y. Kim, S. J. Kim, K. R. Park, H. J. Chung, S. H. Leem and S. I. Kim. 2004. Proteomic analysis of *Acinetobacter Lwoffii* K24 by 2-D gel electrophoresis and electrospray ionization quadrupole-time of flight mass spectrometry. Journal of Microbiological Methods. **57**: 337-349.

Kim, S. I. S. Kim, M. H. Nam, S. Kim, K. Ha, K. Oh, J. Yoo and Y. Park. 2002. Proteome analysis of aniline-induced proteins in *Acinetobacter lwoffii* K24. Current Microbiology. **44**: 61-66.

Kim, S. I., S. Song, K. Kim, E. Ho and K. Oh. 2003. Proteomic analysis of the benzoate degradation pathway in *Acinetobacter* sp. KS-1. Research in Microbiology. **154**: 697-703.

Kim, S., O. Kweon and C.E. Cerniglia. 2009. Proteomic applications to elucidate bacterial aromatic hydrocarbon metabolic pathways. Current Opinion in Microbiology. **12**: 301-309.

Kim, S.I., J.S. Choi and H.Y. Kahng. 2007. A proteomics strategy for the analysis of bacterial biodegradation pathways. OMICS A Journal of Integrative Biology. **11**: 280-294.

Kloos, K., J. C. Munch and M. Schloter. 2006. A new method for the detection of alkane-monoxygenase homologous genes (alkB) in soils based on PCR-hybridization. Journal of Microbiological Methods. **66**: 486–496.

Koma, D., F. Hasumi, E. Yamamoto, T. Ohta, S. Chung and M. Kubo.2001. Biodegradation of long chain *n*-paraffins from waste oil of car engine by *Acinetobacter* sp. Journal of Bioscience and Bioengineering. **91**: 94–96.

Laemmli, U. K. 1970. Cleavage of structural proteins during the assembly of the head of bacteriophage T4. Nature. **227**: 680-685.

Lal, B., and S. Khanna. 1996. Mineralization of [14C] octacosane by *Acinetobacter calcoaceticus* S30. Canadian Journal of Microbiology. **42**:305-315.

Leahy, J. G., and R. R. Colwell. 1990. Microbial degradation of hydrocarbons in the environment. Microbiological Reviews. **54:** 305-315.

Li, L., X. Liu, W. Yang, F. Xu, W. Wang, L. Feng, M. Bartlam, L. Wang and Z. Rao. 2008. Crystal structure of long-chain alkane monooxygenase (LadA) in complex with coenzyme FMN: unveiling the long-chain alkane hydroxylase. Journal of Molecular Biology. **376** (2): 453-465.

Lilley, K. S., A. Razzaq, and P. Dupree. 2001. Two-dimensional gel electrophoresis: recent advances in sample preparation, detection and quantitation. Current Opinion in Chemical Biology. **6**: 46-50.

Lower, B. H., M. F. Hochella, and S. K. Lower. 2005. Putative mineral-specific proteins synthesized by a metal reducing bacterium. American Journal of Science. **305**: 687-710.

Luckarift H. R., S. R. Sizemore, K. E Farrington, P. A. Fulmer, J. C. Biffinger, L. J. Nadeau and G. R Johnson. 2011. Biodegradation of medium chain hydrocarbons by *Acinetobacter venetianus* 2AW immobilized to hair-based adsorbent mats. Biotechnology Progress. **27**: 1580-1586.

Maeng, J. H., Y. Sakai, Y. Tani and N. Kato. 1996a. Isolation and characterization of a novel oxygenase that catalyzes the first step of n-alkane oxidation in *Acinetobacter* sp. strain M-1. Journal of Bacteriology. **178**: 3695-3700.

Maeng, J.H., Y. Sakai, I. Takeru, Y. Sakai, Y. Tani and N. Kato. 1996b. Diversity of dioxygenases that catalyze the first step oxidation of long-chain-alkanes in *Acinetobacter* sp. M-1. FEMS Microbiology letters. **141**: 177-182.

Maier, T., H. Förster, O. Asperger and U. Hahn. 2001. Molecular characterization of the 56-kDa CYP153 from *Acinetobacter* sp. EB104. Biochemical and Biophysical Research Communications. **286**: 652-658.

Mandri, T., and J. Lin. 2007. Isolation and characterization of engine oil degrading indigenous microorganisms in KwaZulu Natal, South Africa. African Journal of Biotechnology. **6**:23-27.

Manilla-Pérez, E., A.B. Lange, S. Hetzler and A. Steinbüchel. 2010. Occurrence, production, and export of lipophilic compounds by hydrocarbonoclastic marine bacteria and their potential use to produce bulk chemicals from hydrocarbons. Applied Microbiology and Biotechnology. **86**: 1693-1706.

Marchal, R., S. Pennet, F. Solano-Serena and J. P Vandecasteele. 2003. Gasoline and diesel oil biodegradation. Oil and Gas Science and Technology Review. **58**: 441-448.

Marín, M. M., L. Yuste and F. Rojo. 2003. Differential expression of the components of the two alkane hydroxylases from *Pseudomonas aeruginosa*. Journal of Bacteriology. **185**: 3232-3237.

Marino, F. 1998. Biodegradation of paraffin wax. Masters thesis. National Library of Canada. Accessed from:[http://www.collectionscanada.gc.ca/obj/s4/f2/dsk1/tape8/PQDD_0030/MQ50640.pdf] on 18/11/11

Marko-Varga, G. 2004. Proteomics principles and challenges. Pure and Applied Chemistry. **76**: 829-837.

Martí, S., J. Sánchez-Céspedes, E. Oliveira, D. Bellido, E. Giralt and J. Vila. 2006. Proteomic analysis of a fraction enriched in cell envelope proteins of *Acinetobacter baumannii*. Proteomics. **6**: S82-S87.

Mazzoli, R., P. Fattori, C. Lamberti, M. G. Giuffrida, M. Zapponi, C. Giunta and E. Pessione. 2010. High isoelectric point sub-proteome analysis of *Acinetobacter radioresistens* S13 reveals envelope stress responses induced by aromatic compounds. Molecular Biosystems. **7**: 598-607.

Mohebali, G., and A. S. Ball. 2008. Biocatalytic desulfurization (BDS) of petrodiesel fuels. Journal of Microbiology. **154**: 2169-2183.

Munir, E., T. Hattori, and M. Shimada. 2002. Purification and characterization of malate synthase from glucose-grown wood-rotting basidiomycete *Fomitopsis palustris*. Bioscience, Biotechnology, and Biochemistry. **66**: 576-581.

Navon-Venezia S., Z. Zosim, A. Gottlieb, R. Legmann, S. Carmeli, E.Z. Ron, and E. Rosenberg.1995. Alasan, a new bioemulsifier from *Acinetobacter radioresistens*. Applied and Environmental Microbiology. **61**: 3240-3244.

Nisar, S., C S. Lane, A. F. Wilderspin, K. J. Welham, W. J. Griffiths, L. H. Patterson. 2004. Short communication: A proteomic approach to the identification of cytochrome P450 isoforms in male and female rat liver by nanoscale liquid chromatography-electrospray ionization-tandem mass spectrometry. Drug Metabolism and Disposition. **32**: 382-386.

Nyssonen, M. 2009. Functional genes and gene array analysis as tools for monitoring hydrocarbon biodegradation. VTT publications 711 accessed from: http://urn.fi/URN:ISBN:978-951-38-7347-9 on 30/11/11.

Okoh, A. I. 2006. Biodegradation alternative in the cleanup of petroleum hydrocarbon pollutants. Biotechnology and Molecular Biology Review. **1**: 38-50.

Okoh, A. I., and M. R. Trejo-Hernandez. 2006. Remediation of petroleum hydrocarbon polluted systems: exploiting the bioremediation strategies. African Journal of Biotechnology. **5**: 2520-2525.

Okoro C. C. 2011. Influence of growth media composition on the emulsifying activity of bioemulsifiers produced by four bacterial isolates with wide substrate specificity. American Journal of Biotechnology and Molecular Sciences. **1**: 1-7.

Orozco, M., J. Tirado-Rives, and W. L. Jorgensen. 1993. Mechanism for rotamase activity of FK506 binding protein from molecular dynamics simulations. Biochemistry. **32**: 12864-12874.

Parche, S., W. Geiβdorfer, and W. Hillen. 1997. Identification and characterization of *xcp*R encoding a subunit of the general secretory pathway necessary for dodecane degradation in *Acinetobacter calcoaceticus* ADP1. Journal of Bacteriology. **179**: 4631-4634.

Park, M. O. 2005. New pathway for long-chain *n*-alkane synthesis via l-alcohol in *Vibrio furnissii* M1. Journal of Bacteriology. **187:** 1426-1429.

Paul, D. R. Kumar, B. Nanduri, T. French, K. Pendarvis, A. Brown, M. Lawrence, S. C. Burgess. 2011. Proteome and membrane Fatty acid analysis on *Oligotropha carboxidovorans* OM5 grown under chemolithoautotrophic and heterotrophic conditions. PLoS ONE 6(2): e17111. Doi:10.1371/journal.pone.0017111

Peixoto, R. S., A. B. Vermelho, and A. S. Rosado. 2011. Petroleum-degrading enzymes: Bioremediation and New Prospects. Enzyme Research. Doi:10.4061/2011/475193.

Penet, S., R. Marchal, A. Sghir, and F. Monot. 2004. Biodegradation of hydrocarbon cuts used for diesel oil formulation. Applied Microbiology and Biotechnology. **66**: 40-47.

Pessione, E., M. G. Giuffrida, L. Prunotto, C. Barello, R. Mazzoli, D. Fortunato, A. Conti, C. Giunta. 2003. Membrane proteome of *Acinetobacter radioresistens* S13 during aromatic exposure. Proteomics. **3**: 1070-1076.

Piccolo, L. L., C. De Pasquale, R. Fodale, A. M. Puglia, and P. Quatrini. 2011. Involvement of an alkane hydroxylase system of *Gordonia* sp. strain SoCg in degradation of solid *n*-alkanes. Applied and Environmental Microbiology. **77**: 1204-1213.

Pieper, R., S. Huang, D. J. Clark, J. M. Robinson, H. Alami, P. P. Parmar, M. Suh, S. Kuntumalla, C. L. Bunai, R. D. Perry, R. D. Fleischmann, and S. N. Peterson. 2009. Integral and peripheral association of proteins and protein complexes with *Yersinia pestis* inner and outer membranes. Proteome Science. **7** (5) Doi: 10.1186/1477-5956-7-5.

Pirog, T. P., I. G. Sokolov, Y. V Kuz'minskaya, Y. R. Malashenko. 2002. Peculiarities of ethanol metabolism in an *Acinetobacter* sp. mutant strain defective in exopolysaccharide synthesis. Microbiology. **73**: 189-195.

Plohl, K., H. Leskovsek, and M. Bricelj. 2002. Biological degradation of motor oil in water. Acta Chimica Slovenica. **49**: 279-289.

Ratajczak, A., W. Geiβdorfer and W. Hillen. 1998a. Alkane hydroxylase from *Acinetobacter* sp. strain ADP1 is encoded by *alkM* and belongs to a new family of bacterial integral-membrane hydrocarbon hydroxylases. Applied and Environmental Microbiology. **64**: 1175-1179.

Ratajczak, A., W. Geiβdorfer and W. Hillen. 1998b. Expression of alkane hydroxylase from *Acinetobacter* sp. strain ADP1 is induced by a broad range of *n*-alkanes and requires the transcriptional activator AlkR. Journal of Bacteriology. **180**: 5822-5827.

Rattanasomboon, N., S. R. Bellara, C. L. Harding, P. J. Fryer, C. R. Thomas, M. Al-Rubeai, C. M. McFarlane. 1999. Growth and enumeration of the meat spoilage bacterium *Broncothrix thermosphacta*. International Journal of Food Microbiology. **51**: 145-158.

Reichert-Schwillinsky, F., C. Pin, M. Dzieciol, M. Wagner and I. Hein. 2009**.** Stress-and growth rate-related differences between plate count and real-time PCR data during growth of *Listeria monocytogenes*. Aplied and Environmental Microbiology. **75**: 2132-2138.

Rios, L.M., C. Moore, and P. R. Jones. 2007. Persistent organic pollutants carried by synthetic polymers in the ocean environment. Marine Pollution Bulletin. **54**: 1230-1237.

Rodriguez-Trigo, G., J.P. Zock, and I. I. Montes. 2007. Health Effects of Exposure to Oil Spills. Arch Bronconeumol. **43**: 628-635.

Rojo, F. 2009. Degradation of alkanes by bacteria. Environmental Microbiology. **11**: 2477-2490.

Rojo, R. 2005. Guest commentaries: Specificity at the end of the tunnel: understanding substrate length discrimination by the AlkB alkane hydroxylase. Bacteriology. **187**: 19-22.

Rosenberg E, R. Legmann, A. Kushmaro, R. Taube, E. Adler, and E. Ron. 1992. Petroleum bioremediation: a multiphase problem. Biodegradation. **3**: 337–350.

Sabirova, J. S., M. Ferrer, D. Regenhardt, K. N. Timmis, and P. N. Golyshin. 2006. Proteomic insights into metabolic adaptations in *Alkanivorax borkumensis* induced by alkane utilization. Journal of Bacteriology. **188**: 3763-3773.

Sakai, Y., J. H. Maeng, Y. Tanu, and N. Kato. 1994. Short communication: Use of long-chain *n*-alkanes (C13-C44) by an isolate, *Acinetobacter* sp. M-1. Bioscience, Biotechnology and Biochemistry. **58**: 2128-2130.

Sakai, Y., J. H. Maeng, S. Kubota, A. Tani, Y. Tani and N. Kato. 1996. A non-conventional dissimilation pathway for long chain *n*-alkanes in *Acinetobacter* sp. M-1 that starts with a dioxygenase reaction. Journal of Fermentation and Bioengineering. **81**: 286-291.

Sheppard, P. J., E. M. Adetutu, T. H. Makadia, and A. S. Ball. 2011. Microbial community analysis of bioremediated weathered hydrocarbon-contaminated soil. Soil Research. **49**: 261-269.

Sikkema, J., J. A. M. de Bont and B. Poolman. 1995. Mechanisms of membrane toxicity of hydrocarbons. Microbiological Reviews. **59**: 201-222.

Singh, C. and J. Lin. 2008. Isolation and characterization of diesel-degrading indigenous microorganisms in Kwazulu-Natal, South Africa. African Journal of Biotechnology. **7**: 1927-1932.

Singh, O.V, and N.S. Nagaraj. 2006. Transcriptomics, proteomics and interactomics: unique approaches to track the insights of bioremediation. Briefings in Functional Genomics and Proteomics. **4**: 355-362.

Smits T. H. M., S. B. Balada, B. Witholt and J. B van Beilen. 2002. Functional analysis of alkane hydroxylases from Gram-negative and Gram-positive Bacteria. Journal of Bacteriology. **184**: 1733-1742.

Smits, T. H. M., M. Röthlisberger, B. Witholt and J. B. van Beilen. 1999. Molecular screening for alkane hydroxylase genes in Gram-negative and Gram-positive strains. Environmental Microbiology. **1**: 307-317.

Soares, N. C., M. P. Cabral, J. R. Parreira, C. Gayoso, M. J. Barba, and G. Bou. 2009. 2-DE analysis indicates that *Acinetobacter baumannii* displays a robust and versatile metabolism. Proteome Science. **7**: 37-47.

Sood, N., and B. Lal. 2008. Isolation and characterization of a potential paraffin-wax degrading thermophillic bacterial strain *Geobacillus kaustophilus* TERI NSM for application in oil wells with paraffin deposition problems. Chemosphere. **70**: 1445-1451.

Sugiura, K., M. Ishihara, T. Shimauchi, and S. Harayama. 1997. Physicochemical properties and biodegradability of crude oil. Environmental Science and Technology. **31**: 45-51.

Tani, A., T. Ishige, Y. Sakai and N. Kato. 2001. Gene structures and regulation of the alkane hydroxylase complex in *Acinetobacter* sp. Strain M-1. Journal of Bacteriology. **183**: 1819-1823.

Thomas, M.C. 1996. Bacterial diversity and the environment. Trends in Biotechnology. **14**: 327-329.

Throne-Holst, M., A. Wentzel, T. E. Ellingsen, H. K. Kotlar, and S. B Zotchev. 2007. Identification of novel genes involved in long-chain *n*-alkane degradation by *Acinetobacter* sp. strain DSM 17874. Applied and Environmental Microbiology. **73**: 3327–3332.

Toolsi, R. 2008. Real-time quantitative PCR analysis of diesel-degrading genes of *Acinetobacter calcoaceticus* isolates. Masters thesis. University of Kwazulu Natal, Westville campus.

Van Beilen, J. B., and E. G. Funhoff. 2005. Expanding the alkane oxygenase toolbox: new enzymes and applications. Current Opinion in Biotechnology. **16**: 308-314.

Van Beilen, J. B., and E. G. Funhoff. 2007. Alkane hydroxylases involved in microbial alkane degradation. Applied Microbiology and Biotechnology. **74**: 13-21.

Van Beilen, J. B., Z. Li, W. A Duetz, T. H. M. Smits, and B Witholt. 2003. Diversity of alkane hydroxylase systems in the environment. Oil and Gas Science and Technology. **58**: 427-440.

Van Gestel, K., J. Mergaert, J. Swings, J. Coosemans, and J. Ryckeboer. 2003. Bioremediation of diesel oil-contaminated soil by composting with biowaste. Environmental Pollution. **125**: 361-368.

Van Hamme, J.D., A. Singh, and O.P. Ward. 2003. Recent advances in petroleum microbiology. Microbiology and Molecular Biology Reviews. **67**: 503-549.

Vanbroekhoven, K., A. Ryngaert, P. Wattiau, R. De Mot, and D. Springael. 2004. *Acinetobacter* diversity in environmental samples assessed by 16S rRNA gene PCR-DGGE fingerprinting. FEMS Microbiology Ecology. **50**: 37-50.

Vanzella, T. P., C. B. R. Martinez, and I. M. S. Colus. 2007. Genotoxic and Mutagenic effects of diesel oil water soluble fraction on a neotropical fish species. Journal of Mutation Research/Genetic Toxicology and Environmental Mutagenesis. **631**: 36-43.

Vasconcellos, S. P., B. M Dellagnezze, A. Wieland, J. H. Klock, E.V. Santos Neto, A. J. Marsaioli, V. M. Oliveira, and W. Michaelis. 2011. The potential for hydrocarbon biodegradation and production of extracellular polymeric substances by aerobic bacteria isolated from a Brazillian petroleum reservoir. World Journal of Microbiology and Biotechnology. **27**: 1513-1518.

Wang, L., Y. Tung, S. Wang, R. L. Liu, M. Z. Liu, Y. Zhang, F. L. Liang, and L. Feng. 2006. Isolation and characterization of a novel thermophillic bacillus strain degrading long-chain *n*-alkanes. Extremophiles. **10**: 347-356.

Wentzel, A., T. E. Ellingson, H. K. Kotlar, S. B. Zotchev, and M. Throne-Holst. 2007. Bacterial metabolism of long-chain *n*-alkanes. Applied Microbiology Biotechnology. **76**: 1209-1221.

Westermeier, R. and R. Marouga. 2005. Protein detection methods in proteomics research. Bioscience Reports. **25**: 19-32.

Whyte, L. G., J. Hawari, E. Zhou, L. Bourbonniere, W. Inniss and C. W. Greer. 1998. Biodegradation of variable-chain-length alkanes at low temperatures by a psychrotrophic *Rhodococcus* sp. Applied and Environmental Microbiology. **64**: 2578-2584.

Wilkinson, L. 1988. Systat computer software: The system for statistics, Version 4. Evanston SYSTAT, Inc.

Wilmes, P., and P. L. Bond. 2006. Metaproteomics: studying functional gene expression in microbial ecosystems. Trends in Microbiology. **14**: 92-97.

Wissing, J., S. Heim, L. Flohe, V. Bilitewski, and R. Frank. 2000. Enrichment of hydrophobic proteins via Triton X-114 phase partitioning and hydroxyapatite column chromatography for mass spectrometry. Electrophoresis. **21**: 2589-2593.

Yamahira, K., K. Hirota, K. Nakajima, N. Morita, Y. Nodasaka and I. Yumoto. 2008. *Acinetobacter* sp. strain Ths, a novel psychrotolerant and alkalitolerant bacterium that utilizes hydrocarbon. Extremophiles. **12**: 729-734.

Zanaroli, G., S. Di Toro, D. Todaro, G. C Varese, A. Bertolotto and F. Fava. 2010. Characterization of two diesel fuel degrading microbial consortia enriched from a non acclimated, complex source of microorganisms. Microbial Cell Factories. **9** (10). Doi:10.1186/1475-2859-9-10.

Zhao, Z. and J.W.C. Wong. 2009. Biosurfactants from *Acinetobacter calcoaceticus* BU03 enhance the solubility and biodegradation of phenanthrene, Environmental Technology. **30**: 291-299.

Zheng, Q., J. Song, K. Doncaster, E. Rowl, and D.M. Byers. 2007. Qualitative and quantitative evaluation of protein extraction protocols for apple and strawberry fruit suitable for two-dimensional electrophoresis and mass spectrometry analysis. Journal of Agricultural Food Chemistry. **55**: 1663-1673.

Zhu, X., A.D. Venosa, and M.T. Suidan. 2004. Literature review on the use of commercial bioremediation agents for the cleanup of oil-contaminated estuarine environments. Accessed online from [http://www.epa.gov/oem/docs/oil/edu/litreviewbiormd.pdf] on 10/03/2010.

APPENDICES

APPENDIX I: Media and Reagents

Composition of the Bushnell-Hass Agar:

- K_2HPO_4 1.0 g/litre
- KH_2PO_4 1.0 g/litre
- NH_4NO_3 1.0 g/litre
- $CaCl_2.H_2O$ 0.02 g/litre
- $FeCl_3$ 0.05 g/litre
- $MgSO_4.7H_20$ 0.2 g/litre
- Agar 15 g/litre
- pH 7.0 ± 0.2 at 25 °C

Composition of the Nutrient Agar (Merck):

- Meat extract 1.0 g/litre
- Peptone 5.0 g/litre
- Yeast extract 2.0 g/litre
- NaCl 8.0 g/litre
- Agar 15.0 g/litre
- pH 7.1 ± 0.2 at 25 °C

Phosphate buffered saline (1 litre)

- Dissolve 8 g NaCl, 0.2 g KCl, 0.12 g KH_2PO_4, 0.91 g Na_2HPO_4 in 800 ml distilled water
- Stir to dissolve
- Adjust pH to 7.2-7.4
- Bring volume up to 1 L with distilled water
- Autoclave
- Store at room temperature

1 × Bradfords reagent (1 litre)

- Dissolve 100 mg Coomassie brilliant blue G-250 in 50 ml 95% ethanol
- Add 100 ml 85% phosphoric acid and mix thoroughly
- Bring volume up to 1 L with distilled water
- Filter through Whatman no. 1 filter paper until OD_{595nm} is <0.2
- Store at 4°C in dark bottle

1× SDS Gel-loading buffer

- To 100 ml 50 mM Tris-HCl (pH 6.8) add 2 g SDS or SLS
- Mix well and add 0.1 g Bromophenol blue
- Add 10 ml glycerol.
- Mix well and store in aliquots at 4°C

10% SDS

- Autoclave 100 ml distilled water
- Add 10 g SDS powder
- Filter sterilize

5 × Tris-Glycine-SDS buffer (1 litre, makes 5 litre)

- Mix 15.1 g Tris base with 94 g Glycine in 900 ml distilled water
- Autoclave
- Add 50 ml of 10% SDS stock (filter sterilized)
- Top up to 1 litre with autoclaved distilled water
- Dilute to 1 × buffer before use with distilled water

30% Acrylamide (1 litre)

- To 600 ml distilled water, carefully dissolve 290 g Acrylamide and 10 g N,N-methylene-bisacrylamide with the application of heat in a hot water bath
- Once dissolved, bring volume up to 1 litre with double distilled water
- Filter sterilize to remove particulate matter with Whatman no. 1 filter paper
- Store at 4°C in a dark bottle

10% Ammonium persulphate

- Dissolve 0.1 g Ammonium persulphate in 1.0 ml distilled water prior to use
- Do not store, use only when required

1.5 M Tris_HCl pH 8.8 (1 Litre)

- Dissolve 182.1 g Tris base into 800 ml distilled water
- Adjust pH to 8.8 with HCl
- Bring volume up to 1 litre with distilled water
- Autoclave
- Store at room temperature

1M Tris-HCl pH 6.8 (1 Litre)

- Dissolve 121.1 g Tris base into 800 ml distilled water
- Adjust pH to 6.8 with HCl
- Bring volume up to 1 litre with distilled water
- Autoclave
- Store at room temperature

50 mM Tris-HCl

- Dilute 5 ml 1M Tris-HCl into 95 ml autoclaved water

Coomassie blue stain

- Dissolve 0.25 g Coomassie brilliant blue R250 in 90 ml Methanol: water (1:1 v/v)
- Add 10 ml glacial acetic acid
- Filter through whatman no. 1 filter paper to remove particulate matter
- Prepare destaining solution the same as above, excluding the coomassie stain

Staining Procedure:

- Immerse gel in staining solution overnight at room temperature with agitation
- Remove staining solution (reusable)
- Immerse gel in destaining solution, changing the destain solution repeatedly
- Application of heat may speed up the destaining process
- Reuse destain by passing it through a filter containing activated carbon to remove stain molecules

Oriole (BIORAD) staining procedure:

- To 590 ml of diluents in 1 litre bottle, add 400 ml methanol and then 10 ml Oriole fluorescent gel stain concentrate
- Mix well by shaking
- Place the gel into a clean tray containing 100 ml of diluted oriole stain
- Cover tray and place on a rocker for 90 min
- Transfer the gel to water prior to imaging
- Gels can be stored in water, in the dark for up to 6 months at 2-8°

0.15 M NaCl

- Dissolve 4.39 g NaCl in 500 ml distilled water
- Autoclave
- Store at room temperature

APPENDIX II: tetradecane assay

Table IIA : Percentage degradation of C14 over 20 days, performed in triplicate

	Hydrocarbon Degradation (Round 1)											
Day	V2				LT1A				AB control			
	w1	w2	w1-w2	% degradation	w1	w2	w1-w2	% degradation	w1	w2	w1-w2	% degradation
HC day 0	41.2639	42.0049	0.741	0	41.2639	42.0049	0.741	0	41.2639	42.0049	0.741	0
HC day 1	43.8867	43.9495	0.0628	91.52	41.0966	41.3561	0.2595	64.98				
HC day 3	41.2665	41.3924	0.1259	83	34.5840	34.7400	0.156	78.95				
HC day 5	43.8858	44.0043	0.1185	84	41.096	41.2318	0.1358	81.67				
HC day 10	43.8859	43.9107	0.0248	96.7	41.0938	41.1673	0.0735	90	41.2637	41.6692	0.4055	45.3
HC day 14	43.8835	43.9601	0.0766	89.66	41.0941	41.1613	0.0672	90.9				
HC day 17	43.8836	43.9212	0.0376	94.9	41.0936	41.2741	0.1805	75.6				
HC day 20	43.8847	43.9701	0.0854	88.5	41.0943	41.2	0.1057	85.7	34.5822	35.0519	0.4697	36.6

	Hydrocarbon Degradation (Round 2)											
Day	V2				LT1A				AB control			
	w1	w2	w1-w2	% degradation	w1	w2	w1-w2	% degradation	w1	w2	w1-w2	% degradation
HC day 0	43.8823	44.6513	0.769	0	43.8823	44.6513	0.769	0	43.8823	44.6513	0.769	0
HC day 1	43.8843	44.0285	0.1442	81.25	41.2637	41.4437	0.18	76.59			0	
HC day 3	43.8863	43.9976	0.1113	85.53	41.2664	41.3443	0.0779	89.87			0	
HC day 5	43.8856	44.0766	0.191	75.16	41.266	41.3113	0.0453	94.11			0	
HC day 10	41.1106	41.258	0.1474	80.83	41.2654	41.3378	0.0724	90.59	36.6641	37.2477	0.5836	24.11
HC day 14	36.6624	36.771	0.1086	85.88	41.2649	41.3783	0.1134	85.25			0	
HC day 20	36.6625	36.7217	0.0592	92.3	41.096	41.1592	0.0632	91.78	48.7286	49.2334	0.5048	34.36

Table IIA : continued…

	Hydrocarbon Degradation (Round 3)											
Day	V2				LT1A				AB control			
	w1	w2	w1-w2	% degradation	w1	w2	w1-w2	% degradation	w1	w2	w1-w2	% degradation
HC day 0	41.0963	41.8511	0.7548	0	41.0963	41.8511	0.7548	0	41.0963	41.8511	0.7548	0
HC day 1	41.0944	41.2289	0.1345	82.18	48.7272	48.9214	0.1942	74.27			0	
HC day 3	41.1968	41.3182	0.1214	83.92	48.7293	48.9360	0.2067	72.62			0	
HC day 5	34.5828	34.679	0.0962	87.25	48.729	48.8363	0.1073	85.78			0	
HC day 10	34.5836	34.7208	0.1372	81.82	48.7292	48.8195	0.0903	88.04	43.1557	43.68	0.5243	30.54
HC day 14	34.5828	34.6724	0.0896	88.13	48.7287	48.8559	0.1272	83.15			0	
HC day 20	41.2663	41.3081	0.0418	94.46	34.584	34.6535	0.0695	90.79	43.8867	44.3971	0.5104	32.38

Where:

w1: weight of beaker

w2: weight of beaker plus hydrocarbon

AB: Abiotic control

Table IIA2 : Percentage degradation of C14 over 20 days, summary of triplicate results

	V2					LT1A					AB control					
Day	**% degradation**			std. deviation	Ave.	**% degradation**			std. deviation	Ave	**% degradation**				std. deviation	Ave.
HC day 0	0	0	0	0	0	0	0	0	0	0	0	0	0	0	0	0
HC day 1	91.52	81.25	82.18	5.68	84.98	64.98	76.59	74.27	6.14	71.95						
HC day 3	83	85.53	83.92	1.28	84.15	78.95	89.87	72.62	8.73	80.48						
HC day 5	84	75.16	87.25	6.26	82.14	81.67	94.11	85.78	6.34	87.19						
HC day 10	96.7	80.83	81.82	8.89	86.45	90	90.59	88.04	1.33	89.54	45.3	24.11	24	30.54	10.02	30.99
HC day 14	89.66	85.88	88.13	1.90	87.89	90.9	85.25	83.15	4.01	86.43						
HC day 20	88.5	92.3	94.46	3.02	91.75	85.7	91.78	90.79	3.26	89.42	36.6	34.36	27.7	32.38	3.79	32.76

Table IIB : Bacterial enumeration on nutrient agar for C14 assay over a period of 20 days

Day	V2 round 1		V2 round 2		V2 round 3		Stats.	
	log cfu/ml	log cfu/ml	log cfu/ml	log cfu/ml	log cfu/ml	log cfu/ml	std. deviation	ave log cfu/ml
Day 0	-	-	7.46	7.48	7.38	7.38	0.052599113	7.425
Day 1 no HC	-	-	8.99	8.96	8.97	9.01	0.022173558	8.9825
HC day 0	8.78	9.07	8.83	8.72	9.03	9.09	0.161987654	8.92
HC day 1	9.28	9.13	8.98	8.97	9.14	9.09	0.115137599	9.098333333
HC day 3	9.43	9.45	9.39	9.49	9.16	9.14	0.15331884	9.343333333
HC day 5	9.49	9.57	9.64	9.69	9.48	9.56	0.082320512	9.571666667
HC day 10	9.62	9.54	9.64	9.72	9.59	9.68	0.064005208	9.631666667
HC day 14	9.76	9.72	9.73	9.76	9.49	9.53	0.121778487	9.665
HC day 20	9.17	9.31	9.34	9.23	9.41	9.32	0.08477421	9.296666667
Day	**LT1A round 1**		**LT1A round 2**		**LT1A round 3**		**Stats**	
	log cfu/ml	log cfu/ml	log cfu/ml	log cfu/ml	log cfu/ml	log cfu/ml	std. deviation	ave log cfu/ml
Day 0	-	-	7.54	7.52	7.48	7.04	0.23797759	7.395
Day 1 no HC	-	-	8.94	8.94	9.03	9.08	0.06946222	8.9975
HC day 0	8.64	9.21	8.88	8.96	9.05	9.06	0.194490788	8.966666667
HC day 1	9.26	9.23	9.23	9.29	9.18	9.23	0.036696957	9.236666667
HC day 3	9.84	9.74	9.66	9.54	9.32	9.37	0.206341141	9.578333333
HC day 5	9.85	9.77	9.77	9.79	9.45	9.51	0.166373075	9.69
HC day 10	9.52	9.63	9.63	9.52	9.41	9.43	0.094162979	9.523333333
HC day 14	10.69	10.87	9.23	9.32	9.36	9.28	0.768880138	9.791666667
HC day 20	9.22	9.09	9.11	9.15	9.12	9.17	0.047187569	9.143333333

Where:

HC: Hydrocarbon

Day 0: cells grown on sodium acetate as sole carbon source

HC day 0: Cells grown on sodium acetate for 3 days, then spiked with hydrocarbon

Table IIC : Optical Density at 600nm for C14 assay over a period of 20 days

Day	V2 round 1	V2 round 2	V2 round 3	ave.	std. deviation
Day 0	-	0.059	0.062	0.0605	0.00212132
Day 1 no HC	-	0.681	0.655	0.668	0.018384776
HC day 0	0.659	0.535	0.642	0.612	0.067223508
HC day 1	1.154	1.111	1.253	1.172666667	0.072817123
HC day 3	1.497	1.503	1.516	1.505333333	0.009712535
HC day 5	1.441	1.718	1.78	1.646333333	0.180505771
HC day 10	1.84	1.772	1.764	1.792	0.041761226
HC day 14	1.878	0.981	1.799	1.552666667	0.496651118
HC day 20	1.281	1.974	1.826	1.693666667	0.364960728

Day	LT1A round 1	LT1A round 2	LT1A round 3	ave.	std. deviation
Day 0	-	0.044	0.068	0.056	0.016970563
Day 1 no HC	-	0.72	0.458	0.589	0.185261977
HC day 0	0.71	0.744	0.72	0.724667	0.01747379
HC day 1	0.887	1.507	0.523	0.972333	0.497519179
HC day 3	1.64	1.634	1.714	1.662667	0.044557079
HC day 5	1.792	1.729	1.773	1.764667	0.032316147
HC day 10	1.932	1.82	1.482	1.744667	0.234267653
HC day 14	1.967	1.722	2.021	1.903333	0.159343445
HC day 20	1.977	1.689	1.870	1.845333	0.145575868

Where:

HC: Hydrocarbon

Day 0: cells grown on sodium acetate as sole carbon source

HC day 0: Cells grown on sodium acetate for 3 days, then spiked with hydrocarbon

Table IID : Bovine serum albumin standard curve raw data. 1/10 dilutions of protein samples were prepared and diluted 1:50 with Bradford reagent, and then measured spectrophotometrically at OD 595nm

BSA concentration (mg/ml)	Reading 1	Reading 2	Reading 3	Reading 4	ave
0	0	0	0	0	0
0.1	0.059	0.056	0.053	0.051	0.05475
0.2	0.118	0.109	0.108	0.102	0.10925
0.3	0.158	0.154	0.151	0.149	0.153
0.4	0.203	0.196	0.195	0.191	0.19625
0.5	0.245	0.242	0.235	0.233	0.23875
0.6	0.275	0.273	0.273	0.275	0.274
0.75	0.331	0.321	0.32	0.323	0.32375

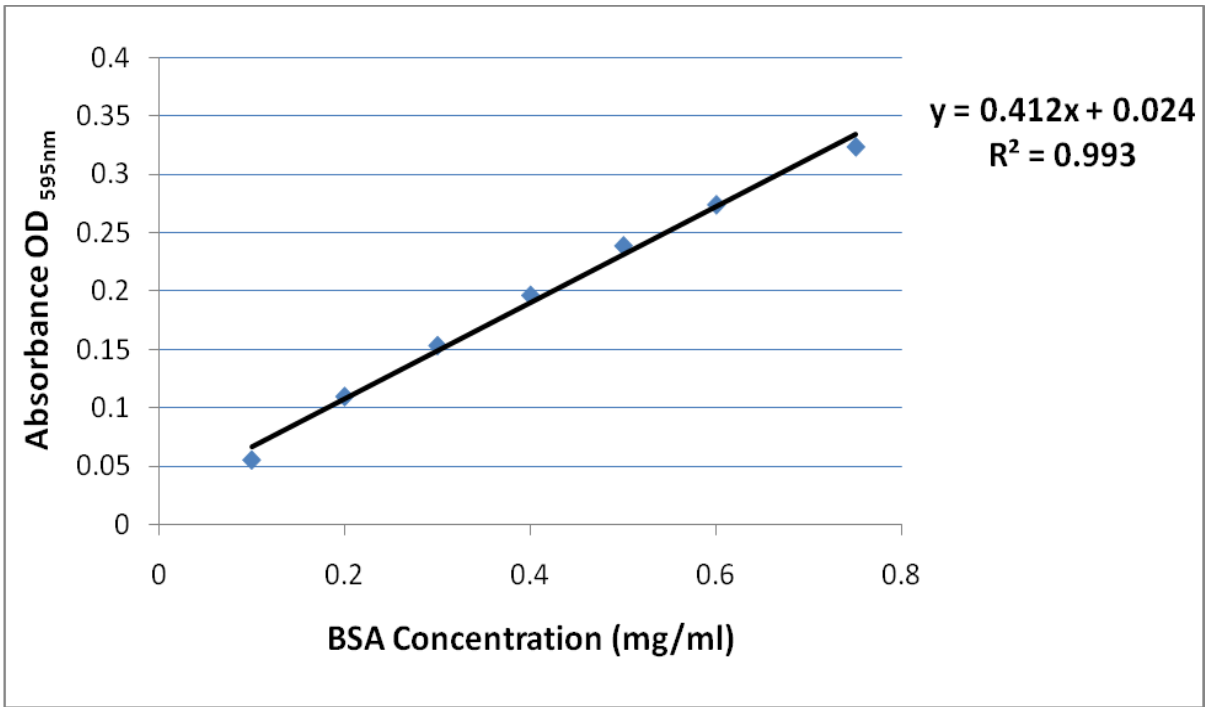

Figure IIA : Bovine serum albumin standard curve plotted from average values obtained in table IID above. Equation obtained from standard curve used to determine unknown protein concentrations in Table IIE.

Table IIE : Protein concentrations as determine by Bradford assay for C14 **equation: y=0.412x + 0.024

						(note: multiply values by 10 since 1/10 dilution)		Final concentration	Procedure to standardize
Sample	**Reading 1**	**Reading 2**	**Reading 3**	**Reading 4**	**ave**	**Concentration (mg/ml)****	**x10**	**µg/100µl**	**std to 50**
V2 day 0	0.034	0.048	0.043	0.052	0.04425	0.042231	0.42231	42.2	Increase load
LT1A day 0	0.091	0.098	0.095	0.095	0.09475	0.063037	0.63037	63.04	dilute
V2 day 1	0.096	0.101	0.101	0.099	0.09925	0.064891	0.64891	64.89	dilute
LT1A day 1	0.107	0.112	0.109	0.105	0.10825	0.068599	0.68599	68.6	dilute
V2 day 5	0.059	0.059	0.063	0.065	0.0615	0.049338	0.49338	49.3	
LT1A day 5	0.054	0.057	0.055	0.06	0.0565	0.047278	0.47278	47.3	
V2 day 10	0.1	0.101	0.103	0.104	0.102	0.066024	0.66024	66	dilute
LT1A day 10	0.133	0.133	0.125	0.137	0.132	0.078384	0.78384	78.4	dilute
V2 day 14	0.077	0.07	0.076	0.079	0.0755	0.055106	0.55106	55.1	dilute
LT1A day 14	0.084	0.096	0.096	0.103	0.09475	0.063037	0.63037	63	dilute
V2 day 20	0.071	0.068	0.078	0.095	0.078	0.056136	0.56136	56.1	dilute
LT1A day 20	0.081	0.084	0.087	0.113	0.09125	0.061595	0.61595	61.6	dilute
Round 2									
V2 day 0	0.058	0.062	0.062	0.063	0.06125	0.049235	0.49235	49.24	
LT1A day 0	0.078	0.075	0.08	0.077	0.0775	0.05593	0.5593	55.93	dilute
V2 day 1	0.072	0.111	0.078	0.107	0.092	0.061904	0.61904	61.90	dilute
LT1A day 1	0.072	0.066	0.075	0.1	0.07825	0.056239	0.56239	56.2	dilute
V2 day 5	0.086	0.082	0.088	0.113	0.09225	0.062007	0.62007	62	dilute
LT1A day 5	0.121	0.122	0.123	0.147	0.12825	0.076839	0.76839	76.8	dilute
V2 day 10	0.071	0.072	0.074	0.069	0.0715	0.053458	0.53458	53.4	
LT1A day 10	0.133	0.136	0.137	0.135	0.13525	0.079723	0.79723	79.7	dilute
V2 day 14	0.105	0.132	0.135	0.133	0.12625	0.076015	0.76015	76	dilute
LT1A day 14	0.184	0.183	0.181	0.186	0.1835	0.099602	0.99602	99.6	dilute
V2 day 20	0.117	0.115	0.11	0.116	0.1145	0.071174	0.71174	71.1	dilute
LT1A day 20	0.17	0.168	0.17	0.174	0.1705	0.094246	0.94246	94.2	dilute

Table IIF: Spot distribution patterns in terms of molecular weight and *p*I (isoelectric point) for those proteins showing a 2-fold increase or decrease in expression levels for organisms V2 and LT1A from day 0 to day 20 as determined by PDQuest™ Advanced 2-D analysis software (version 8.0.1, BIO-RAD, USA).

V2 C14			LT1A C14		
Spot number	Molecular weight (kDa)	pI	Spot number	Molecular weight (kDa)	pI
203	25	4.8	4503	25.75	4.5
1	15.59	4.91	4201	14.07	4.94
101	20.59	4.92	5401	24.02	5.25
1001	11.88	5.07	5601	48.04	5.27
1902	117.54	5.08	5902	100	5.3
1201	24.97	5.12	5402	24.02	5.44
1601	45.35	5.15	5001	8.76	5.48
1401	40.16	5.19	6402	24.16	5.57
1104	22.28	5.21	6903	100.1	5.61
1801	100	5.3	6203	17.67	5.73
1903	140.14	5.33	6401	23.79	5.74
1203	24.29	5.45	6606	38.16	5.85
1002	13.61	5.46	6505	32.24	6
1103	22.7	5.49	5202	16.9	6.03
2002	14.95	5.57	7901	100.06	6.13
2901	138.03	5.6	7801	73.5	6.14
2902	154.14	5.63	7301	19.09	6.38
2701	69.37	5.66	7302	20.57	6.81
2801	102.89	5.68	7701	59.72	7.08
2201	23.55	5.74	7002	8.7	7.11
2101	18.89	5.74	8101	10.08	7.46
3901	134.44	5.94	8002	8.6	7.82
3902	155.23	5.97	9701	68.33	8.88
3601	49.34	5.98			
3401	37	6			
3301	32.17	6.01			
3903	137.55	6.05			
3402	37.99	6.07			
3002	17.18	6.09			
3904	108.62	6.11			
3302	31.29	6.13			
3101	19.3	6.13			
4001	13.83	6.15			
4201	23.07	6.18			
4301	25.64	6.19			

V2 C14		
Spot number	Molecular weight (kDa)	pI
4501	41.15	6.21
4601	45.31	6.22
4002	12.63	6.24
5101	19.19	6.28
5902	131.82	6.28
5201	23.78	6.3
5601	47.35	6.3
5001	15.39	6.36
5602	47.02	6.37
5202	25.03	6.42
5102	18.36	6.45
6101	20.43	6.49
6901	124.4	6.5
6003	16.08	6.55
6402	40.07	6.56
6001	13.21	6.56
6602	47.93	6.6
6701	66.78	6.64
6702	66.17	6.74
7601	46.32	6.8
7005	12.04	6.91
7302	30.94	6.99
7001	16	7
7701	61.16	7.13
7303	30.37	7.26
7602	47.24	7.27
8601	47.06	7.64
8304	31.4	7.66
8701	59.18	7.69
8401	36.57	7.96
8301	32.56	7.98

Table IIG: Experiment summary report for PDQuest analysis of 2D gel images

V2 C14						
Gel Name	Replicate Group	Spots	Matched	Match Rate 1	Match Rate 2	Correlation Coefficient
C14 d0.1	day 0	147	66	44%	41%	0.041
C14 d0.2	day 0	150	50	33%	31%	0.382
C14 d5.1	day 5	69	44	63%	27%	0.438
C14 d5.2	day 5	123	51	41%	32%	0.503
C14 d10.1	day 10	130	65	50%	40%	0.765
C14 d10.2	day 10	75	22	29%	13%	0.391
C14 d14.1	day 14	104	48	46%	30%	0.575
C14 d14.2	day 14	180	62	34%	38%	0.634
*** C14 d20.1**	day 20	136	136	100%	85%	1
C14 d20.2	day 20	117	46	39%	28%	0.512
LT1A C14						
Gel Name	Replicate Group	Spots	Matched	Match Rate 1	Match Rate 2	Correlation Coefficient
C14 d0.1	day 0	83	40	48%	26%	0.694
***C14 d0.2**	day 0	91	91	100%	61%	1
C14 d5.1	day 5	109	51	46%	34%	0.705
C14 d5.2	day 5	186	65	34%	43%	0.802
C14 d10.1	day 10	97	52	53%	34%	0.815
C14 d10.2	day 10	188	64	34%	42%	0.797
C14 d14.1	day 14	138	65	47%	43%	0.726
C14 d14.2	day 14	234	74	31%	49%	0.826
C14 d20.1	day 20	144	61	42%	40%	0.693
C14 d20.2	day 20	227	66	29%	44%	0.734

*Master gel image
Match rate 1: spots matched to member
Match rate 2: spots matched to master
Correlation coefficient based on master gel

Table IIH: Normalization reports for PDQuest analysis of 2D gel images for isolate LT1A and V2 respectively

Normalization Report - LT1A C14		
Gel Image Name	**Pixel Count**	**Total Density**
lt1a c14 d0 r1 no 4	717920	48062972
lt1a do r2 no.4	717920	1.58E+08
lt1a c14 d10 r1 no.2	717920	33572040
lt1a c14 d10 r2 no.2	717920	2.94E+08
lt1a c14 d14 r1	717920	35352832
lt1a c14 d14 r2	717920	3.75E+08
lt1a c14 d20 r1 no.2	717920	47658140
lt1a c14 d20 r2	717920	3.09E+08
lt1a c14 d5 r1 no.2	717920	1.05E+08
lt1a c14 d5 r2 no.4	717920	3.87E+08

Normalization Report - V2 c14		
Gel Image Name	**Pixel Count**	**Total Density**
v2 c14 d0 r1 no.4	717920	48506972
v2 d0 r2 no.3	717920	1.26E+08
V2C14d5 r1	402617	1647215
v2 c14 d10 r1 no.2	717920	1.28E+08
v2 c14 d10 r2 no.2	717920	1.29E+08
v2 c14 d14 r1 no.2	717920	81676392
v2 c14 d14 r2 no.3	717920	79991272
v2 c14 d20 r1 no.3	717920	5.82E+08
v2 c14 d20 r2 no.2	717920	80439768
v2 c14 d5 r2 no.3	717920	1.09E+08

APPENDIX III: Octacosane assay

Table IIIA : Percentage degradation of C28 over 20 days, performed in triplicate

	Hydrocarbon Degradation (Round 1)											
Day	V2				LT1A				AB control			
	w1	w2	w1-w2	% degradation	w1	w2	w1-w2	% degradation	w1	w2	w1-w2	% degradation
HC day 0	-	-	0.4743	0	-	-	0.4743	0	-	-	0.4743	0
HC day 1	33.7548	34.2252	0.4704	0.82	30.234	30.6978	0.4638	2.21			0	
HC day 3	33.7546	34.1963	0.4417	6.87	30.2326	30.7039	0.4713	0.63			0	
HC day 5	33.7548	34.1673	0.4125	13.03	30.2329	30.5613	0.3284	30.76			0	
HC day 10	33.7543	34.1847	0.4304	9.26	30.2326	30.629	0.3964	16.42	39.7093	40.1562	0.4469	5.78
HC day 14	33.7539	33.9733	0.2194	53.74	30.2323	30.5686	0.3363	29.1			0	
HC day 20	33.7538	33.9753	0.2215	53.3	30.2328	30.4101	0.1773	62.62	33.755	34.2229	0.4679	1.35

	Hydrocarbon Degradation (Round 2)											
Day	V2				LT1A				AB control			
	w1	w2	w1-w2	% degradation	w1	w2	w1-w2	% degradation	w1	w2	w1-w2	% degradation
HC day 0	-	-	0.4743	0	-	-	0.4743	0	-	-	0.4743	0
HC day 1	39.6996	40.1653	0.4657	1.81	31.9848	32.4483	0.4635	2.28			0	
HC day 3	33.7551	34.2214	0.4663	1.69	30.2336	30.7049	0.4713	0.63			0	
HC day 5	39.7018	40.088	0.3862	18.57	31.985	32.3633	0.3783	20.24			0	
HC day 10	33.7552	34.1601	0.4049	14.63	31.9852	32.3774	0.3922	17.31	30.2341	30.7113	0.4772	-0.61
HC day 14	33.7539	34.1632	0.4093	13.7	31.9842	32.401	0.4168	12.12			0	
HC day 20	39.7093	40.055	0.3457	27.11	30.2324	30.5798	0.3474	26.76	30.2329	30.7043	0.4714	0.61

Table IIIA : continued…

	Hydrocarbon Degradation (Round 3)											
Day	V2				LT1A				AB control			
	w1	w2	w1-w2	% degradation	w1	w2	w1-w2	% degradation	w1	w2	w1-w2	% degradation
HC day 0	41.0963	41.8511	0.7548	0	41.0963	41.8511	0.7548	0	41.0963	41.8511	0.7548	0
HC day 1	41.0944	41.2289	0.1345	82.18	48.7272	48.9214	0.1942	74.27			0	
HC day 3	41.1968	41.3182	0.1214	83.92	48.7293	48.9360	0.2067	72.62			0	
HC day 5	34.5828	34.679	0.0962	87.25	48.729	48.8363	0.1073	85.78			0	
HC day 10	34.5836	34.7208	0.1372	81.82	48.7292	48.8195	0.0903	88.04	43.1557	43.68	0.5243	30.54
HC day 14	34.5828	34.6724	0.0896	88.13	48.7287	48.8559	0.1272	83.15			0	
HC day 20	41.2663	41.3081	0.0418	94.46	34.584	34.6535	0.0695	90.79	43.8867	44.3971	0.5104	32.38

Where:

w1: weight of beaker
w2: weight of beaker plus hydrocarbon
AB: Abiotic control

Table IIIA2 : Percentage degradation of C14 over 20 days, summary of triplicate results

Hydrocarbon Degradation of all 3 repeats C28															
	V2					**LT1A**					**AB control**				
Day	**% degradation**			std. deviation	ave	**% degradation**			std. deviation	ave	**% degradation**			std. deviation	ave
HC day 0	0	0	0	0	0	0	0	0	0	0	0	0	0	0	0
HC day 1	0.82	1.81	0.51	0.6789	0.95	2.21	2.28	1.98	0.1570	1.66					
HC day 3	6.87	1.69	10.12	4.2517	5.73	0.63	0.63	7.97	4.2378	3.37					
HC day 5	13.03	18.57	20.35	3.8176	13.94	30.76	20.24	12.59	9.1227	18.18					
HC day 10	9.26	14.63	22.54	6.6804	13.28	16.42	17.31	27.58	6.2023	16.88	5.78	-0.61	3.04	3.2057	2.85
HC day 14	53.74	13.7	56.21	23.8621	36.88	29.1	12.12	26.76	9.2026	19.30					
HC day 20	53.3	27.11	52.65	14.9367	37.0	62.62	26.76	33.73	19.0138	35.53	1.35	0.61	2.57	0.9897	1.38

Table IIIB : Bacterial enumeration on nutrient agar for C28 assay over a period of 20 days

Day	V2 round 1		V2 round 2		V2 round 3		Stats	
	log cfu/ml	log cfu/ml	log cfu/ml	log cfu/ml	log cfu/ml	log cfu/ml	std. deviation	ave log cfu/ml
Day 0	7.49	7.53	7.71	7.83	8.51	7.95	0.373238083	7.836666667
Day 1 no HC	8.89	8.95	9.11	9.16	9.41	9.38	0.214382835	9.15
HC day 0	8.95	9.11	9.02	9.03	9.06	9.02	0.052694086	9.031666667
HC day 1	8.70	8.72	8.86	8.87	8.79	8.92	0.088090862	8.81
HC day 3	9.10	9.04	8.81	8.89	8.76	8.87	0.132274966	8.911666667
HC day 5	9.30	9.22	9.67	9.61	9.71	9.63	0.208390659	9.523333333
HC day 10	8.62	8.68	9.11	9.07	9.37	9.34	0.319463091	9.031666667
HC day 14	9.62	9.58	9.16	9.19	9.35	9.38	0.191311265	9.38
HC day 20	9.68	9.69	7.24	7.48	9.5	9.63	1.17405281	8.87
Day	**LT1A round 1**		**LT1A round 2**		**LT1A round 3**		**Stats**	
	log cfu/ml	log cfu/ml	log cfu/ml	log cfu/ml	log cfu/ml	log cfu/ml	std. deviation	ave log cfu/ml
Day 0	7.08	7.36	7.81	7.76	7.3	8.28	0.435909012	7.598333
Day 1 no HC	9.04	9.11	8.96	9.01	9.18	9.32	0.131250397	9.103333
HC day 0	9.04	9.03	8.96	8.85	9.00	9.06	0.076941536	8.99
HC day 1	9.00	9.03	9.24	9.16	8.79	8.85	0.17313771	9.011667
HC day 3	9.06	8.9	9.1	9.12	9.06	9.16	0.090037029	9.066667
HC day 5	9.62	9.59	9.6	9.49	9.33	9.29	0.144591378	9.486667
HC day 10	9.02	9.12	9.4	9.38	9.6	9.51	0.224714634	9.338333
HC day 14	9.46	9.49	9.42	9.28	9.37	9.36	0.076070143	9.396667
HC day 20	9.64	9.73	7.45	7.48	9.53	9.64	1.12241555	8.911667

Where:

HC: Hydrocarbon

Day 0: cells grown on sodium acetate as sole carbon source

HC day 0: Cells grown on sodium acetate for 3 days, then spiked with hydrocarbon

Table IIIC : Optical Density at 600nm for C28 assay over a period of 20 days

Day	V2 round 1	V2 round 2	V2 round 3	std. deviation	ave.
Day 0	0.042	0.121	0.054	0.042571508	0.072333333
Day 1 no HC	0.618	0.701	0.681	0.043316663	0.666666667
HC day 0	0.529	0.551	0.584	0.027682726	0.554666667
HC day 1	0.361	0.33	0.388	0.029022979	0.359666667
HC day 3	0.56	0.403	0.851	0.227315493	0.604666667
HC day 5	1.623	1.642	1.943	0.179518801	1.736
HC day 10	0.882	1.358	1.806	0.462070702	1.348666667
HC day 14	2.044	1.466	1.964	0.313179395	1.824666667
HC day 20	1.989	1.884	1.645	0.176296152	1.839333333

Day	LT1A round 1	LT1A round 2	LT1A round 3	std. deviation	ave.
Day 0	0.08	0.155	0.066	0.047857427	0.100333333
Day 1 no HC	0.41	0.779	0.786	0.215091453	0.658333333
HC day 0	0.602	0.578	0.493	0.057274194	0.557666667
HC day 1	0.723	0.529	0.451	0.140061891	0.567666667
HC day 3	0.553	0.672	1.0013	0.232225602	0.7421
HC day 5	1.542	1.638	1.004	0.341715281	1.394666667
HC day 10	1.313	1.403	1.926	0.331008056	1.547333333
HC day 14	1.959	1.457	1.729	0.251292658	1.715
HC day 20	1.922	1.879	1.86	0.03176476	1.887

Where:

HC: Hydrocarbon

Day 0: cells grown on sodium acetate as sole carbon source

HC day 0: Cells grown on sodium acetate for 3 days, then spiked with hydrocarbon

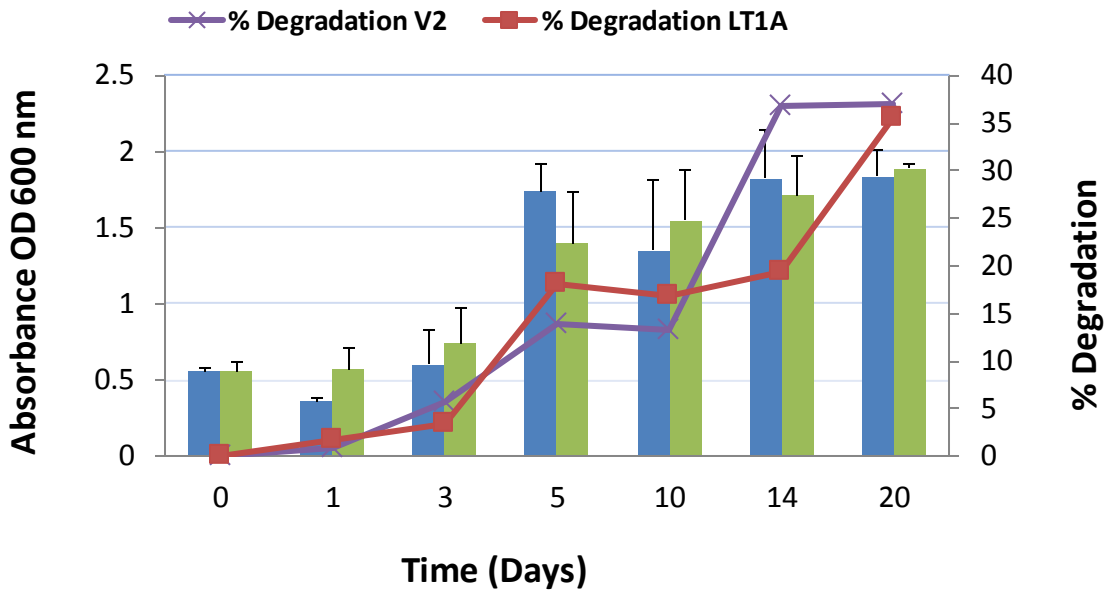

FigureIIIA Degradation profile for *Acinetobacter* sp. V2 and LT1A grown in Bushnell Haas medium spiked with 0.5% Octacosane (C_{28}), showing the microbial populations as determined spectrophotometrically at OD_{600nm} and the % C_{28} degradation over 20 days. Blue bars represent growth of V2, green bars represent growth of LT1A (*n*=3).

Table IIID : Protein concentrations as determine by Bradford assay for C28
**equation: y=0.412x + 0.024

						(note: multiply values by 10 since 1/10 dilution)		Final concentration	Procedure to standardize
Sample	**Reading 1**	**Reading 2**	**Reading 3**	**Reading 4**	**ave**	**Concentration (mg/ml)****	**x10**	**µg/100µl**	**std to 50**
V2 day 0	0.034	0.048	0.043	0.052	0.04425	0.042231	0.42231	42.2	Increase load
LT1A day 0	0.091	0.098	0.095	0.095	0.09475	0.063037	0.63037	63.04	dilute
V2 day 1	0.037	0.033	0.035	0.038	0.03575	0.038729	0.38729	38.7	Increase load
LT1A day 1	0.061	0.058	0.059	0.064	0.0605	0.048926	0.48926	48.9	Increase load
V2 day 5	0.077	0.073	0.073	0.076	0.07475	0.054797	0.54797	54.8	dilute
LT1A day 5	0.167	0.161	0.161	0.163	0.163	0.091156	0.91156	91.1	dilute
V2 day 10	0.116	0.113	0.111	0.114	0.1135	0.070762	0.70762	70.8	dilute
LT1A day 10	0.086	0.114	0.112	0.112	0.106	0.067672	0.67672	67.7	dilute
V2 day 14	0.292	0.284	0.273	0.269	0.2795	0.139154	1.39154	139.1	dilute
LT1A day 14	0.225	0.226	0.222	0.224	0.22425	0.116391	1.16391	116.4	dilute
V2 day 20	0.246	0.245	0.244	0.247	0.2455	0.125146	1.25146	125.1	dilute
LT1A day 20	0.235	0.231	0.236	0.232	0.2335	0.120202	1.20202	120.2	dilute
Round 2									
V2 day 0	0.058	0.062	0.062	0.063	0.06125	0.049235	0.49235	49.24	
LT1A day 0	0.078	0.075	0.08	0.077	0.0775	0.05593	0.5593	55.93	dilute
V2 day 1	0.04	0.035	0.044	0.035	0.0385	0.039862	0.39862	39.86	Increase load
LT1A day 1	0.033	0.034	0.03	0.032	0.03225	0.037287	0.37287	37.29	Increase load
V2 day 5	0.157	0.162	0.159	0.159	0.15925	0.089611	0.89611	89.6	dilute
LT1A day 5	0.176	0.176	0.172	0.171	0.17375	0.095585	0.95585	95.6	dilute
V2 day 10	0.136	0.137	0.134	0.135	0.1355	0.079826	0.79826	79.8	dilute
LT1A day 10	0.156	0.158	0.156	0.153	0.15575	0.088169	0.88169	88.2	dilute
V2 day 14	0.16	0.152	0.151	0.151	0.1535	0.087242	0.87242	87.2	dilute
LT1A day 14	0.168	0.168	0.166	0.166	0.167	0.092804	0.92804	92.8	dilute
V2 day 20	0.086	0.088	0.086	0.086	0.0865	0.059638	0.59638	59.6	dilute
LT1A day 20	0.073	0.077	0.074	0.075	0.07475	0.054797	0.54797	54.8	dilute

Table IIIE: Spot distribution patterns in terms of molecular weight and *p*I (isoelectric point) for those proteins showing a 2-fold increase or decrease in expression levels for organisms V2 and LT1A from day 0 to day 20 as determined by PDQuest™ Advanced 2-D analysis software (version 8.0.1, BIO-RAD, USA).

V2 C28			LT1A C28		
Spot number	Molecular weight (kDa)	pI	Spot number	Molecular weight (kDa)	pI
1304	27.45	4.44	3003	6.52	5.16
1306	28.92	4.56	3104	13	5
1402	31.98	4.44	3201	27.63	4.86
1407	35.26	4.36	3202	28.17	5.19
1803	95.28	4.36	3504	44.5	5.2
2103	16.42	5.07	4104	10.5	5.69
2202	22.53	5.16	4202	23	5.4
2306	26.87	5.17	4203	27.54	5.4
2604	45	5	4207	27.23	5.64
2608	47.67	5.18	4208	17.29	5.65
3002	11.39	5.43	4211	27.17	5.49
3102	15.34	5.47	4301	33.15	5.52
3104	18.72	5.64	4805	121.12	5.64
3209	22.94	5.72	5004	6.96	5.87
3301	28.17	5.2	6102	10.41	6.27
3304	26.46	5.62	6301	32.63	6.12
3501	38.57	5.63	6401	36.65	6.18
3703	77.79	5.62	6402	38.38	6.25
3806	89.12	5.6	6502	45.01	6.16
4102	19.24	5.83	7101	10.12	6.49
4104	18.73	6.07	7203	26.49	6.5
4407	33.01	6.14	7302	30.64	6.89
4503	38.41	5.87	7404	41.65	6.98
4504	44.61	5.93	7703	116.63	6.86
4505	37.67	6.05	8002	6.82	7.66
4701	55.88	5.94			
4804	98.3	5.89			
5202	20.16	6.29			
5502	43.11	6.23			
5604	46.64	6.57			
5803	105.21	6.38			
7103	17.45	7.58			
7601	48.1	7.2			

V2 C28		
Spot number	Molecular weight (kDa)	pI
7604	47.72	7.48
8101	15.91	8.11
8102	17.21	8.4

Table IIIF : Experiment summary report for PDQuest analysis of 2D gel images

V2 C28						
Gel Name	Replicate Group	Spots	Matched	Match Rate 1	Match Rate 2	Correlation Coefficient
C14 d0.1	day 0	99	62	62%	22%	0.326
C14 d0.2	day 0	81	40	49%	14%	0.54
C14 d5.1	day 5	220	219	99%	80%	1
C14 d5.2	day 5	139	95	68%	34%	0.243
C14 d10.1	day 10	112	65	58%	23%	0.41
C14 d10.2	day 10	235	138	58%	50%	0.779
C14 d14.1	day 14	156	91	58%	33%	0.344
C14 d14.2	day 14	197	94	47%	34%	0.61
*** C14 d20.1**	day 20	277	146	52%	53%	0.561
C14 d20.2	day 20	178	111	62%	40%	0.599
LT1A C28						
Gel Name	Replicate Group	Spots	Matched	Match Rate 1	Match Rate 2	Correlation Coefficient
C14 d0.1	day 0	113	60	53%	30%	0.499
C14 d0.2	day 0	102	57	55%	28%	0.422
C14 d5.1	day 5	104	75	72%	37%	0.724
***C14 d5.2**	day 5	176	170	96%	85%	1
C14 d10.1	day 10	88	72	81%	36%	0.543
C14 d10.2	day 10	241	128	53%	64%	0.566
C14 d14.1	day 14	97	69	71%	34%	0.752
C14 d14.2	day 14	178	118	66%	59%	0.799
C14 d20.1	day 20	89	48	53%	24%	0.681
C14 d20.2	day 20	172	100	58%	50%	0.563

*Master gel image

Match rate 1: spots matched to member

Match rate 2: spots matched to master

Correlation coefficient based on master gel

Table IIIG: Normalization reports for PDQuest analysis of 2D gel images for isolate LT1A and V2 respectively

Normalization Report - LT1A C28		
Gel Image Name	**Pixel Count**	**Total Density**
lt1a c14 d0 r1 no 4	717920	51437512
lt1a do r2 no.4	717920	1.71E+08
lt1a c28 d5 r1 no.2	717920	1.25E+08
lt1a c28 d5 r2 no.2	717920	4.42E+08
lt1a c28 d10 r1 no.2	717920	1.18E+08
lt1a c28 d10 r2 n0.3	717920	5.05E+08
lt1a c28 d14 r1 no.2	717920	1.1E+08
lt1a c28 d14 r2 no.2	717920	3.49E+08
lt1a c28 d20 r1 no.3	717920	78222392
lt1a c28 d20 r2 no.2	717920	4.2E+08

Normalization Report - v2 c28		
Gel Image Name	**Pixel Count**	**Total Density**
v2 c28 d5 r2	717920	2.95E+08
v2 c28 d5 r1 no.4	717920	1.55E+08
v2 c28 d10 r1 (41) no.2	717920	1.47E+08
v2 c28 d10 r2 no.3	717920	2.78E+08
v2 c28 d14 r1 (45)	717920	2.94E+08
v2 c28 d14 r2 (57 repeat)	717920	3.69E+08
v2 c28 d20 r1 (47) no.3	717920	3.68E+08
v2 c28 d20 r1 (59 repeat)	717920	4.37E+08
v2 c14 d0 r1 no.4	717920	45954584
v2 d0 r2 no.3	717920	1.18E+08

Table IIH: Statistical analysis for C14 and C28 assays (SPSS V. 19)

Paired Samples Statistics							
		Mean	N	Std. Deviation	Std. Error Mean	Correlation	Sig.
Pair 1	V2C14	73.9086	7	32.73322	12.37199	.984	.000
	LT1AC14	72.1443	7	32.41871	12.25312	.318	.486
Pair 2	AbioticControlC14	9.1071	7	15.56180	5.88181	.365	.421
	V2C14	73.9086	7	32.73322	12.37199	.886	.008
Pair 3	LT1AC14	72.1443	7	32.41871	12.25312	.227	.625
	AbioticControlC14	9.1071	7	15.56180	5.88181	.466	.292
Pair 4	V2C28	15.3971	7	15.67401	5.92422	.984	.000
	LT1AC28	13.5600	7	12.76267	4.82384	.318	.486
Pair 5	V2C28	15.3971	7	15.67401	5.92422	.365	.421
	AbioticControlC28	.6043	7	1.11585	.42175	.886	.008
Pair 6	LT1AC28	13.5600	7	12.76267	4.82384	.227	.625
	AbioticControlC28	.6043	7	1.11585	.42175	.466	.292

Table IIH: Statistical analysis for C14 and C28 assays (SPSS V. 19) continued….

Paired Samples Test									
		Paired Differences					t	df	Sig. (2-tailed)
		Mean	Std. Deviation	Std. Error Mean	95% Confidence Interval of the Difference				
					Lower	Upper			
Pair 1	V2C14 - LT1AC14	1.76429	5.83198	2.20428	-3.62940	7.15797	.800	6	.454
Pair 2	AbioticControlC14 - V2C14	-64.80143	31.45237	11.88788	-93.89002	-35.71284	-5.451	6	.002
Pair 3	LT1AC14 - AbioticControlC14	63.03714	30.41042	11.49406	34.91219	91.16209	5.484	6	.002
Pair 4	V2C28 - LT1AC28	1.83714	7.35530	2.78004	-4.96538	8.63966	.661	6	.533
Pair 5	V2C28 - AbioticControlC28	14.79286	15.45942	5.84311	.49528	29.09044	2.532	6	.045
Pair 6	LT1AC28 - AbioticControlC28	12.95571	12.28295	4.64252	1.59588	24.31554	2.791	6	.032

APPENDIX IV

Table IV: UKZN MALDI TOF MS Data (UWC)*

SAMPLE	ID	Accession No. and Protein Name
A	Yes	gi|293611044, conserved hypothetical protein [Acinetobacter sp. SH024]
B	Yes	gi|293611044, conserved hypothetical protein [Acinetobacter sp. SH024]
C	"Yes Low Score	63 for gi|293611044, conserved hypothetical protein [Acinetobacter sp. SH024]
D		Low score
E		Low score
F		Low score
G	"Yes" borderline	gi|327540314, protein containing DUF1559 [Rhodopirellula baltica WH47]
H		Spectra very poor
I	Yes	gi|299769565, peptidyl-prolyl cis-trans isomerase precursor (PPIase) (rotamase) [Acinetobacter sp. DR1]
J		Low score
K	Yes	gi|239501694, putative TonB-dependent receptor protein [Acinetobacter baumannii AB900]
L	Yes	gi|239501694, putative TonB-dependent receptor protein [Acinetobacter baumannii AB900]
M	Yes	gi|239501694, putative TonB-dependent receptor protein [Acinetobacter baumannii AB900]
N	Yes	gi|293611044, conserved hypothetical protein [Acinetobacter sp. SH024]

*Data output from UWC

APPENDIX V: Photographs and gel images

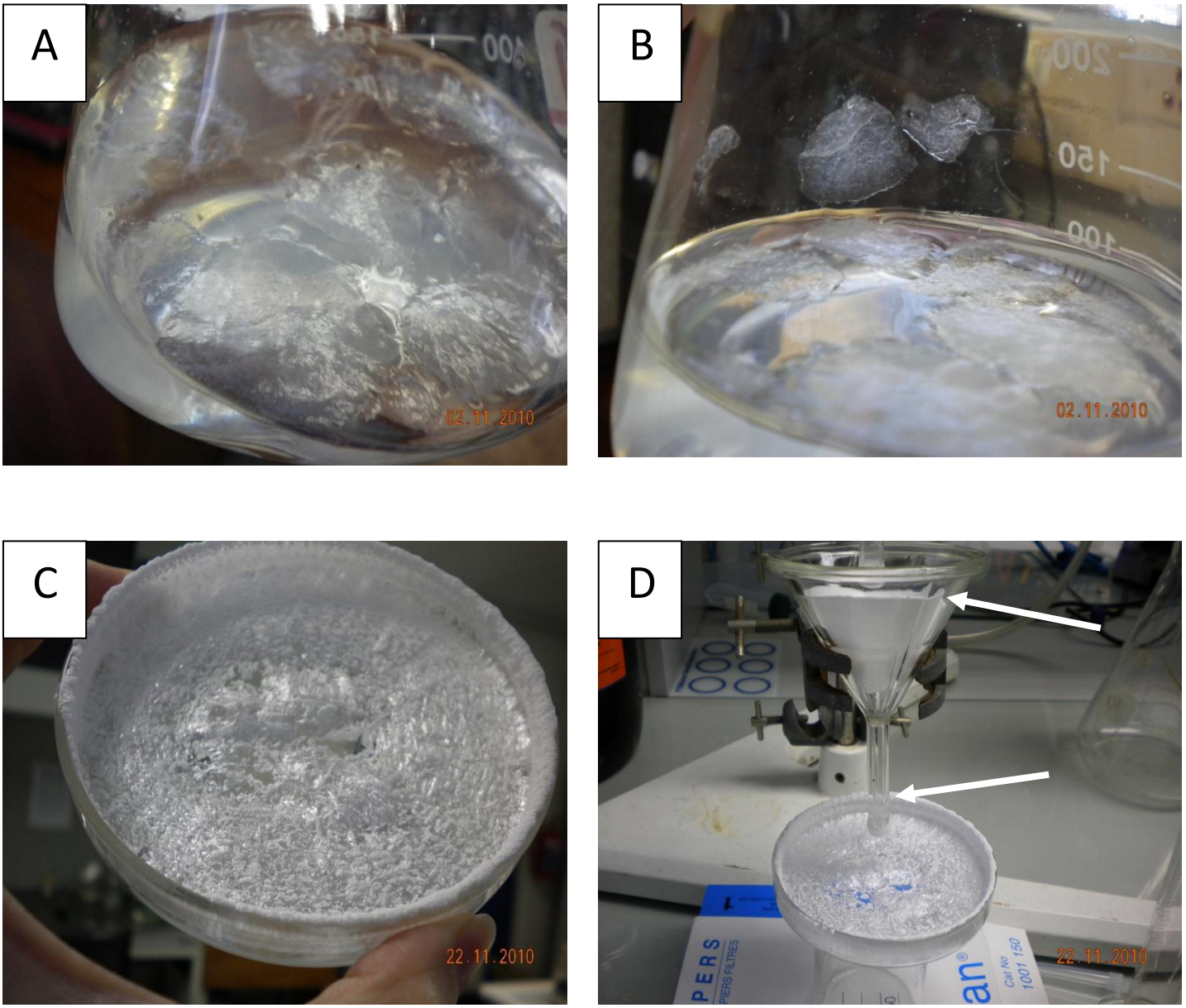

Figure VA A, B: Images of C_{28} after autoclaving. The plastic appearance of the octacosane is clearly seen in these images. It was found to float on the surface of the medium, smaller pieces would disperse after a period of time on the shaker, which was found to complicate OD readings.

C, D: The extraction process. As can be seen, the fine crystalline form of C_{28} is found covering the entire surface of the evapouration plate/beaker and any surfaces that came into contact with the evapourating hexane-C_{28} phase as indicated by the arrows.

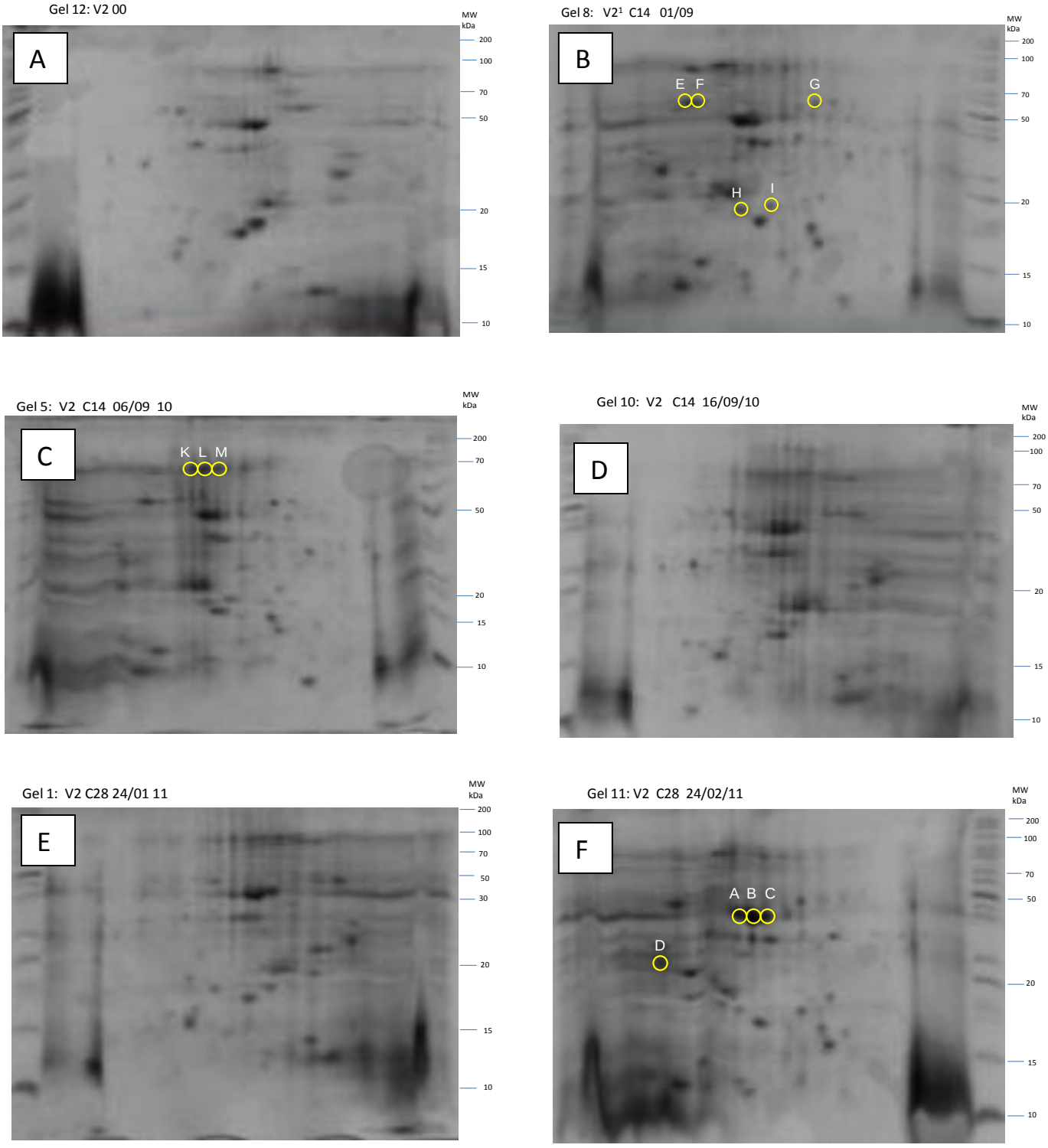

Figure VB V2 2D SDS PAGE gel images of selected, pooled samples for C_{14} (A,B,C,D) and C_{28} (E,F) assays (Run at proteomics facility, UWC). A: Day 0 sample; B: Day 5 sample; C: Day 10 sample; D: Day 20 sample; E: Day 10 sample; F: Day 20 sample. Gels stained with Coomassie blue. pH 4-7 IPG strips from R-L. Circles and letters correspond to sequenced proteins in Table IV.

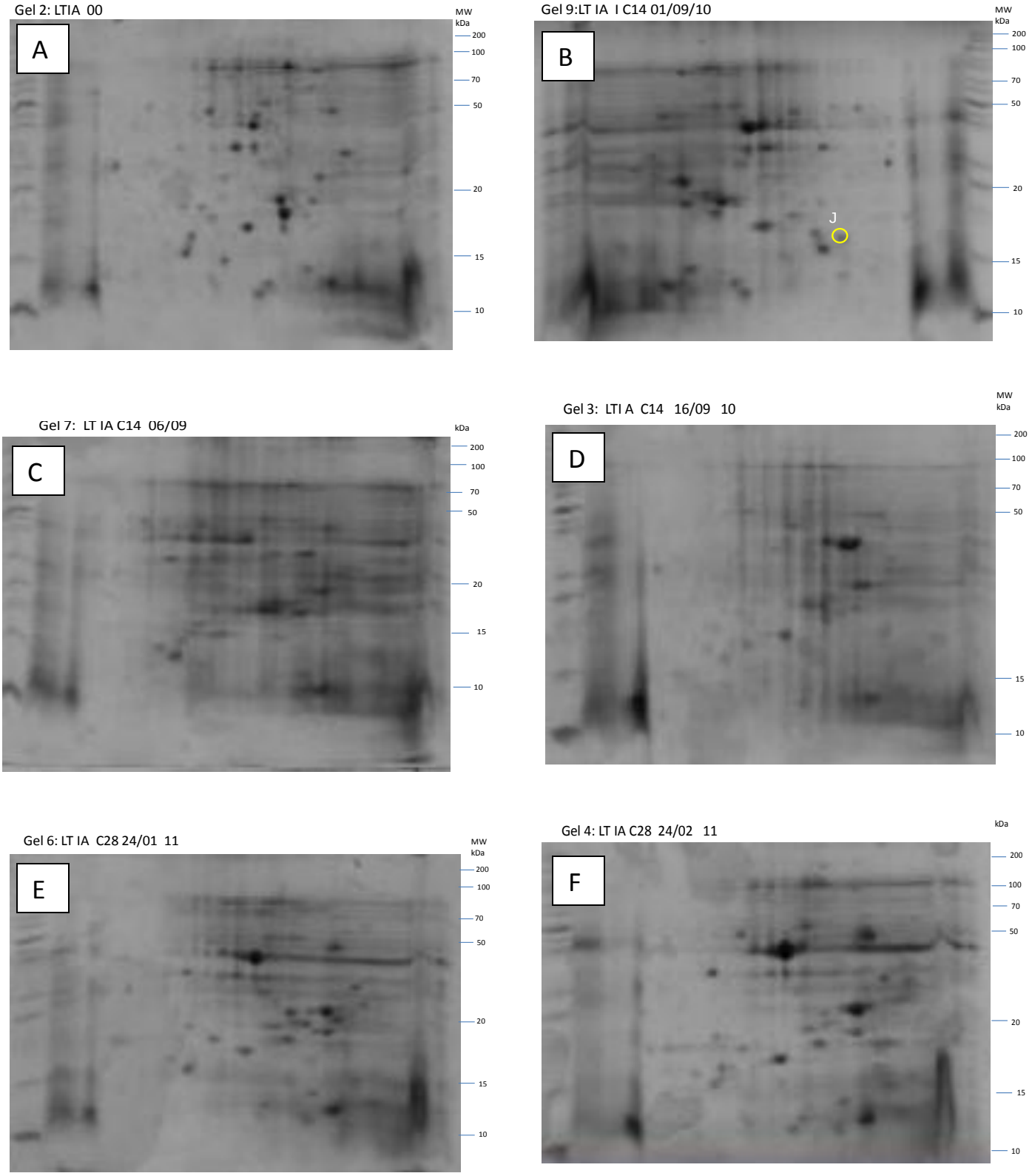

Figure VC LT1A 2D SDS PAGE gel images of selected, pooled samples for C_{14} (A,B,C,D) and C_{28} (E,F) assays (Run at proteomics facility, UWC). A: Day 0 sample; B: Day 5 sample; C: Day 10 sample; D: Day 20 sample; E: Day 10 sample; F: Day 20 sample. Gels stained with Coomassie blue. pH 4-7 IPG strips from R-L. Circles and letters correspond to sequenced proteins in Table IV.

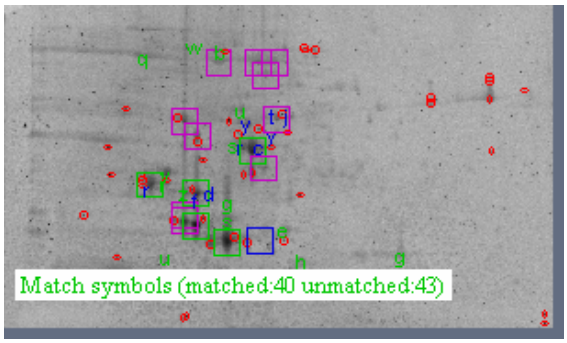

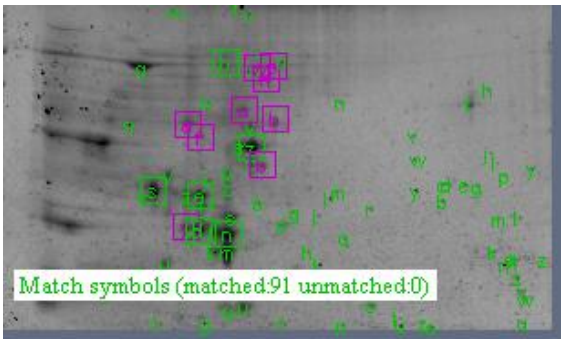

LT1A Day 0

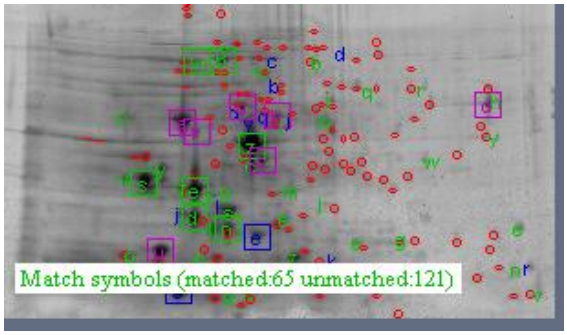

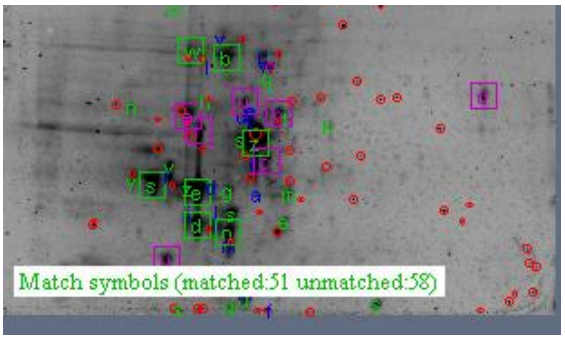

LT1A C14 Day 5

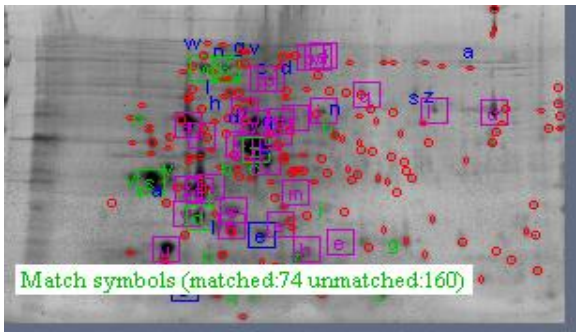

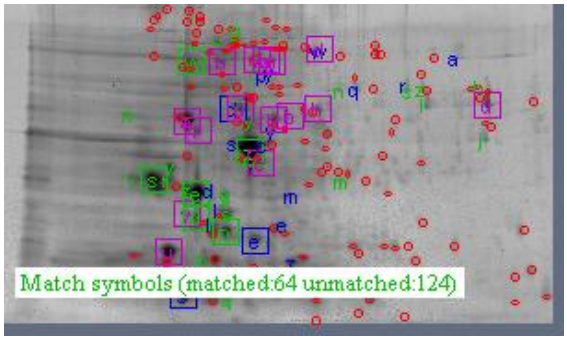

LT1A C14 Day 10

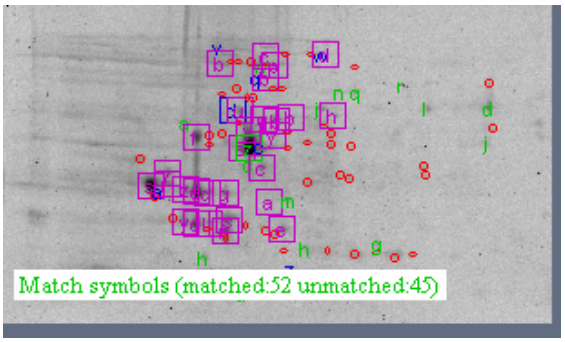

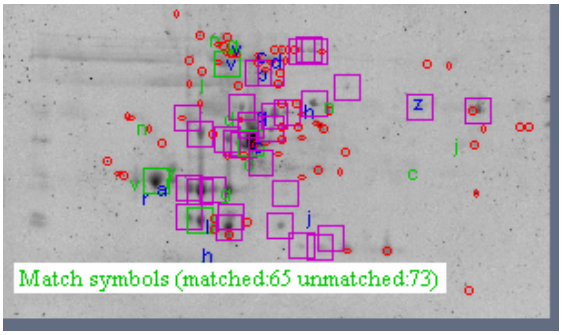

LT1A C14 Day 14

Figure VD 2D SDS PAGE gel images showing match symbols as determined using PDQuest image analysis software. Identity of Gel images as indicated below each pair (duplicate)

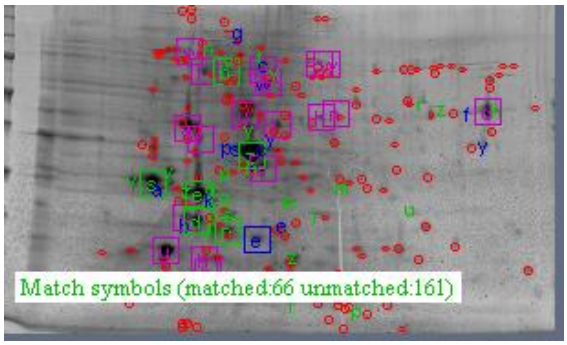

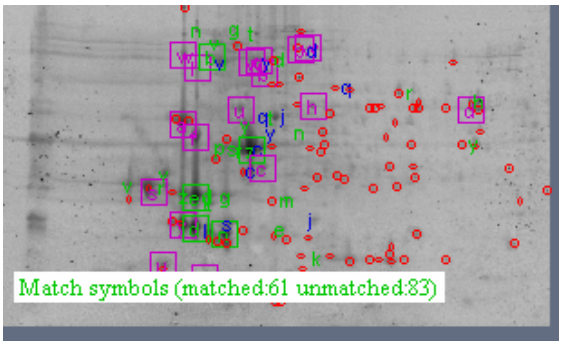

LT1A C14 Day 20

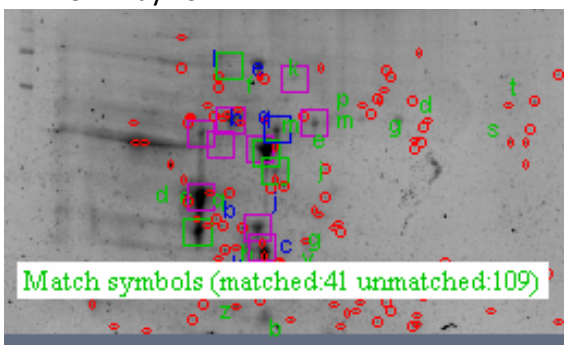

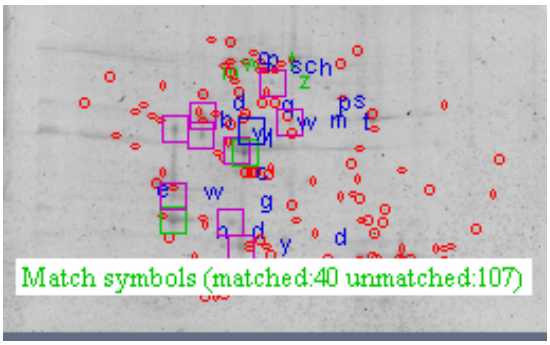

V2 Day 0

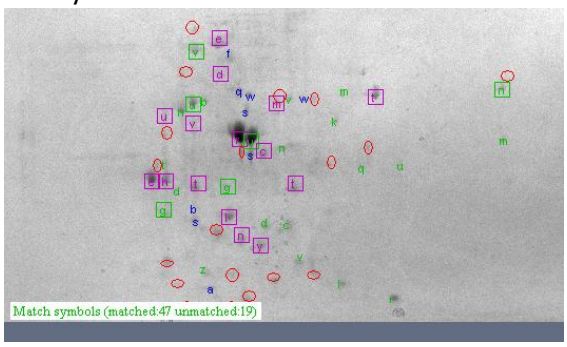

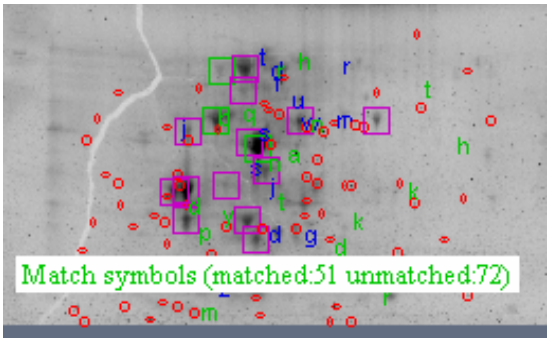

V2 C14 Day 5

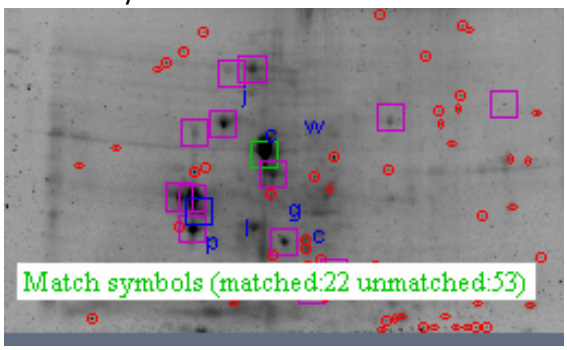

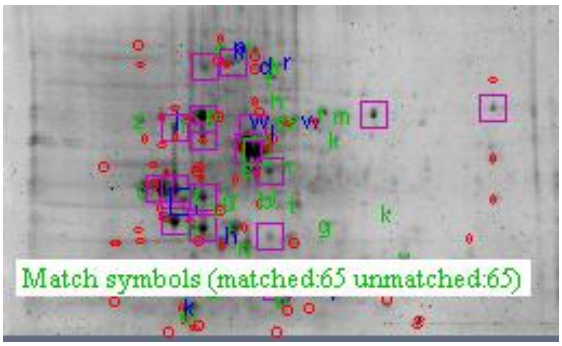

V2 C14 Day 10

Figure VD 2D SDS PAGE gel images showing match symbols as determined using PDQuest image analysis software. Identity of Gel images as indicated below each pair (duplicate)

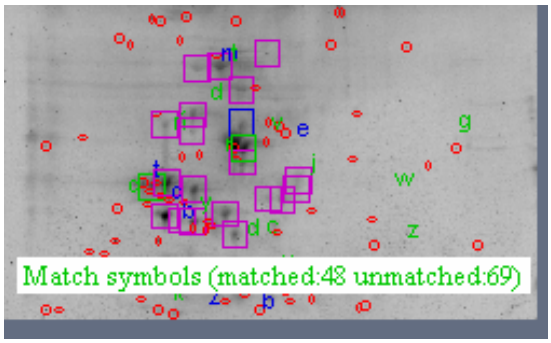

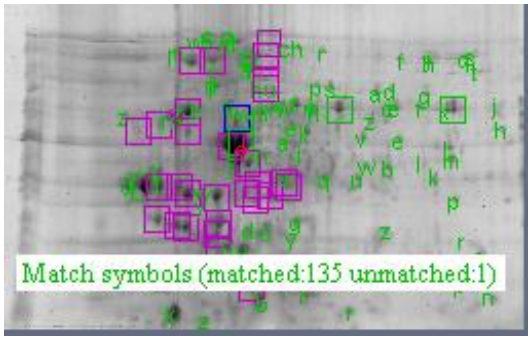

V2 C14 Day 20

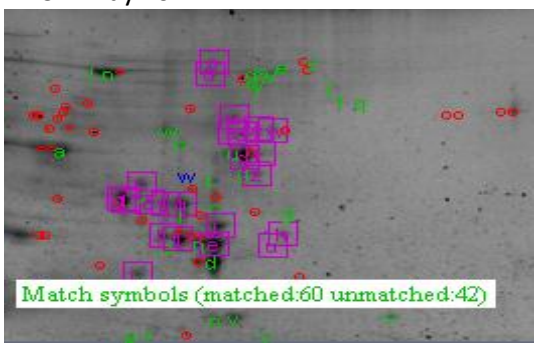

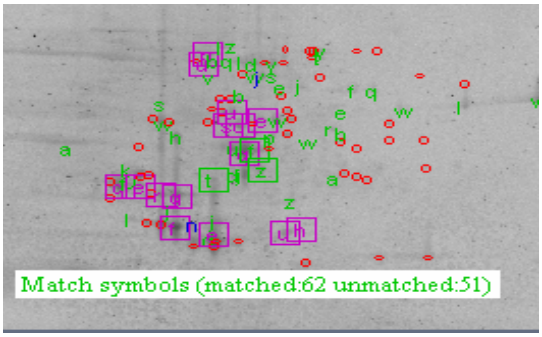

LT1A Day 0

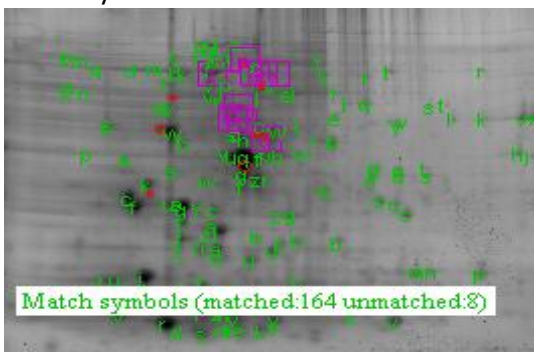

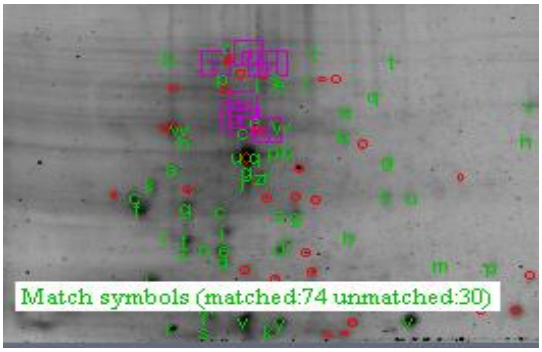

LT1A C28 Day 5

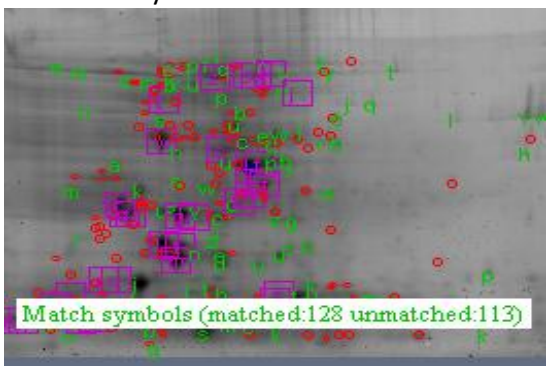

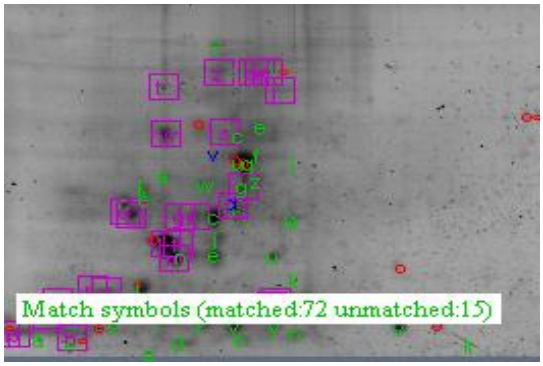

Figure VD 2D SDS PAGE gel images showing match symbols as determined using PDQuest image analysis software. Identity of Gel images as indicated below each pair (duplicate)

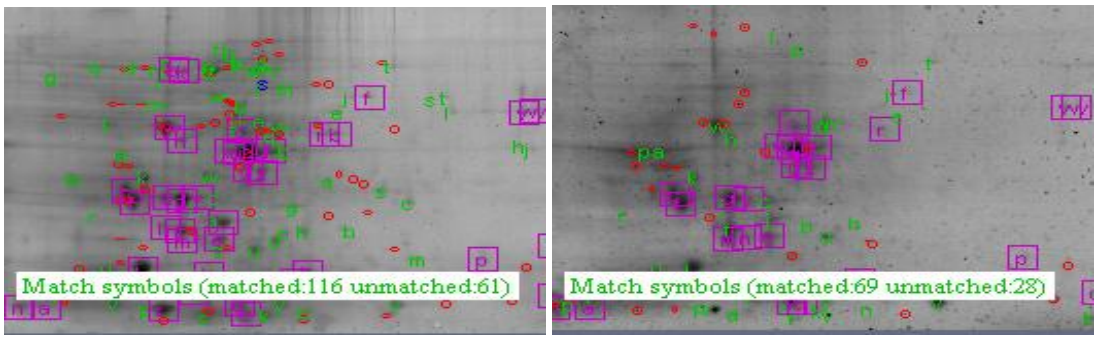

LT1A C28 Day 14

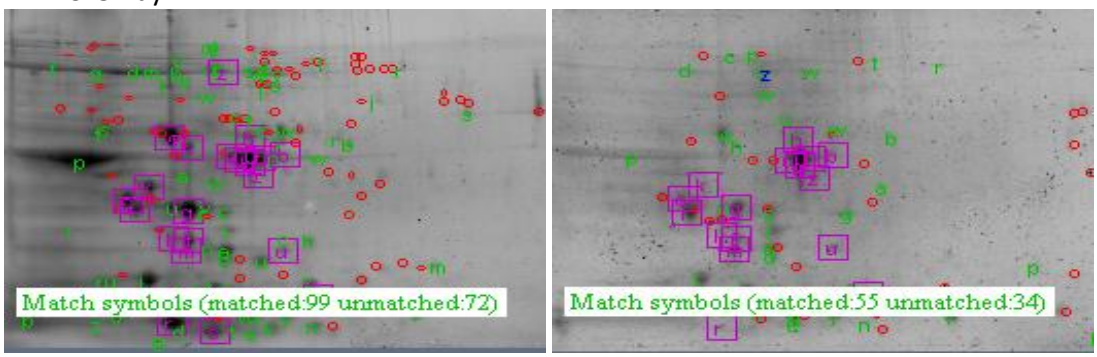

LT1A C28 Day 20

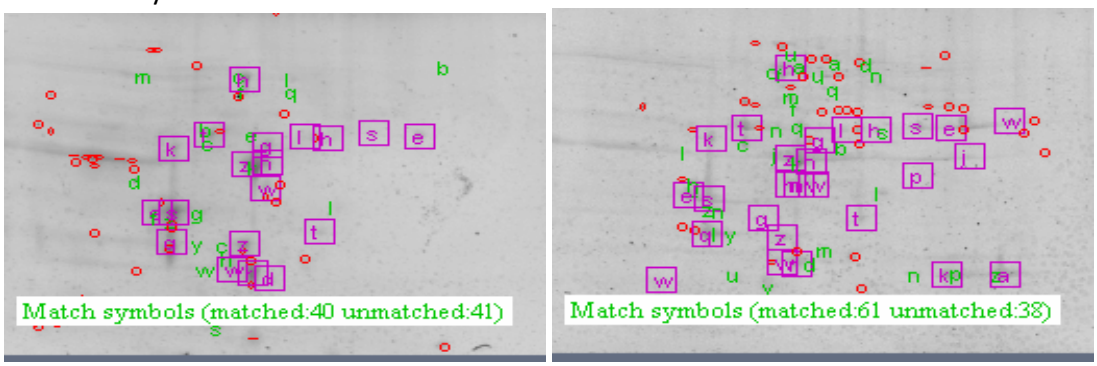

V2 Day 0

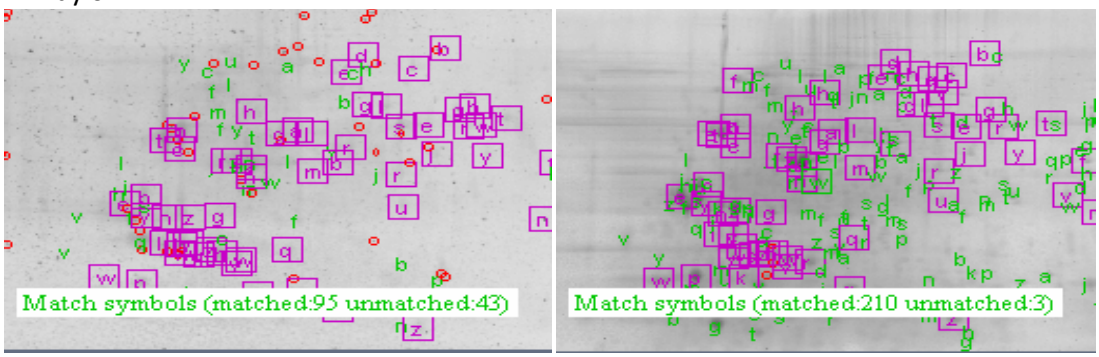

V2 C28 Day 5

Figure VD 2D SDS PAGE gel images showing match symbols as determined using PDQuest image analysis software. Identity of Gel images as indicated below each pair (duplicate)

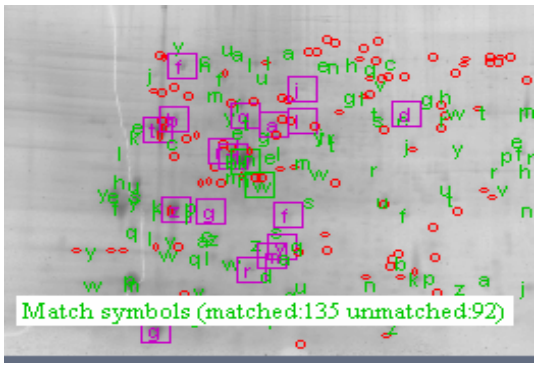

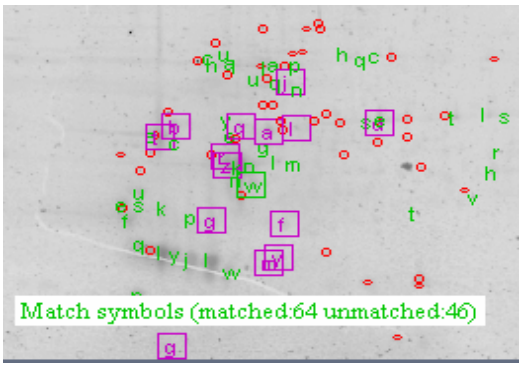

V2 C28 Day 10

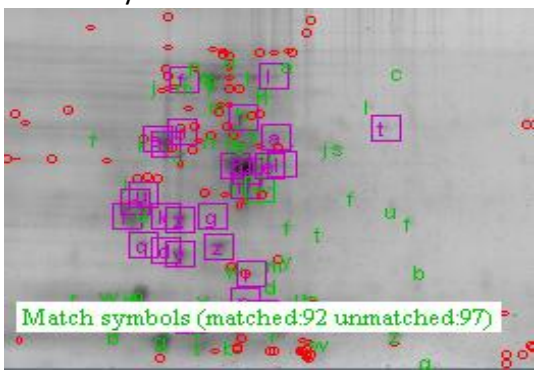

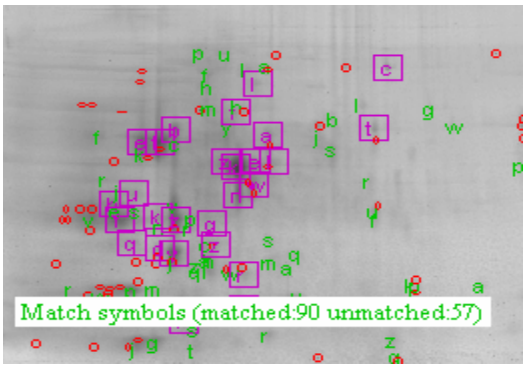

V2 C28 Day 14

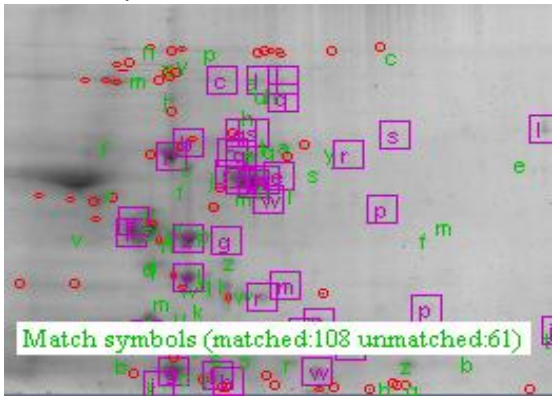

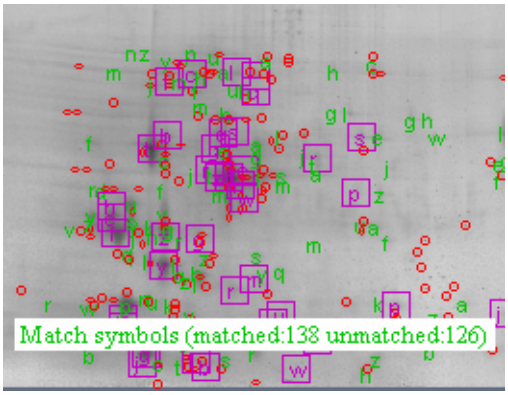

V2 C28 Day 20

Figure VD 2D SDS PAGE gel images showing match symbols as determined using PDQuest image analysis software. Identity of Gel images as indicated below each pair (duplicate)